Electrophysiological assessment of human spinal circuits

Volume 1

Stefane Aline Aguiar

Doctor of Philosophy

Supervisors: Prof. Stuart N. Baker
Dr. Mark Baker

Faculty of Medical Sciences
Institute of Neuroscience
Newcastle University

February 2018

Abstract

Assessing the function of spinal cord circuits non-invasively in humans is crucial both to understand healthy function and pathology. This thesis focuses on the assessment of different human spinal circuits through techniques such as peripheral nerve stimulation, transcranial magnetic stimulation (TMS) and intermuscular coherence with the aim of understanding their function in health and disease.

The thesis investigates human spinal circuits in five studies. 1. An experimental protocol is developed measuring of the flexor carpi radialis (FCR) H-reflex conditioned by electrical stimulation of the extensor carpi radialis (ECR) muscle. At the interval of 30ms between the two stimuli there was a clear facilitation of the H-reflex and at 70ms interval a clear suppression. Several human and monkey experiments revealed that the facilitation was generated by a spinal circuit with convergent input from FCR afferents and ECR Ib afferents to the wrist flexor. 2. In stroke survivors the facilitation at 30ms was similar to in healthy subjects while the later inhibition was weak or absent, which could represent either excessive facilitation or loss of inhibition. 3. Possible descending inputs to these spinal circuits were investigated using TMS to activate the corticospinal tract and click sounds to activate the reticulospinal tract. 4. Intermuscular coherence between lower limb muscles was measured during natural spasms in spinal cord injury patients. Results showed that the spinal cord is capable of producing intermuscular coherence at low frequencies. 5. The ability of peripheral nerve stimulation to reduce tremor by producing plastic changes at the spinal cord level were explored by optimizing phase cancellation of 10 Hz oscillations in motor cortex and spinal cord.

Dedicado aos meus pais.

Acknowledgements

This thesis would not have been possible without the help of many people. I hope they all know how grateful I am for their support.

First, I would like to thank my parents, Indaia and Nilson. For teaching me patience and determination. For supporting me no matter what for so much time, throughout so many things… For their love.

Thank you to my brother and sister, Eric and Jéssica, for being so awesome. You are great friends! And thank you to the entire Aguiar family. I cannot express how important you are for me.

A huge thank you goes to my supervisor, Stuart. Thank you for the incredible patience and for teaching me so much in the past three years.

Thank you to the Baker lab members, in special to Damar, Georgia, Riashad, Alexis, Boubker, Yasuaki, Isabel, Supriyo and Bony, and the non-members Zoltan and Lisa, for helping me so much and for making this experience more enjoyable. Thank you to my other friends Syema, Anderson, Morag, Anselmo, Gabriel, Rodrigo and Rafa, for your support and friendship.

I would like to thank all volunteers, who generously gave up their time to contribute to my research. A special thanks goes to Irene, my favourite volunteer and an incredible person.

I would like to thank my friends from my previous lab, the LAMfriends. In special thank you to Mel, Milena, Marcela and Kauê for giving me great support and being amazing friends. An enormous thank you goes to my former professors and friends Sérgio, Barela, Paulo, Paula and Ana for teaching me so much allowing me to get here.

Finally, I would like to thank the Brazilian government for their financial support (CNPq), which made this entire work possible.

Table of Contents

List of figures

Chapter 1.
Introduction

For many decades extensive work in humans and animals have been developed which allowed us to better comprehend the functioning of spinal cord circuits. From the description of very basic circuits such as the so-called monosynaptic response termed the Hoffman or H-reflex to very complex circuits containing converging inputs from interneurons, descending connections from the brain and inputs from receptors in muscles and the skin, the knowledge gathered from these studies helped us understand the role of spinal circuitry in the control of voluntary movement and how its malfunction can affect the control of movement in numerous neurological disorders. Nevertheless, many advancements are still to be achieved to fully comprehend spinal circuits already being studied and novel circuits which are yet to be described and understood. This thesis aims to contribute towards this goal, investigating human spinal circuitry and its role in the control of voluntary movement as well as understanding what goes wrong in disease.

Assessing the function of spinal cord circuits non-invasively in humans is crucial both to understand healthy function and pathology. Great progress has been achieved in the past decades with a number of well-established techniques which describe and assess the function of different human spinal circuits. Most spinal circuits involve neurons located not only in the spinal cord but also with projections to and from muscles in the periphery as well as projections to and from the brain. As exemplified in the schematic representation in Figure 1 this chapter will introduce concepts related to spinal circuits at the brain, spinal cord and muscle levels. Subsequently, techniques and analysis tools used to assess spinal circuit function are presented as well as what goes wrong within spinal circuitry in disease.

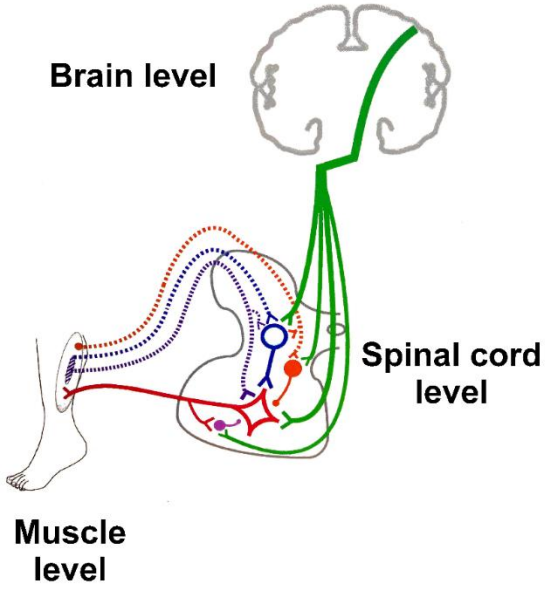

Figure 1. Schematic representation of spinal circuits, which can involve neurons at the brain, spinal cord and muscle levels. Modified from Pierrot-Deseilligny and Burke (2012).

1.1 Brain level

1.1. 1 Descending pathways

There are five major motor pathways contributing to movement control: corticospinal tract, reticulospinal tract, tectospinal tract, vestibulospinal tract and rubrospinal tract, as shown in Figure 2. They originate from the cerebral cortex and brainstem and serve functions which include control of balance and muscle tone, mediation of reflex movements in response to visual stimuli and the control of skilled refined movements (Crossman and Neary, 2010). These pathways send projections to other parts of the nervous system such as the brainstem and spinal cord and ultimately reach the motoneuron level which is the final common pathway to produce muscle activity (see Figure 2). The motor pathways most relevant for this thesis, the corticospinal and reticulospinal tracts, are presented in more detail subsequently.

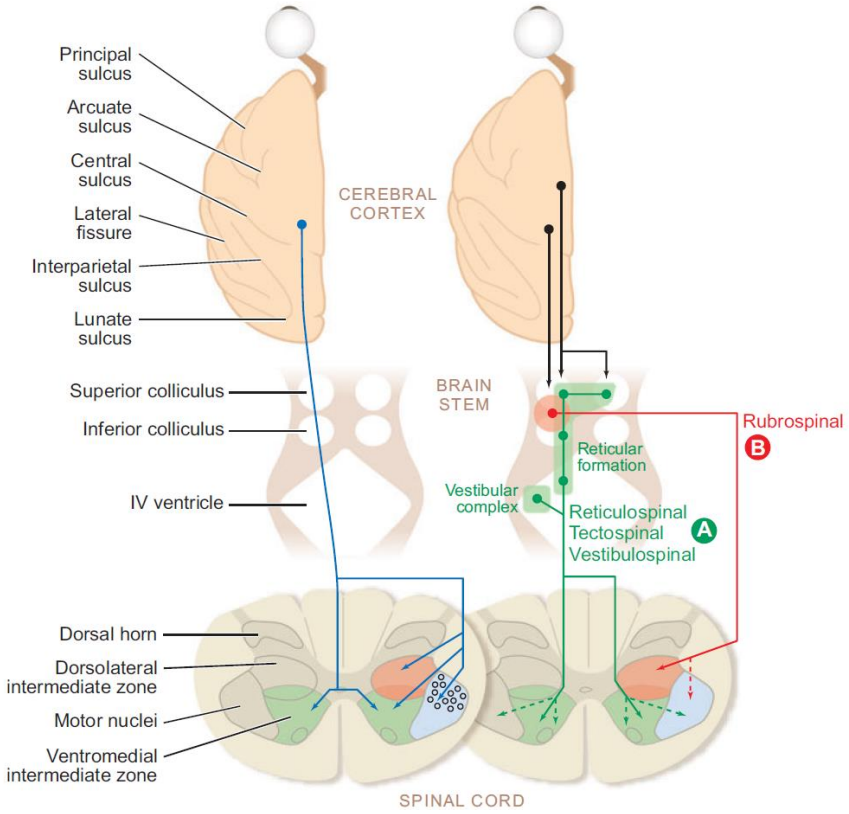

Figure 2. Schematic representation of descending pathways in motor control. From Lemon (2008).

1.1. 2 Corticospinal tract

The corticospinal tract is the largest and most important and extensively studied motor pathway. It originates in the primary motor cortex (M1) and several other cortical areas (Lemon, 2008). As shown in Figure 2, the corticospinal tract projects from the cortex to brainstem structures and at the level of the medullary pyramids most of its fibres (~85%) decussate, i.e., cross to the contralateral side of the body in the dorsolateral portion of the spinal cord (Rosenzweig *et al.*, 2009). These fibres can either make direct monosynaptic connections to motoneurons or connect to more interneurnons before reaching the motoneuron level. The monosynaptic connections between M1 and motoneurons are important for the control of fine, fractionated movements, especially of the hand (Witham *et al.*, 2016). The corticospinal tract can be activated using transcranial magnetic stimulation (TMS), explained in more detail in section 1.4.2.

1.1. 3 Reticulospinal tract

The reticulospinal tract originates in the reticular formation, a structure located in the brainstem. As shown in Figure 2 reticulospinal fibres project from the brainstem to the spinal cord in both ipsilateral and contralateral sides (Lemon, 2008). The reticulospinal tract is traditionally thought to be involved in the control of gross movements such as locomotion and posture. However, recent evidence shows that the reticulospinal tract is also involved in the control of fine hand movements (Soteropoulos *et al.*, 2012). This is particularly important after a corticospinal lesion (e.g., stroke), since the reticulospinal tract could assume a crucial role in the recovery of hand function (Baker, 2011). The reticulospinal tract can be activated by click sounds (Fisher *et al.*, 2012a), which is described in more detail in section 1.4.3.

1.2 Muscle level

In the periphery, sensory receptors located in muscles and the skin provide important information such as muscle length, tendon tension, skin pressure and temperature. This information is carried through afferent fibres to the spinal cord where other synaptic connections will take place. The sensory receptors which are most relevant for this thesis are the muscle spindles and Golgi tendon organs, described in more detail below.

1.2. 1 Muscle spindle

Muscle spindles are sensory receptors located in muscle fibres, as shown in Figure 3A. They fire in response to muscle stretch, which is why they are also called stretch receptors. Muscle spindles constantly detect changes in muscle length, providing useful information about how the body is positioned and moving in space (Matthews, 1972). Information from muscle spindles is transmitted to the spinal cord via their afferents, called Ia afferents, which make monosynaptic connections with the motoneurons of the same muscle, as shown in Figure 3B. The stretch reflex resulting from this spinal circuit is a monosynaptic reflex since it involves only one synapse

between Ia afferents, firing when the muscle is stretched, and motoneurons, which respond firing and causing the contraction of the muscle. Muscle spindles are the only receptors that have a monosynaptic connection with motoneurons (Bear *et al.*, 2007). Muscle spindle contains not only the described extrafusal fibres, located outside the spindle, but also intrafusal fibres, located within the fibrous capsule of spindles. While extrafusal fibres are innervated by alpha motorneurons, intrafusal fibres receive innervation from gamma motorneurons. Activity from alpha and gamma motorneurons affects differently the response of spindle through the firing of their Ia afferents: alpha motorneuron activation decreases Ia activity while gamma motorneuron activation increases Ia activity (Bear *et al.*, 2007).

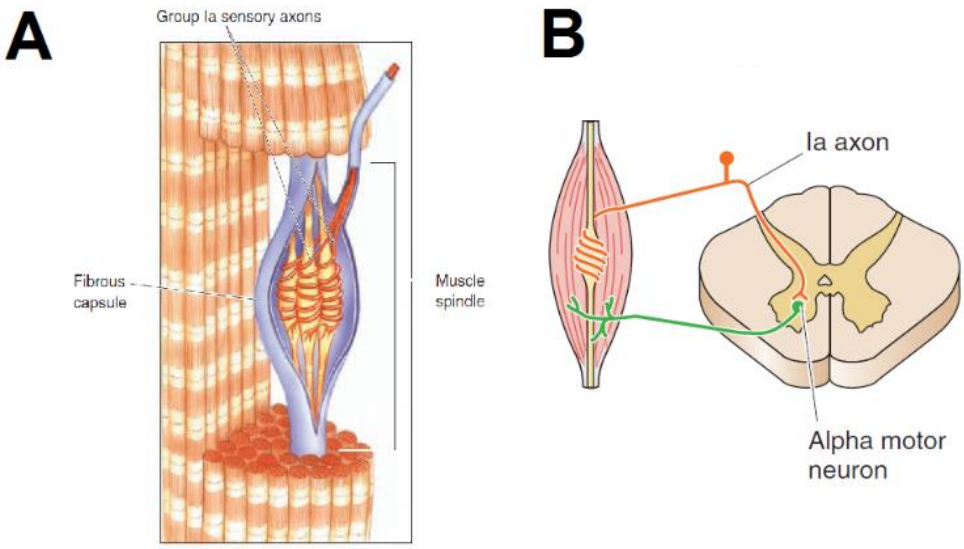

Figure 3. **A**, schematic representation of muscle spindles and Ia axons. **B**, schematic representation of spinal circuit producing the stretch reflex with monosynaptic connection between Ia afferents from muscle spindles with motoneurons of the same muscle. Modified from Bear *et al.* (2007).

1.2. 2 Golgi tendon organs

Golgi tendon organs are contraction-sensitive mechanoreceptors located on the musculotendinous junction (Jami, 1992). They are positioned therefore in series with muscle fibres (see Figure 4A), as opposed to muscle spindles which are located in parallel with muscle fibres. Golgi tendon organs fire mainly in response to changes in muscle tension (Bear *et al.*, 2007). Their afferents are called Ib afferents, which, as shown in Figure 4B, synapse with inhibitory interneurons which in turn synapse with

the motoneurons of the same muscle, inhibiting its contraction. This disynaptic pathway is called autogenic or non-reciprocal inhibition (Jami, 1992).

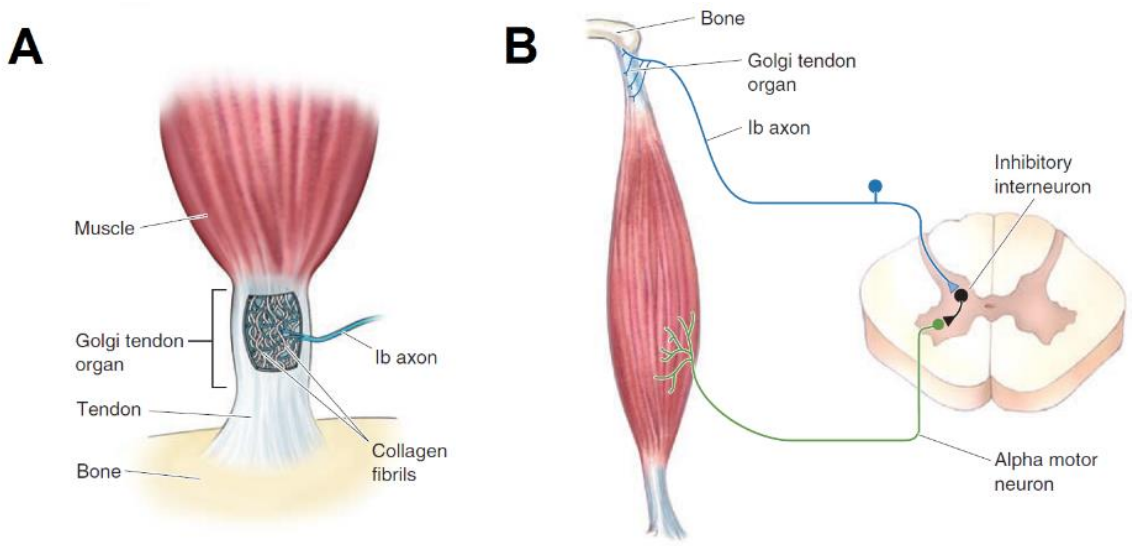

Figure 4. **A**, schematic representation of Golgi tendon organs and Ib axons. **B**, schematic representation of spinal circuit producing non-reciprocal inhibition caused by Ib afferents originating from Golgi tendon organs. Modified from Bear *et al.* (2007).

1.2. 3 Afferent fibres

Several different types of afferent fibres transmit sensory information from the periphery to the brain and spinal cord. These fibres range from the largest diameter and fastest conducting afferents carrying information from proprioceptors in skeletal muscles (named group I) to smaller and slower fibres which carry information from mechanoreceptors in muscles and the skin and about pain and temperature (groups II, III and IV) (Bear *et al.*, 2007).

The main interest of this thesis focus on the group I afferent fibres, specifically Ia and Ib afferents which transmit sensory information from muscle spindles and Golgi tendon organs, respectively. Ia afferents are slightly larger in diameter and have slightly faster conduction velocities than Ib afferents; around 82 m/s in Ia and 90 m/s in Ib reported in the cat (Willis *et al.*, 1976). Figure 5A and B shows the firing patterns of muscle spindles and Golgi tendon organ afferents in response to a muscle twitch and stretch, respectively. On the onset of a muscle twitch Ib afferents from Golgi tendon organs rapidly increase their firing while Ia afferents go silent. A somewhat

inverse process occurs for a muscle stretch, which causes Ia afferents to rapidly increase their firing while Ib afferents go silent for a while (Matthews, 1972).

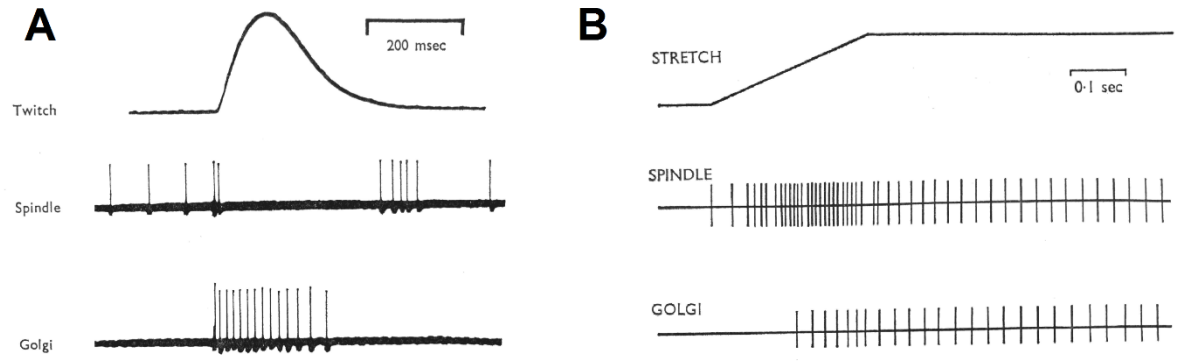

Figure 5. Firing of muscle spindles and Golgi tendon organs in response to a muscle twitch (**A**) and a muscle stretch (**B**). Modified from Matthews (1972).

Ia afferent fibres have non-linear firing characteristics, which allows them to be activated in response even to very initial and small changes in muscle length. These fibres arrive from the primary endings of muscle spindles and make several connections at the spinal cord level; these include connections in the dorsal column and in the ventral horn, where Ia afferents synapse with motorneurons of the homonymous and synergistic muscles (Pierrot-Deseilligny and Burke, 2012). Ib afferent fibres, on the other hand, are more powerfully stimulated by a muscle contraction rather than a stretch. A Ib afferent fibre, usually originated by a single Golgi tendon organ, can signal very small variations in contractile force (Pierrot-Deseilligny and Burke, 2012). They are also insensitive to vibration of the relaxed muscle, which opens possibilities of experimental protocols to distinguish effects from Ib afferents compared to Ia afferents, which are sensitive to such stimuli (Coppin *et al.*, 1970).

Another important group of afferents fibres are the group II afferents. As the name suggests they are smaller diameter fibres and therefore have slower conduction velocities and higher threshold for electrical activation when compared to group I fibres. Group II afferents originating from muscle spindles signal activity from spindles secondary endings, which are more sensitive to the static component of the muscle stretch than the dynamic component or the vibration of the muscle. These afferent fibres connect to group II interneurons and the fastest pathways described are disynaptic (Pierrot-Deseilligny and Burke, 2012). The selective activation of group

II afferents can be achieved by experiments using a technique consisting on the cooling of the nerve being examined (Grey *et al.*, 2001; Marque *et al.*, 2005).

1.3 Spinal cord level

After extensive work on human and animal experiments on the past decades several spinal circuits have been described in the literature. Subsequently, some of the different spinal circuits described in the literature are presented as well as techniques for the assessment of their function in humans.

1.3. 1 Reciprocal inhibition

Figure 6 describes the spinal circuit producing reciprocal inhibition. The muscle spindles fire their Ia afferents which synapse with inhibitory Ia interneurons, which in turn synapse with the motoneurons of the antagonist muscle, causing the inhibition of activity from the antagonist muscle. Reciprocal Ia inhibition therefore involves a disynaptic pathway (Pierrot-Deseilligny and Burke, 2012). Reciprocal inhibition can be assessed in the human forearm by measuring the H-reflex in the flexor carpi radialis (FCR) muscle (explained in detail on section 1.4.1) conditioned by a radial nerve shock. The H-reflex is a response in the flexor muscle caused by the monosynaptic connection of Ia afferents, stimulated by a shock to median nerve, and the motoneurons of this same muscle. When the median nerve shock is conditioned with a shock to the radial nerve at an appropriate interval the stimulation coming from extensor afferents will cause the flexor to be inhibited, decreasing the size of its response, i.e., the H-reflex (Araki *et al.*, 1960; Day *et al.*, 1984).

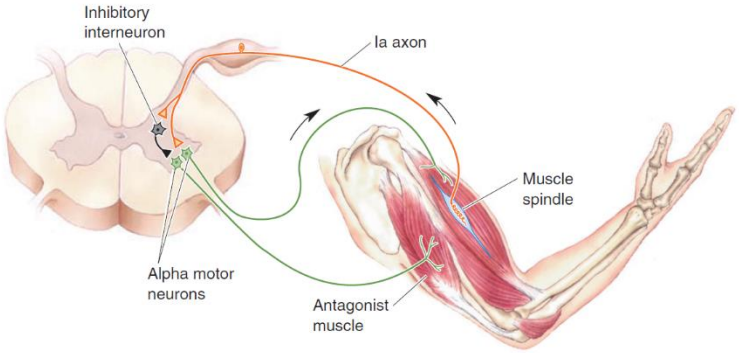

Figure 6. Schematic representation of spinal circuit producing reciprocal inhibition. From Bear *et al.* (2007).

1.3. 2 Recurrent inhibition (Renshaw cells)

Figure 7 shows the spinal pathway responsible for recurrent inhibition due to Renshaw cells. Recurrent collateral of motorneurons axons excite Renshaw cells which in turn inhibit the same motorneurons. Recurrent inhibition was the first pathway to be identified and one of the first to have a reliable method of investigation in humans (Pierrot-Deseilligny and Burke, 2012). To assess recurrent inhibition in humans one can evoke the H-reflex after a conditioning H-reflex on the same muscle. By using appropriate intervals between the two shocks and intensities of each shock this method will cause a collision in the motorneuron axons between the orthodromic conditioning reflex volley and the antidromic volley elicited by the test stimulus. The decrease in the reflex muscle response is caused by recurrent inhibition due to the action of Renshaw cells (Bussel and Pierrot-Deseilligny, 1977).

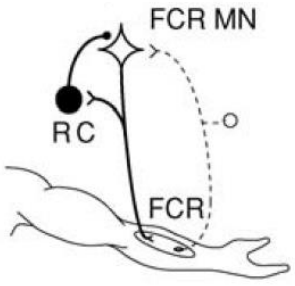

Figure 7. Schematic representation of spinal circuit producing recurrent inhibition due to Renshaw cells. Modified from Pierrot-Deseilligny and Burke (2012).

1.3. 3 Pre-synaptic inhibition

Spinal circuits may also involve pre-synaptic inhibition of Ia terminals, which modulates the efficacy of synapses involving Ia afferents. The pre-synaptic inhibition of Ia terminals can be controlled by descending input from supraspinal centres (Pierrot-Deseilligny and Burke, 2012). Berardelli and colleagues (1987) have demonstrated the assessment of pre-synaptic inhibition between human antagonist forearm muscles. Using the same method described for the measurement of reciprocal inhibition (i.e., the FCR H-reflex conditioned by radial nerve stimulation), the authors demonstrated inhibition of the FCR H-reflex with longer intervals between test and conditioning stimuli (5 to 40ms, as opposed to -1 to 3ms in the case of reciprocal inhibition). The inhibition shown was proved to be caused by large group I extensor afferents acting on the FCR H-reflex at a premotoneuronal site (Berardelli *et al.*, 1987).

1.3. 4 Ib pathways

The most basic and well described Ib pathway is the one producing non-reciprocal inhibition, caused by the activation of Ib afferents from Golgi tendon organs, synapsing with Ib inhibitory interneurons which in turn inhibit motorneurons of the same muscle, as described previously (see Figure 4B). The assessment of such pathway in the human upper limb, however, still represents a challenge. Burne and Lippold (1996) proposed a method in which electrical stimulation is given percutaneously over muscle tendons. The inhibition of ongoing EMG activity was claimed to be caused by the described Ib non-reciprical inhibition pathway (Figure 8). Priori and colleagues (1998) criticized the work, however, not only due to the long latency of the effect (~55ms in the forearm extensor), not compatible with such disynaptic pathway, but also due to the location of stimulation over muscle tendons, since Golgi tendon organs are not located in the actual tendon but in the musculotendineous junction (Jami, 1992). It was ultimately shown that the effect was probably caused by group III tendon afferents producing pre-synaptic inhibition of Ia fibres (Priori *et al.*, 1998).

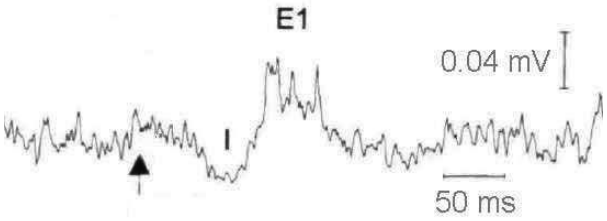

Figure 8. Autogenic/non-reciprocal inhibition of ongoing muscle activity. From Burne and Lippold (1996).

Another Ib pathway, extremely relevant to this thesis (particularly in chapter 2), is a trisynaptic pathway by which Ib afferents excite motorneurons of the antagonist muscle. As shown in Figure 9, Ib afferents from Golgi tendon organs in the forearm extensor synapse with Ib interneurons, which synapse with another set of interneurons, which in turn excite motorneurons of the flexor (antagonist) muscle (Pierrot-Deseilligny and Burke, 2012). The assessment of this pathway in the human upper limb is extremely challenging. Cavallari and colleagues (1985) have demonstrated the effects of radial nerve stimulation on the FCR H-reflex, showing a facilitation (caused by this excitatory Ib pathway) which follows the Ia reciprocal inhibition and is potentiated by cutaneous stimulation. The authors argue, however, that in most cases is not possible to observe a clear-cut facilitation, but instead a facilitation that only manifests itself as a hump superimposed on the decay of the Ia inhibition (Cavallari *et al.*, 1985). This makes such method not ideal to asses this Ib pathway. Chapter 2 describes a study which developed a novel method that can potentially assess the function of this pathway.

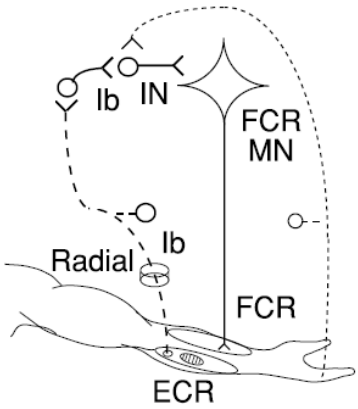

Figure 9. Schematic representation of trisynaptic Ib pathway by which Ib afferents cause excitation of motorneurons of the antagonist muscle. Modified from Pierrot-Deseilligny and Burke (2012).

1.3. 5 Other spinal pathways

Several other spinal circuits have been described in the literature. They include recurrent inhibition due to Renshaw cells – measured by evoking the H-reflex conditioned by nerve stimulation at appropriate intervals and intensities (Bussel and Pierrot-Deseilligny, 1977) –, cutaneousmuscular reflexes – which is revealed by changes in ongoing EMG activity in response to stimulation of a digital nerve (Jenner and Stephens, 1982) –, group II pathways – involving slower conducting group II afferents fibres originating from secondary endings of muscle spindles – and propriospinal pathways – which involve neurons connecting different segments of the spinal cord (Pierrot-Deseilligny and Burke, 2012).

1.4 Techniques and analysis tools

There are a number of electrophysiological techniques and analysis tools which are crucial to investigate human spinal circuits. The ones relevant to this thesis are described in more detail below. The techniques include the H-reflex measurement (used in chapters 2, 3 and 4), TMS, and click sounds to activate the reticular formation (both used in chapter 4). The analysis tools include spectral and intermuscular coherence analysis (used in chapters 5 and 6).

1.4. 1 H-reflex

The Hoffman reflex, most commonly referred to as the H-reflex was first described and named after Paul Hoffman, in 1910, and used in numerous investigations ever since (Magladery and Mc, 1950; Magladery *et al.*, 1951; Burke, 2016). It consists of the recording of the EMG signal from a muscle in response to an electrical stimuli given to the nerve that controls this same muscle. Figure 10A shows a schematic representation of the H-reflex mechanism and measurement. The nerve shock depolarizes the membrane of axons from both efferent and afferent fibres. The activation of efferent fibres, which are the motorneurons controlling the muscle, will

result in a direct muscle response of short latency, named M-wave. The activation of afferent fibres, which are the Ia afferents from muscle spindles, will travel to the spinal cord where one synapse will occur with the motorneurons of that same muscle, which subsequently will lead to a muscle response of later latency than the M-wave, called the H-reflex. The H-reflex is therefore a monosynaptic reflex, at least in its first response component lasting around 1ms; later components of the reflex response are influenced by other more complex pathways including oligosynaptic connections (e.g., Grey *et al.*, 2001). It is one of the most basic and simple reflex responses of the motor system and it has been extensively studied in this field.

The H-reflex is commonly studied in the lower limb, on the soleus muscle, where its measurement is fairly easy and straightforward making it possible for measurements to be taken even during the different phases of walking (e.g., Raffalt *et al.*, 2015). This thesis, however will focus on the FCR H-reflex on the upper limb, which can at times be a challenging experimental protocol compared to the soleus H-reflex. Nevertheless, the FCR H-reflex has also been the subject of numerous investigations and its methodology has been well described in the literature (Jabre, 1981). Figures 10B and C show the most efficient procedure for electrodes placement for the recording of the FCR H-reflex. Technical difficulties on the measurement of the FCR H-reflex in humans include the amount of body fat of participants being tested. Small to medium amounts of body fat can already make the measurement difficult not only because body fat in between the median nerve and the stimulating electrode will make the shock reach the nerve with less intensity, forcing the experimenter to apply pressure on the stimulating electrode against the skin, but also body fat will compromise the EMG recordings, which will not present such clear signals due to the body fat in between the recording electrodes and the muscle underneath the skin. Another issue for the measurement of the H-reflex is the fact that some subjects present an extremely variable H-reflex, with small fluctuations in the general state of alertness of the participant causing significant changes in the size of the response, which makes this measurement not ideal in an experimental session lasting a few hours. The H-reflex measurement can also become extremely challenging in subjects with difficulties to remain still, in a relaxed position, since any sudden movements or contractions will greatly influence the H-reflex response, as explained in more detail below.

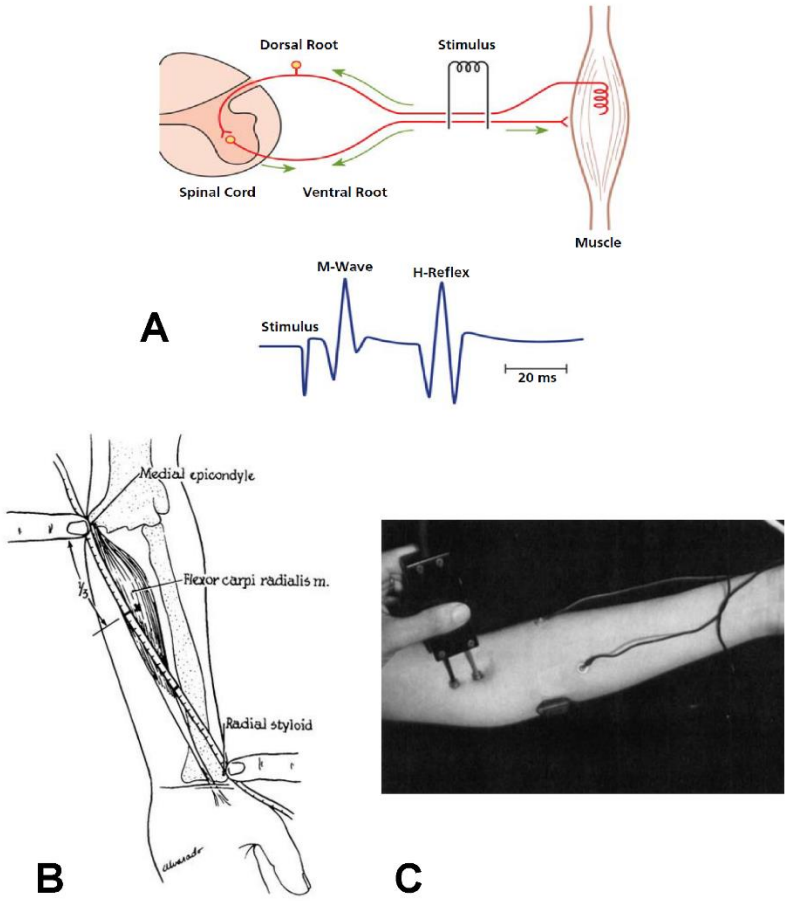

Figure 10. **A**, schematic representation of nerve stimulation activating both efferent and afferent fibres giving rise to the M-wave and H-reflex, respectively. From Wynne *et al.* (2006). B and C show placement of electrodes for the measurement of the FCR H-reflex. **B**, placement of recording electrode over FCR muscle belly. **C**, placement of EMG electrodes, one over FCR muscle belly and one over brachioradialis, and placement of stimulation electrode over the median nerve. Modified from Jabre (1981).

Several methodological details are important for the successful measurement of the FCR H-reflex. The already mentioned placement of recording electrodes is an important factor as well as the placement of the stimulating electrode over the median nerve at the cubital fossa, which can be challenging since usually pressure needs to be applied on the electrodes so the shock can reach the nerve that is located deep inside the arm. This also means maintaining the stimulating electrode in the same position throughout the entire experiment can be difficult as even small movements of the person might move the electrode and therefore change the intensity of the shock and consequently the size of the response. The background EMG activity greatly influences the size of the H-reflex. In fact, that is one important criteria to identify a response as an H-reflex: the response needs to increase during a weak voluntary contraction compared to rest (Burke, 2016). Other important criteria

include the latency of the response, which for the FCR muscle is usually around 15ms (Khosrawi *et al.*, 2015), and fluctuations in the size of both M-wave and H-reflex according to changes in the intensity of the median nerve shock, as demonstrated in Figure 11 (Jabre, 1981). As the median nerve shock intensity increases a small M-wave will start to appear and the H-reflex size will increase up until a certain point, where is maximal. Passed this point increments in the intensity of the median nerve stimulation will cause the H-reflex to decrease and the M-wave to increase until the point where the M-wave is maximal and the H-reflex disappears. This happens since for these high intensities more and more efferent fibres are recruited producing an M-wave response and the antidromic volley in these fibres will collide with and eliminate the H-reflex response (Pierrot-Deseilligny and Burke, 2012).

Another important factor during the measurement of the FCR H-reflex is the pulse width for median nerve stimulation. Such pulse duration is known to influence the recruitment of fibres producing the reflex response (Hindle *et al.*, 2014); in our studies pulse duration was kept at 500 μs, which is within the range (500-1000 μs) most commonly used in experiments investigating spinal circuits such as the ones explored in this thesis (e.g., Jabre, 1981). The median nerve stimulation rate is also extremely important since subsequent median nerve shocks with short intervals in between will cause homosynaptic depression and decrease the size of the H-reflex; intervals of at least 3 to 4 seconds in between stimuli are recommended to avoid this problem (Pierrot-Deseilligny and Burke, 2012). Finally, the intensity of median nerve stimulation is crucial as well since it alters the size of the H-reflex response, as described previously.

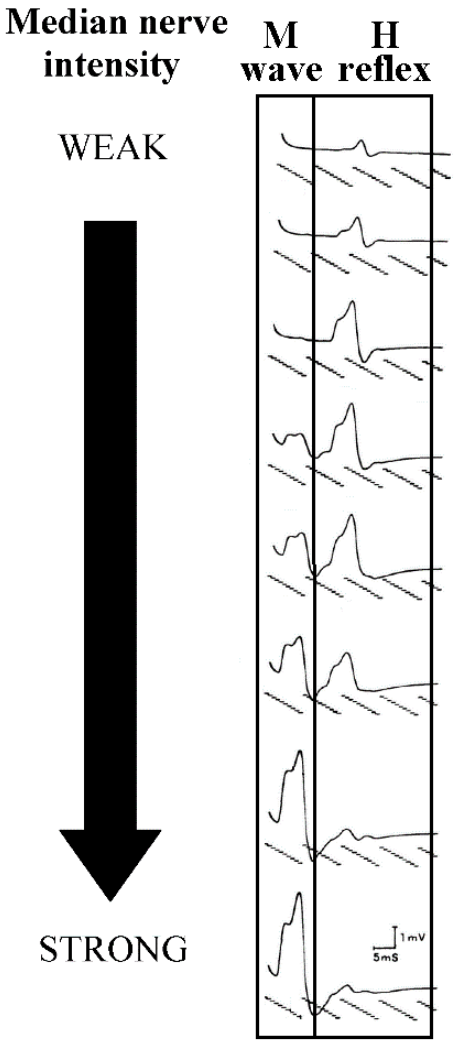

Figure 11. Changes in FCR H-reflex and M wave according to increase in median nerve shock intensity, from weak (top) to strong (bottom). Modified from Jabre (1981).

1.4. 2 Transcranial magnetic stimulation (TMS)

TMS is a technique for non-invasive brain stimulation first introduced in the 1980s (Barker *et al.*, 1985), serving as a very efficient alternative for transcranial electric stimulation (TES), which uses electrodes placed in the scalp delivering high currents to depolarize neurons in the cortex causing discomfort and pain (Klomjai *et al.*, 2015). As demonstrated in Figure 12A, the technique consists of the placement of commonly a figure-of-eight shaped coil – to provide focused rather than more widespread stimulation, achieved with a circular coil (Klomjai *et al.*, 2015) – over the motor cortex, which delivers magnetic stimulation that passes through the scalp and reaches neurons in the cortex, and recording of EMG signals of the target muscle.

Figure 12B shows a simplified schematic representation of the mechanism of action of TMS. TMS is delivered over motor cortex activating the corticospinal tract ultimately reaching the motorneurons of the target muscle on the contralateral side of the body and generating a motor evoked potential (MEP).

Since most corticospinal tract fibres decussate TMS is usually applied over motor cortex on the contralateral side of the target muscle. Although most TMS studies investigate the corticospinal tract, it has been shown that TMS can also activate the reticular formation, which gives rise to the reticulospinal tract, as described in more detail below (Fisher *et al.*, 2012a). Important methodological aspects of TMS experiments involve the intensity of stimulation and orientation of the coil, which will change the direction of current causing direct (D) and indirect (I) waves of different latencies in the muscle responses (Day *et al.*, 1989; Sakai *et al.*, 1997; Di Lazzaro and Rothwell, 2014). Even the population investigated can be important in TMS experiments, as it has been shown that Chinese subjects have significantly higher threshold of TMS intensity to produce a MEP (Yi *et al.*, 2014).

Depending on the specific parameters of stimulation including coil type and positioning, stimulation intensity, amongst others, TMS can activate different motor pathways. TMS has even been used in investigations aiming at testing the connectivity between different cerebral areas (Paus *et al.*, 1997), showing for example connections between the motor cortex in the two cerebral hemispheres (Ferbert *et al.*, 1992) and between the premotor cortex and the primary motor cortex (Parmigiani *et al.*, 2018).

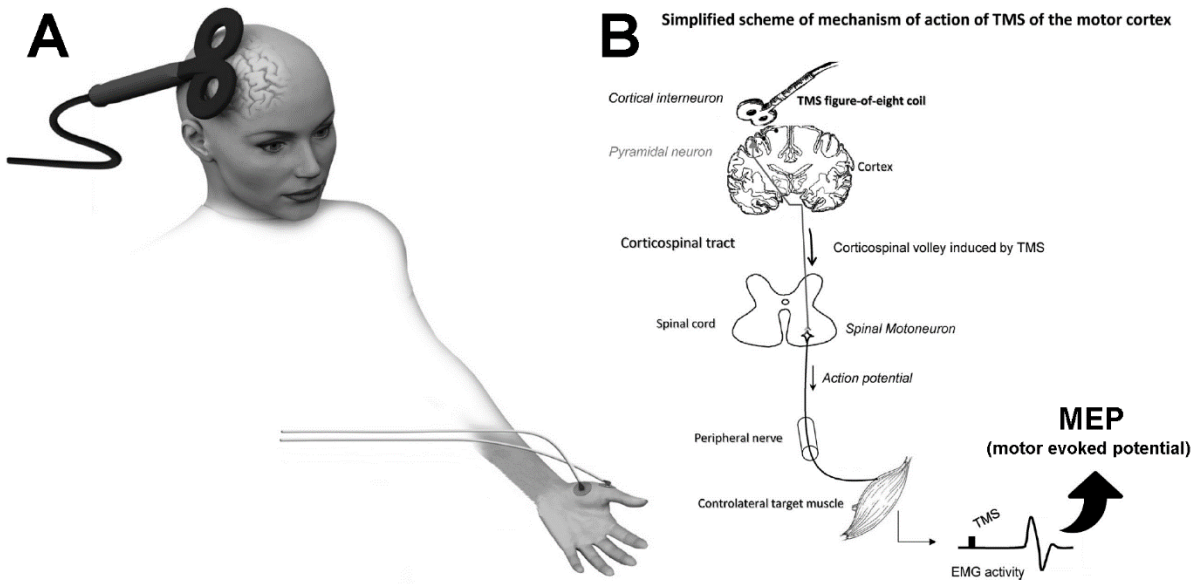

Figure 12. Transcranial magnetic stimulation (TMS) technique. **A**, coil positioning over motor cortex and EMG electrodes on contralateral target muscle. Modified from Kamke *et al.* (2016). **B**, simplified schematic representation of mechanism of action of TMS over motor cortex. Modified from Klomjai *et al.* (2015).

1.4. 3 Click sound for stimulation of the reticular formation

Recently, a study conducted in monkeys showed long-latency responses (7-25 ms) of reticular formation cells to TMS, which were most likely caused by the TMS sound. Such conclusion was evident since the reticular formation cells responded even when the TMS coil was lifted off the head and the TMS sound reproduced via a bone vibrator produced similar responses (Fisher *et al.*, 2012a). This study provided an important contribution since it showed a non-invasive method to activate the reticular formation and consequently the reticulospinal tract: click sounds.

Such discovery was used in a human study aiming at producing plastic changes in reticulospinal pathways. Foysal and colleagues (2016) paired two stimuli known to activate reticulospinal pathways, auditory click stimuli and electrical stimulation around motor threshold over the biceps muscle, at appropriate intervals to induce spike timing-dependent plasticity (STDP) in the brainstem – both long-term potentiation (LTP) and depression (LTD). After receiving paired stimulation for around 7 hours subjects showed modulation of the amplitude of the biceps long-latency stretch reflex according to the timing of stimulation. The biceps long-latency stretch reflex may be partly mediated by the reticulospinal tract (Foysal *et al.*, 2016).

Plastic induced changes in the reticulospinal tract can be important to recover limb function after stroke, when the corticospinal tract is lesioned (Baker *et al.*, 2015).

1.4. 4 Spectral and coherence analysis

Fourier transforms can be used to quantify the amplitude of a signal in the frequency domain (spectral analysis). Such approach has been widely used in motor control studies and is particularly important in measuring oscillations on different nervous system structures influencing motor output (e.g., Ramos-Murguialday and Birbaumer, 2015). Oscillations in different frequency bands are observed during various motor tasks, such as isometric contractions and eye movements (Grosse *et al.*, 2002). Specifically, oscillations in the 8-12 Hz frequency band are seen generating physiological tremor in humans. These are believed to be centrally generated and although the exact neural structure of origin is unknown the M1 area and the spinal cord are thought to be good candidates (Elble and Koller, 1990; Williams *et al.*, 2010). These oscillations will be explored in more detail in chapter 6.

Spectral analysis can be used further to quantify coupling between oscillations from two structures (e.g., brain and muscle, brain and spinal cord, muscle and muscle, etc). Coherence is the most common analysis serving this purpose, which shows the amplitude of the correlation between two signals in the frequency domain. Important insight into the motor system functioning has been gathered from coherence analysis studies, showing for example the differentiation between pathways converging onto motorneurons (corticomuscular coherence, Boonstra, 2013) and muscle groups sharing common input (intermuscular coherence, Nazarpour *et al.*, 2012). Intermuscular coherence will be explored in more detail in chapter 5.

1.5 What goes wrong with spinal circuitry in disease

Diseases which affect the nervous system can modify the function of spinal cord circuits and cause great impact on motor output. The ones relevant to this thesis and their effect on spinal circuitry are described below, namely spinal cord injury, stroke,

and pathological tremor. Spinal cord injury is investigated in chapters 3 and 5, stroke is investigated in chapter 3 and tremor is explored in chapter 6.

1.5. 1 Spinal cord injury

Figure 13 shows a schematic representation of the main typical consequences of a spinal cord injury on spinal cord functioning. Descending input from the brain and brainstem remains intact above the lesion. At the lesion epicentre neuron death as well as disruption and demyelination of axons occurs, reducing or abolishing descending control depending on the fraction of motor units damaged by the lesion. Segments below the lesion commonly receive no descending input, which means muscles innervated at these segments will be paralyzed only showing activity such as spasms and spontaneous motor unit activity. Ascending input is usually intact below the lesion and reduced or abolished at the lesion epicentre and above the lesion, which may decrease force production (Thomas *et al.*, 2014a). Imbalanced damage between the two sides of the body is present if the spinal cord lesion is asymmetrical. Several functional consequences of these changes will take place, including changes in motor unit recruitment, changes in motor axon properties and the reorganization of input to motorneurons (Thomas *et al.*, 2014a). Hyperreflexia and spasticity are also seen at times in chronic spinal cord injury (Calancie *et al.*, 1993).

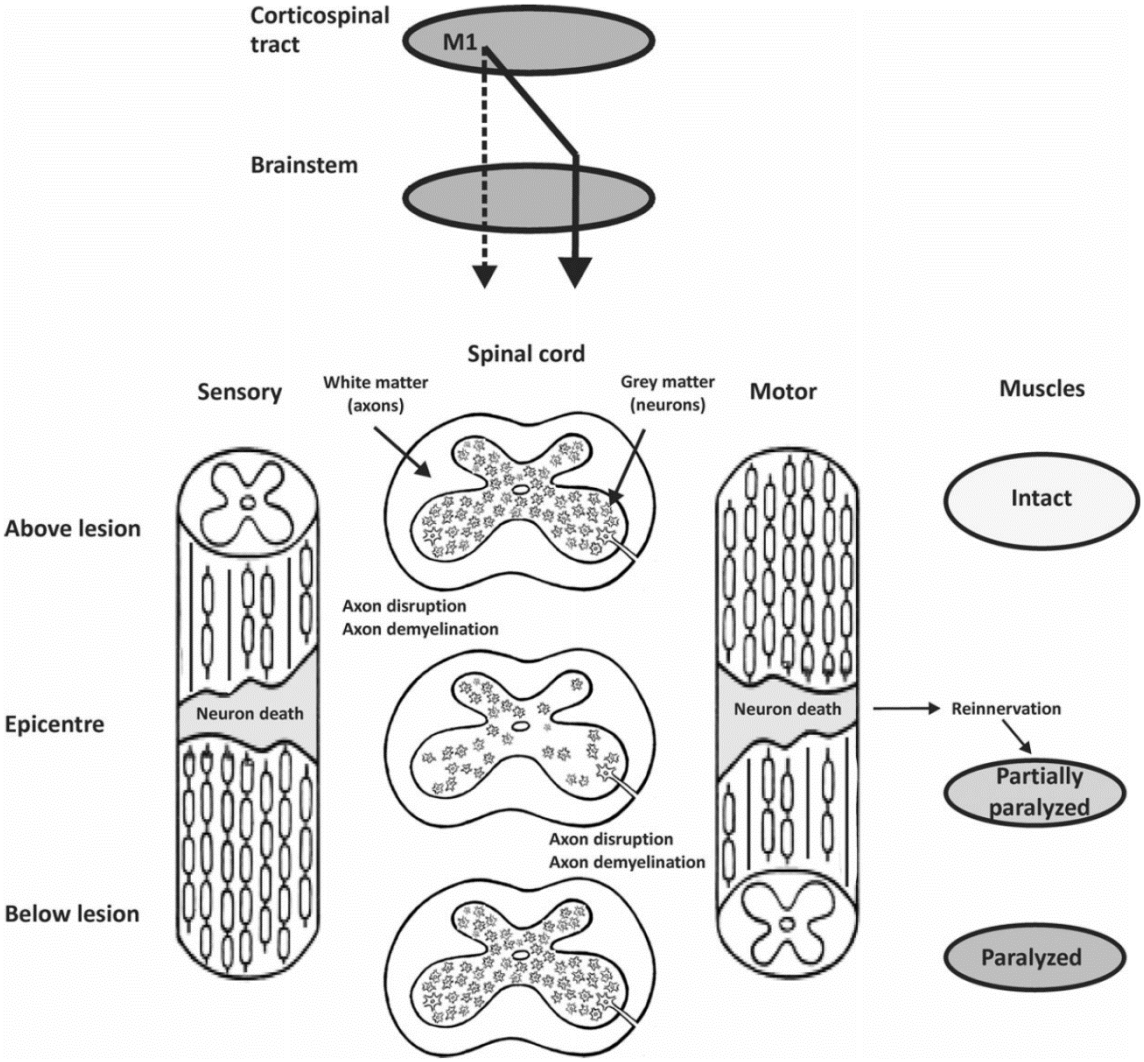

Figure 13. Schematic representation of the typical consequences of a spinal cord injury on spinal cord functioning. From Thomas *et al.* (2014a).

1.5. 2 Stroke

In stroke the death of brain cells, caused by either an obstruction of a blood vessel (ischemic stroke) or intracranial bleedings (haemorrhagic stroke) (Grefkes and Ward, 2014), results in impaired descending inputs to the spinal cord. Since the corticospinal tract functioning is affected, and most of its fibres decussate, the control of muscles in the contralateral side of the lesion is affected (Kloter *et al.*, 2011). Similar to spinal cord injury, stroke is also often associated with hyperreflexia and spasticity (Li and Francisco, 2015). This means reflexes such as the H-reflex might be easier to elicit in these two populations. Spasticity, characterized by an increase in muscle tone, is thought to be a consequence of hyperexcitable spinal reflexes and is

predominantly seen in flexor muscles in stroke survivors (Li and Francisco, 2015). One of the main consequences of a stroke on spinal circuitry is the loss of descending control by the corticospinal tract, however, recent work has shown that plasticity protocols targeting strengthening of alternative routes such as the reticulospinal tract can play an important role in the recovery of descending control and consequently motor function (Baker, 2011; Baker *et al.*, 2015).

1.5. 3 Tremor

One of the most common forms of pathological tremor is essential tremor, a postural tremor exacerbated during voluntary movement (Elble and Koller, 1990). It affects mainly upper limbs but can also occur in lower limbs, trunk, head, face and voice in more uncommon cases. One important aspect of the diagnosis is that essential tremor cannot be accompanied by any neurological disorder (Elble, 2013). Its frequency ranges from 4 to 12 Hz, which overlaps with the frequency of physiological tremor. The origin is unknown and oscillations in several structures such as the cerebellum and thalamus are believed to play a role (Elble, 2013). The most common recommended treatment is pharmacological, with the use of propranolol (Fasano and Deuschl, 2015).

Tremor is one of the main symptoms of Parkinson's disease, present in almost all patients. The frequency of Parkinsonian tremor ranges from 3 to 5 Hz, regardless of the body part, which is why it is believed to be centrally generated, although the mechanisms are still under debate (McAuley and Marsden, 2000). This form of tremor only occurs at rest and the ability of movement to stop tremor decreases as the disease progresses. The most common treatment for this type of tremor is pharmacological (Elble and Koller, 1990).

Cerebellar tremor is another type of pathological tremor, caused by lesions in the cerebellum. It includes static tremor as well as tremor during movement, which gets exacerbated once the individual's movement approaches its final target. The frequency of cerebellar tremor is very irregular for both static and kinetic tremor, ranging from 2 to 8 Hz, depending on the body limb. Pharmacological treatment can be very ineffective and surgical intervention can be used depending on the case (Elble and Koller, 1990).

Other less common forms of pathological tremor include tremor resulting from lesions in midbrain, from peripheral neuropathies, task-specific tremors and posttraumatic tremor (Elble and Koller, 1990).

On the other hand, physiological tremor, which is the one present in healthy individuals, is believed to be driven by three principal components: mechanical oscillations at the limb resonant frequency, oscillations around reflex feedback loops and centrally generated rhythmic motor output (Elble and Koller, 1990).

When mechanically perturbed, a limb will present damped oscillations at its resonant frequency. This frequency depends on the physical characteristics of the limb. The mechanical component of physiological tremor is a function of elastic and inertial properties of the limb. Specifically, mechanical oscillations are directly proportional to the square root of the combined stiffness of the limb and inversely proportional to the square root of the combined inertia (Elble and Koller, 1990). For this reason, the frequency of such mechanical oscillations is different for different limb segments. Accordingly, this frequency is decreased with the addition of inertial loads to the limb and increased with the addition of spring loads (Elble and Koller, 1990).

The stretch reflex also seems to participate in physiological tremor (Hagbarth and Young, 1979). The high sensitivity of muscle spindles to detect small changes in muscle length suggests the stretch reflex oscillates with tremor. Although some controversy exists regarding this matter, the majority of authors seem to agree that the stretch reflex assists tremor that is actually generated somewhere else in the nervous system (Elble and Koller, 1990). Just as for mechanical oscillations, the frequency of this tremor component changes according to the limb, since the length of the arc-reflex loop is different for different limb segments.

The 8-12 Hz component of physiological tremor is believed to be centrally generated, since its frequency is unaltered by the addition of loads to the limb (Elble and Koller, 1990). The origin is unknown but many structures are believed to be good candidates because they present oscillations at this frequency. These include the thalamus, cerebellum, primary motor cortex (M1) and spinal cord (Elble and Koller, 1990; Williams *et al.*, 2010).

Williams and colleagues (2010) demonstrated that in normal conditions (i.e., not in pathology) the spinal cord produces oscillations at tremor frequency (~10 Hz) and these are phase opposite to tremor oscillations in M1. The result from this is phase cancellation at the motorneuron level, which is the reason why physiological tremor

has small amplitude. Spinal systems identified to act contributing to this phase cancellation include Renshaw cells (Williams and Baker, 2009) and intermediate zone interneurons (Williams *et al.*, 2010), but not pre-synaptic inhibition (Galan and Baker, 2015). One of the reasons why pathological tremor has higher amplitude could be therefore that this phase cancellation is not as efficient as in physiological tremor. Kozelj and Baker (2014) showed that the reason why spinal cord interneurons cancel tremor is that they respond to oscillatory sensory input with the opposite phase to neurons in the brain. In chapter 6 a plasticity protocol is developed in which peripheral nerve stimulation is used to change spinal circuits strengthening their connections to optimize the phase cancelling between spinal cord and the brain with the final goal of ameliorating pathological tremor.

1.6 Overview of this thesis

This thesis focuses on the assessment of different human spinal circuits through techniques such as peripheral nerve stimulation, TMS and intermuscular coherence with the aim of understanding their function in health and disease.

Five results chapters are described subsequently which investigate different spinal circuits. In chapter 2 experiments with the H-reflex describe a spinal circuit with convergent input from wrist flexor afferents and extensor Ib afferents to the wrist flexor. Chapter 3 investigates the same circuit when affected by central nervous system lesions. In chapter 4 possible descending inputs to this circuit, from corticospinal and reticulospinal tracts, are explored. Chapter 5 analyses spasms in spinal cord injury patients, and demonstrates that the spinal cord is capable of producing low frequency intermuscular coherence. Finally, in chapter 6 the ability of peripheral nerve stimulation to cause plastic changes enhancing spinal circuits to reduce tremor is investigated.

Chapter 2.
Convergent Spinal Circuits Facilitating Human Wrist Flexors

2.1 Abstract

Non-invasive assessment of spinal circuitry in humans is limited, especially for Ib pathways in the upper limb. We developed a protocol in which we evoke the H-reflex in flexor carpi radialis (FCR) by median nerve stimulation and condition it with electrical stimulation above motor threshold over the extensor carpi radialis (ECR) muscle belly. Eighteen healthy adults (eight male, ten female) took part in the study. There was a clear reflex facilitation at 30 ms inter-stimulus interval (ISI), and suppression at 70 ms ISI, which was highly consistent across subjects. We investigated two hypotheses of the possible source of the facilitation: (i) ECR Ib afferents from Golgi tendon organs, activated by the twitch following ECR stimulation, and (ii) FCR afferents, from spindles and/or Golgi tendon organs, activated by the wrist extension movement that follows ECR stimulation. Several human and monkey experiments indicated a role for both of these sets of afferents. Our results provide evidence for a spinal circuit in which flexor motoneurons receive convergent excitatory input from flexor afferents as well as from extensor Ib afferents; this circuit can be straightforwardly assessed non-invasively in humans.

2.2 Introduction

Assessing spinal circuitry non-invasively in humans is crucial for understanding both healthy function and pathology. For example, Delwaide (2001) suggests that the cause of rigidity in Parkinson's disease is a dysfunction in Ib pathways; a test to assess the function of these circuits would therefore have clinical interest. Unfortunately methods for non-invasive assessments in humans are limited. The measurement of reciprocal inhibition, for instance, is often considered a very challenging protocol since it requires the stimulation of both median and radial nerves simultaneously and recording of changes in the H-reflex according to the interval

between stimuli (Day *et al.*, 1984). Nevertheless, great progress in this field has been achieved with a number of existing and well established techniques to assess different circuits such as cutaneomuscular reflexes (Jenner and Stephens, 1982), recurrent inhibition due to Renshaw cells (Bussel and Pierrot-Deseilligny, 1977) and presynaptic inhibition (Berardelli *et al.*, 1987), amongst others (see Pierrot-Deseilligny and Burke, 2012 for review).

Assessing Ib pathways in human upper limb has been proven to be particularly challenging. Burne and Lippold (1996) used electrical stimulation percutaneously over tendons of different muscles to assess 'autogenic' (non-reciprocal) inhibition of ongoing muscle activity, claimed to be caused by a polysynaptic pathway originated from Ib afferents from Golgi tendon organs. Priori and colleagues (1998) criticized, however, not only the long-latency of this inhibition, which was not compatible with a Ib pathway, but also the location of stimulation over tendons since Golgi tendon organs are actually located in the musculo-tendinous junction (Jami, 1992). Ultimately, this inhibition is more likely generated by slowly-conducting group III tendon afferents producing presynaptic inhibition of Ia fibres (Priori *et al.*, 1998). Another potential test to assess Ib pathways was described by Cavallari and colleagues (1985), who demonstrated a facilitation of the flexor carpi radialis (FCR) H-reflex by a prior radial nerve stimulus at an interval of 2 ms. They suggested that this was mediated by Ib pathways and enhanced by cutaneous stimulation. However, as noted by the authors themselves, in most cases this Ib facilitation was less clear, manifesting only as an inflection superimposed on the decay of the shorter-latency inhibition. The lack of consistency makes this protocol not ideal for assessing the function of Ib pathways in humans.

In this study, we used median nerve stimulation to evoke an H-reflex in the FCR muscle, and conditioned this by previous electrical stimulation above motor threshold to the extensor carpi radialis (ECR) muscle belly. With a 30 ms inter-stimulus interval (ISI), we found a clear facilitation. Two hypotheses were investigated as the source of this effect: (i) ECR Ib afferents from Golgi tendon organs, activated since the high intensity ECR stimulation causes a twitch, pulling on the ECR tendon, and (ii) FCR afferents, from muscle spindles and/or Golgi tendon organs, activated by the wrist extension movement that follows from the ECR contraction. Results from a series of experiments in both human subjects and monkey supported the participation of both ECR Ib afferents and FCR afferents in the effect. Our work reveals novel convergent spinal circuits not yet described in the literature, with flexor motoneurons receiving

convergent input from FCR afferents and ECR Ib afferents, which can be easily assessed non-invasively in humans.

2.3 Methods

- *Experiments in healthy human subjects*

Eighteen healthy human volunteers, 18 to 56 years of age, participated in this study (eight male and ten female). All subjects signed a written consent form prior to participation and all procedures were approved by the Ethical Committee of the Medical Faculty, Newcastle University. Subjects were seated comfortably on a chair with their forearm resting on a table. To measure and evoke the H-reflex, electromyography (EMG) recording electrodes (Kendall H59P, Medcat) were placed on skin overlying the FCR muscle belly, with a reference over the brachioradialis, and connected to a Digitimer NL 824 amplifier (gain 2000, bandpass 30 Hz-2 kHz). A stimulating electrode (bipolar felt pad, P20-4zl, Medcat) was placed over the median nerve just above the elbow (cathode proximal), and connected to an isolated constant current stimulator (Digitimer DS7A except for vibration and threshold protocols, when Digitimer DS5 was used). Electrode placement was according to Jabre (1981). The response was identified as an H-reflex if it had a latency between 12 and 21 ms, an amplitude which increased during voluntary contraction, and the amplitude fluctuated with changes in stimulus intensity together with the M-wave amplitude (all as described in Jabre (1981)). The recordings were made with the amplitude of the H-reflex around 50% of the maximum observed for each subject. The reason for choosing 50% of maximum H-reflex amplitude was the fact that we were interested in exploring effects which could include both facilitation and suppression of the response size, therefore 50% would provide enough space for both effects to be detected. It is important to note, however, that especially for small amplitude responses the control of such amplitude could not be perfect, often making responses smaller than 50% maximum the most commonly recorded. In addition, the possibility of non-linear change in response size at this level needs to be acknowledged. We refer to these responses for simplicity as the ‘FCR H reflex’, but note here that with surface recording electrodes there may be some contribution from other nearby muscles. Background EMG activity was small or negligible since the muscle was at rest. The stimulating electrodes on the median nerve were kept fixed

by a strap wrapped around the subject's arm (monophasic pulse, intensities up to 10 mA, 500 µs pulse width). Stimulating electrodes were also placed on the ECR muscle belly for the conditioning stimuli, with the cathode proximal, stimulating at an intensity 3 x motor threshold (MT) (monophasic pulse, intensities up to 24 mA, 1 ms pulse width). This intensity was chosen as it was strong enough to generate clear effects, but not uncomfortable for the subjects. An assessment of the effect of changing the intensity is reported in Results. MT was defined as the intensity which produced the first visible twitch of the ECR muscle. We did not record EMG signals from the ECR muscle since it was not within the scope of our investigation to explore possible effects of any components of our stimulation protocol on activity from this extensor muscle. A schematic representation of electrode positioning is shown in Figure 14A.

During all protocols, subjects were instructed to remain relaxed, with no contraction of forearm muscles, and to maintain their arm in a constant position. The lack of activity in the FCR recording was constantly monitored by the experimenter. Subjects were randomly selected to take part in the different experimental protocols described subsequently.

Main protocol. The H-reflex was conditioned by previous stimulation of ECR at 18 ISIs: 1.5, 2, 2.5, 3, 3.5, 4, 5, 10, 15, 20, 30, 40, 50, 60, 70, 100, 200 and 1000 ms. The ISIs used were chosen based on previous investigations exploring both reciprocal and presynaptic inhibition in the human upper limb (Day *et al.*, 1984; Berardelli *et al.*, 1987) and adjusted to account for the difference in the timing of effects from stimulation delivered to the radial nerve in the referenced studies compared to stimulation to the ECR muscle used here. Each combination of test and conditioning stimuli were separated by an interval of 4 s and the amplitude of the H-reflex was expressed as a percentage of the control H-reflex (with no conditioning ECR stimulation). Ten repetitions of each ISI and twenty repetitions for the control H-reflex were completed, delivered in pseudo-random order. Reflex amplitude was measured and expressed as a percentage of the control values for each subject. A two-way ANOVA with factors subjects and ISI was performed to investigate whether conditioning ECR stimulation had any effect on H-reflex measurements. If the ANOVA showed a significant effect of interval, we tested which ISIs showed significant differences from 100% across subjects using t-tests, with a significance level of $p<0.05$. A similar approach was used to assess reflex changes in all experiments listed below. For the ISIs of 30 and 70 ms we also conducted a separate analysis for each subject using t-tests on the single sweep reflex amplitudes, in order

to determine how many subjects showed significant facilitation (30 ms ISI) and/or inhibition (70 ms ISI); the significance level was set as $p<0.05$. Data from 17 subjects were gathered for this protocol.

Threshold Intensity. In six subjects, we tested 11 intensities of ECR stimulation (1, 1.2, 1.4, 1.6, 1.8, 2, 2.2, 2.4, 2.6, 2.8 and 3 x MT) only for the ISI of 30 ms.

Threshold Changes after Vibration. In five subjects, we tested the H-reflex conditioned with an ISI of 30 ms at five intensities of ECR stimulation (1.5, 1.8, 2.1, 2.4 and 2.7 x MT) before and after vibration of 25 minutes over the ECR tendon (166 Hz). Subjects were instructed to remain relaxed during the vibration, and no overt contractions of ECR were observed.

ECR Twitch Time. In nine subjects, stimuli were delivered to the ECR muscle at 3 x MT while subjects had their forearm held in a horizontal position (wrist 90 degrees from horizontal plane) and grasped a metal bar attached to a strain gauge which detected force in the direction of flexion-extension. For each subject we recorded 64 to 122 repetitions of the stimulus, and averaged the post-stimulus force profile. The time of the first peak in force production after the ECR stimulation was measured and referred to as the twitch time.

ECR Tendon Taps. In nine subjects, we replaced the conditioning stimulus by a mechanical tap applied directly to the ECR tendon instead of electrical stimulation, with the same 18 ISIs used previously. The tap apparatus (LDS V201 shaker with PA25E power amplifier, Brüel and Kjaer) was positioned above the ECR tendon approximately 3 4 cm more proximal than the wrist, with the tapper applying light pressure on the skin. The tap intensity was at tap threshold (TT), defined as the lowest tap amplitude which produced a visible response in the ECR muscle EMG.

FCR Tendon Taps. This protocol was identical to that described above, except that the mechanical tap was applied to the tendon of the FCR muscle (approximately 3 4 cm more proximal than the wrist). Data from five subjects were gathered for this protocol.

Cutaneous Stimulation. In five subjects, we tested the impact of cutaneous stimuli on the H reflex facilitation. Cutaneous stimulation (200 μs pulse width, intensity 2 x perceptual threshold, Digitimer DS7A stimulator) was given through surface electrodes on the dorsal side of digits 2 and 3 (Cavallari *et al.*, 1985). The H-reflex elicited by the median nerve stimulus was tested with three conditioning conditions: (i) H-reflex + ECR stimulation (30 ms ISI), (ii) H-reflex + cutaneous stimulation (25 ms ISI), and (iii) H-reflex + ECR stimulation + cutaneous stimulation

(both timed relative to median nerve as above). Forty repetitions of each condition and of the control H-reflex were typically measured.

Wrist Flexed. In eight subjects, the main protocol described above was repeated while subjects had their wrist held in a flexed position by a Velcro strap. The degree of wrist flexion adopted was the maximum possible in that subject. In this position, the wrist flexors should have been slack, reducing or eliminating activation of flexor muscle afferents following the ECR twitch. Wrist flexion was achieved passively by the strap, with no active flexion by the subject as judged by the absence of background EMG in the FCR recording.

Passive Movement. In six subjects, the conditioning stimulus was replaced by a passive extension movement around the wrist joint, generated by a torque motor. The extension movement was notably larger than that typically generated by ECR electrical stimulation in the main protocol. The maximum amplitude of the passive movement for the subjects tested was 14.2 ± 1.5 degrees, the time to reach maximum movement amplitude was 110.7 ± 6.5 ms. After the point of maximum extension, the wrist joint returned to its neutral position; the total movement duration was 190.5 ± 13.1 ms (mean ± SD). Note that according to the duration of the main facilitatory effects observed in this study (see Results section) only the first few degrees of movement are likely to be relevant.

Most subjects volunteered for several protocols on the same day, although some subjects returned on multiple days; the numbers of subjects tested in each protocol are listed above. Electrodes were placed consistently within the same subject across days, but any minor differences would not affect results as pairwise comparisons were not made between different protocols.

- *Monkey experiments*

All animal procedures were performed under United Kingdom Home Office regulations in accordance with the Animals Scientific Procedures Act (1986) and were approved by the Animal Welfare and Research Ethics Board of Newcastle University. Recordings were made from four terminally anesthetized female rhesus macaque monkeys (coded PLK, PAT, PDR and TNS in this study; age 9.5, 9.6, 9.8 and 7.1 years, and weight 10.4, 9.5, 9.3 and 6.4 kg, respectively).

Initial surgical preparation. Animals were initially sedated by intramuscular injection of ketamine (10 mg · kg^{-1}); then deep anesthesia was induced with propofol (5–10 mg · kg^{-1}, i.v.). Anaesthesia was then switched to sevoflurane inhalation (1.5-

3%) and an intravenous infusion of alfentanil (11-18 μg · kg^{-1} · h^{-1}) with artificial ventilation. Central arterial and venous lines were inserted via the external carotid artery and external jugular vein, and a tracheotomy made to secure the airway. The bladder was catheterized. Anaesthetic monitoring included central arterial and venous pressure, heart rate, blood oxygen saturation, end-tidal carbon dioxide, and core and peripheral temperature. The animal was kept warm with a thermostatically controlled heating blanket, and a system which surrounded the animal with warmed air (Bair Hugger, 3M). Fluids were provided via a continual intravenous infusion (total rate with drug infusions 5-10 ml · kg^{-1} · h^{-1}).

Stimulation. During the experiments the anaesthetic regimen was switched to intravenous infusions of midazolam (270-460 μg · kg^{-1} · h^{-1}), alfentanil (13-26 μg · kg^{-1} · h^{-1}), and ketamine (5.8-9.0 mg · kg^{-1} · h^{-1}); this regimen was chosen to increase the excitability of the nervous system (Witham *et al.*, 2016). The H-reflex was often difficult to obtain in these animals due to the effects of anaesthesia; we therefore used responses to pyramidal tract (PT) stimulation as a way of assessing the excitability of motoneurons in FCR. Although in an awake monkey the FCR H-reflex can be measured, under anaesthesia, which was a condition necessary for invasive procedures used such as cutting the tendon of a muscle, the general excitability of neurons is decreased which made responses difficult or impossible to obtain even at large median nerve stimulating intensities. The PT stimulation was possible through the use of trains of 2 to 4 stimuli, depending on the animal tested. Another difficulty of the H-reflex measurements in the monkey was the fact that although it is possible to obtain a response in these animals in the normal awake state due to their smaller size and consequently shorter delays sometimes the H reflex and M wave was difficult to distinguish. Fine tungsten stimulating electrodes (LF501G, Microprobes Inc, Gaithersburg, MD, USA) were implanted into the PT on the side contralateral to the arm being tested. PT electrodes were positioned with reference to antidromic volleys recorded epidurally from motor cortex after stimulation through them (Riddle and Baker, 2010). Trains of two to four stimuli through the PT electrode, given 3 ms apart, were necessary to evoke an FCR response (2, 4, 3 and 4 trains of stimuli for monkeys PLK, PAT, PDR and TNS, respectively; biphasic pulse, intensities up to 4 mA, 200 μs pulse width; A-M Systems, Isolated Pulse Stimulator Model 2100). For PT responses, unlike the H-reflex, homosynaptic depression is not a concern. The interval between each pair of test and conditioning stimuli was therefore reduced to 500 ms, instead of the 4 s used for human protocols, to accelerate data acquisition in

these time-limited terminal experiments. The amplitude of the PT response was measured as the area under the curve of the rectified EMG signal from FCR. For the conditioning stimulus to ECR we used fine wire electrodes made of 7-stranded stainless steel wires insulated with Teflon and bared for a few millimeters at the tip (part number FE6320, Advent Research Materials, Oxford, UK); these were introduced by a needle which was then withdrawn. In monkeys PLK, PAT and PDR the muscle was exposed and dissected first. Biphasic stimuli were given through these wires (intensity up to 6 mA, 1 ms pulse width for each phase; second A-M Systems stimulator as above). The forearm was fixed through screws attached to the bones (ulna and radius), near the elbow and wrist, for monkeys PLK, PAT and PDR. Wire electrodes were also inserted in FCR for EMG recording (amplifier Digitimer NL824, gain 500 to 1000, bandpass 30 Hz-2 kHz). A schematic representation of electrode positioning is shown in Figure 18A.

Main protocol. A similar protocol to the man protocol described above for human subjects was delivered to the four monkeys, with PT stimulation used as the test stimulus and ECR stimulation at 3 x MT as the conditioning stimulus. The amplitude of the PT response was expressed as a percentage of the control PT response (with no conditioning ECR stimulation) for all monkey experiments. The same 18 ISIs as in the human studies were used except for the two largest, which were reduced to 150 and 200 ms. In the monkey recordings, ISIs refer to the delay from the conditioned stimulus to the last (effective) stimulus in the train delivered to the PT. A minimum of 20 repetitions of each ISI and 40 repetitions of the control PT response were completed.

ECR Tendon Cut. We tested the main protocol in monkeys PLK, PAT and PDR after cutting the ECR tendon near the wrist. The cut end of the tendon was left free.

FCR Tendon Cut and Re-attached. We tested the main protocol in monkey TNS after cutting the FCR tendon near the wrist. Subsequently, we re-attached it using a suture around the tendon sewn to the skin of the hand, maintaining similar tendon tension to that with the tendon intact.

ECR Tendon Pulls at Large Amplitude. In monkey PDR, after the ECR tendon was cut, we used surgical suture around the lose tendon to attach it to a mechanical puller (305C-I, Aurora Scientific Inc.), maintaining a similar resting muscle tension as before the tendon was cut. Brief mechanical pulls (2mm amplitude, 1 ms duration) were used as conditioning stimuli preceding PT stimulation. The same 18 ISIs as in

the main protocol were used, except that in this case the intervals were defined relative to the first stimulus in the train to the PT.

ECR Tendon Pulls at Variable Amplitude. This was similar to the preceding protocol, except that tendon pulls of different intensities were used (20, 40, 60, 80, 100, 120, 140, 160, 180, 200, 250, 300, 350, 400, 450, 500, 750, 1000, 1500 and 2000 µm; all 1 ms duration). A single ISI of 2.5 ms was used, which had produced a clear facilitation with a 2 mm pull amplitude.

All data analysis was carried out using custom scripts written in the MATLAB environment (version R2015a).

2.4 Results

- *Experiments in Healthy Human Subjects*

Figure 14B shows an example from one subject of the control and conditioned H-reflex with the ISIs 30 and 70 ms, which produced evident facilitation and suppression, respectively. The facilitation at 30 ms ISI was significant in 13 out of 17 participants and the suppression at 70 ms ISI was significant for all 17 volunteers ($p < 0.05$). Figure 14C depicts the H reflex amplitude curve for the 18 conditioning ISIs from the same subject. It shows the typical pattern of facilitation followed by suppression which was a consistent finding. Of the four subjects without significant facilitation at 30 ms ISI, three showed reflex amplitudes close to control; one had a reflex 145% of control, but with high variability (SEM 25.7%) that prevented it from reaching significance. Facilitation was not seen at any other intervals for these four subjects.

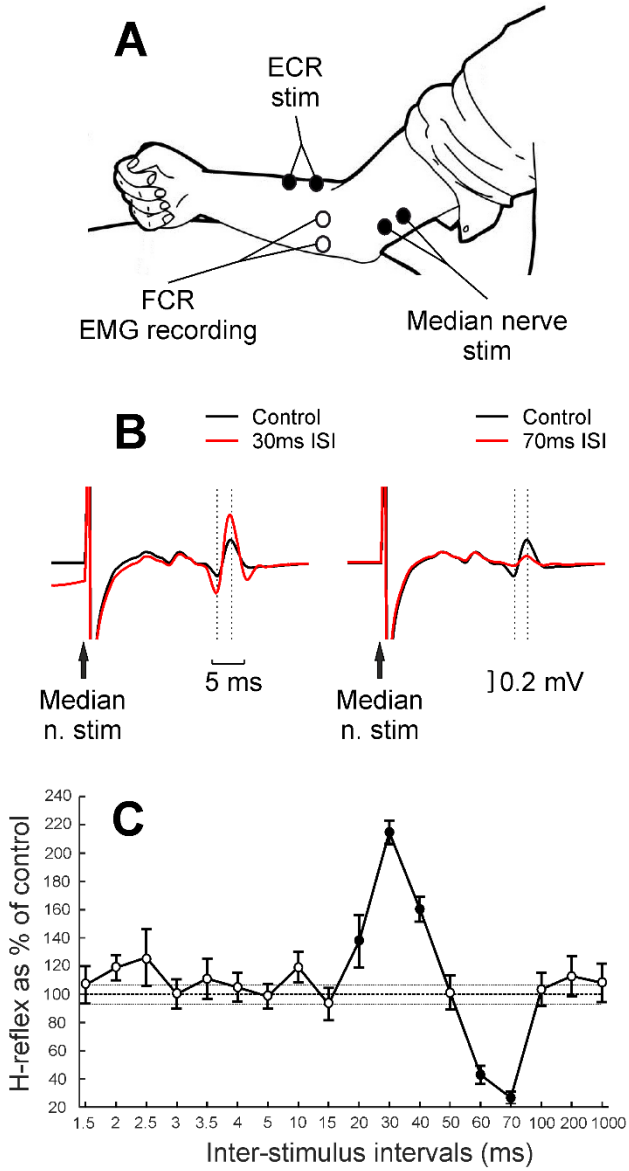

Figure 14. Experimental setup and example of main result in a healthy human subject. **A**, schematic representation of experimental setup. EMG recording electrodes were positioned over FCR muscle belly and stimulating electrodes over the median nerve (to evoke FCR H-reflex) and over the ECR muscle belly. **B**, example from one subject of the comparison between control (black) and conditioned (red) H-reflex at both 30 and 70 ms ISIs between median nerve and conditioning ECR electrical stimulation at 3 x MT; traces are the average of 20 repetitions for control and 10 repetitions for conditioned H-reflex. Dashed lines indicate the times used to measure H-reflex amplitude. **C**, example from the same subject of conditioning curve showing the H-reflex amplitude as percentage of its control amplitude for 18 ISIs between median nerve and conditioning ECR electrical stimulation at 3 x MT. Filled circles represent responses significantly different from control. Error bars represent standard error. Thin dashed horizontal lines indicate standard error of control H-reflex amplitude.

Figure 15 shows the average results across subjects from the main protocol. There was a significant effect of ISI (ANOVA, $F_{(17, 261)} = 22.08$, $p < 0.001$). Significant inhibition was found at ISIs 1.5, 3- 5 ms (t test, all $p < 0.05$), significant facilitation at 30 ms ISI ($p = 0.0001$) and significant inhibition at ISIs 50-1000 ms (t test, all $p <$

0.020). Subsequently, we conducted a number of different experimental protocols to investigate the origin of the facilitation observed at the interval of 30 ms.

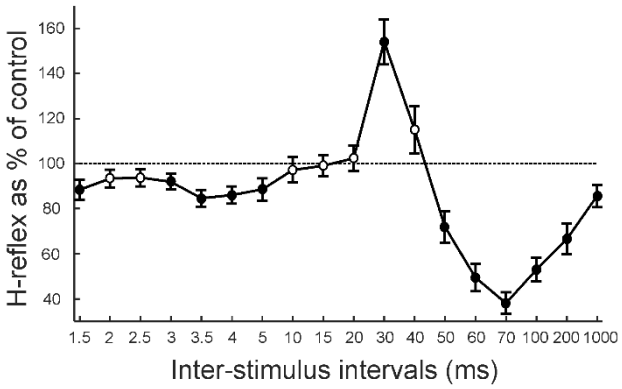

Figure 15. Population averaged data in healthy humans. Average from 17 subjects of H-reflex amplitude, shown as percentage of its control amplitude, for 18 ISIs between median nerve and conditioning ECR electrical stimulation at 3 x MT. Filled circles represent responses significantly different from control. Error bars represent standard error. For one subject data from ISIs up to 5 ms, and for another up to 3 ms, were omitted from the average due to contamination by the stimulus artefact.

One hypothesis for the generation of this facilitation is that the stimulus-evoked twitch in ECR pulls on the extensor tendon, activating Golgi tendon organs which mediate the effect. We first explored the ECR stimulus intensity required to generate the facilitation; results averaged across subjects are shown in Fig. 16A. There was a significant effect of ECR intensity (ANOVA, $F_{(10, 50)} = 7.48$, $p < 0.001$). A significant facilitation at 30 ms ISI was present with ECR conditioning stimuli of 1.8 x MT (t test, $p = 0.0263$) and higher. By definition, 1x MT produces a just-noticeable muscle twitch, although such stimuli are clearly above perceptual threshold. The lack of H reflex facilitation at weaker intensities is thus consistent with generation by ECR Ib afferents.

Another possibility for the origin of the facilitation is Ia afferents from ECR, which could be directly activated by the stimulus to the motor point (Muir and Lemon, 1983). To investigate this we repeated the measurement of the threshold intensity for ECR stimulation to generate the facilitation, after a sustained period of vibrating the ECR tendon (25 minutes, 166 Hz). Such vibration has been proven to increase the threshold for electrical activation of Ia afferents, bringing it to a level higher than the threshold for Ib activation, which does not change (Coppin *et al.*, 1970; Fetz *et al.*, 1979; Katz *et al.*, 1991). If Ia afferents were in fact the source of the facilitation, then

at any stimulus intensity a greater proportion of fibers would be below threshold after sustained vibration. This would lead to a rightwards shift of the curve relating facilitation to stimulus intensity. Figure 16B depicts the results of this experiment. The slight differences in the relationship with intensity between these data and Fig. 16A are likely to reflect inter-individual differences in activation at different percentages of MT; only two subjects participated in both experiments. Sustained vibration had no significant effect on the facilitation (three way ANOVA with factors subjects, intensity and before/after vibration; vibration, $F_{(1, 490)} = 3.37$, $p > 0.05$).

It remains possible that vibration did exert an effect, but that this was too small to be detected within the statistical power of our measurements. To check for this, we measured the standard deviation of the H reflex for each subject at each conditioned intensity, and also fitted a sigmoid curve to the results before vibration shown in Fig. 16B. We then generate simulated data, where H reflex amplitudes before vibration were modelled as Gaussian random numbers, with a mean which followed the sigmoid curve, and a standard deviation as determined from each subject's original data. Data after vibration were similarly generated, except that the sigmoid curve was shifted to the right by a value ΔI. As in the actual data, points were generated for n=5 subjects. We tested for significant differences between these simulated curves, using a three way ANOVA exactly as applied for the experimental data. The process was repeated 1000 times at each ΔI, for ΔI from 0 to 0.5xMT in steps of 0.01xMT. A significant difference between the curves was detected >90% of the time at $p < 0.05$ for shifts of ΔI>0.33xMT. Katz et al. (1991) showed a recruitment curve rightwards shift of around 0.3xMT following sustained vibration, which we estimate would have been detected from our data 83% of the time. We therefore conclude that electrical activation of ECR Ia afferents is unlikely to play a major role in the facilitation of the FCR H reflex which we describe.

If the stimulus delivered to ECR generates the H reflex facilitation via the mechanical consequences of the shock, the muscle would have to generate enough force to activate Ib afferents after less than 30 ms, to allow time for the afferent activity to reach the spinal cord and cause a central effect. Figure 16C illustrates the profile of force produced after the ECR stimulus for one subject; the first peak of the twitch tension occurred in this individual 21 ms after the stimulus. Figure 16D shows a histogram of ECR twitch time across nine subjects. The average twitch time was 24.4 ± 3.5 ms (mean ± SD). This timing is therefore appropriate to generate an H reflex facilitation at the 30 ms interval.

To explore further the possible involvement of mechanical activation of ECR Ib afferents, we tested the effect of replacing the ECR electrical stimulation by a mechanical tap to the ECR tendon at the threshold required to generate a tap reflex in the EMG of the resting ECR muscle (1xTT). As the muscle was at rest, this intensity would be substantially above the threshold for activation of Ia fibers, and both Ia and Ib afferents should be activated (Lundberg and Winsbury, 1960; Katz *et al.*, 1991). Figure 16E shows results averaged across all subjects. There was a significant effect of ISI (ANOVA, $F_{(17, 136)} = 12.56$, $p < 0.001$). Significant facilitation was observed at the ISIs 3.5 and 15 ms (t-test, $p = 0.0057$ and $p = 0.0121$, respectively) and significant inhibition at ISIs 30-1000 ms (t-test, all $p < 0.007$). Thus although a tap to the ECR tendon could generate an H reflex facilitation, the timing of the major facilitation was shifted around 15 ms earlier. This is expected, as the tap was generated within 1 ms, whereas the muscle response to stimulation took an average of 24.4 ms to become maximal. This finding is therefore consistent with the hypothesis that mechanical activation of ECR Ib afferents mediates the H reflex facilitation.

Group Ib pathways in the upper limb are thought to be facilitated by cutaneous stimuli (Cavallari *et al.*, 1985); we accordingly tested whether cutaneous stimulation to the dorsal side of digits 2 and 3 could modify the H reflex facilitation. When the cutaneous stimulus was given 25 ms before the median nerve stimulus, the H-reflex amplitude was unchanged (Fig. 16F, H+cut, $p = 0.2510$). As previously shown, ECR conditioning stimulation 30 ms before the median nerve stimulus facilitated the H reflex (Fig. 16F, H+ECR, $p = 0.0101$). ECR stimulation combined with cutaneous stimulation also caused facilitation of the H-reflex (Fig. 16F, H+ECR+cut, $p = 0.0114$); this facilitation was significantly larger than following ECR stimulation alone ($p = 0.0424$). The enhancement of the facilitation by cutaneous stimuli is further evidence consistent with mediation by Ib pathways.

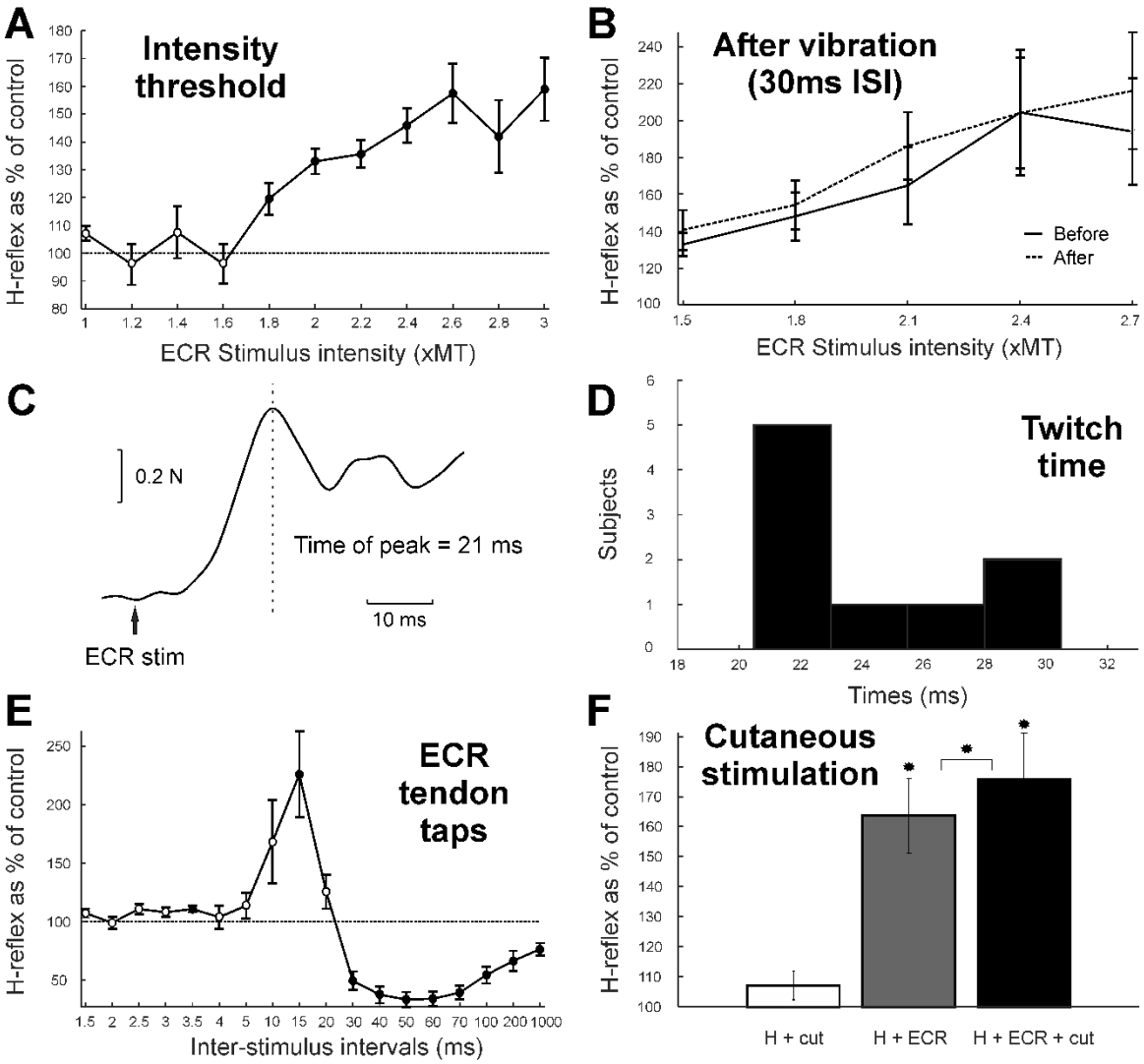

Figure 16. Studies in healthy humans probing which afferents mediate the facilitation. **A**, average from six subjects of H-reflex amplitude with 11 intensities of conditioning ECR electrical stimulation at the ISI of 30 ms between median nerve and conditioning ECR electrical stimulation. **B**, average from five subjects of H-reflex amplitude with 5 intensities of conditioning ECR electrical stimulation at 30 ms ISI between median nerve and conditioning ECR electrical stimulation. Continuous line show measurements before and dashed line after vibration of ECR tendon for 25 min. Filled and opened circles are not displayed here for average values since the analysis comparing conditioned with unconditioned H-reflex was not applied in this protocol. The analysis of this protocol consisted of the comparison between the curves before and after vibration, which were not significantly different, as shown in more detail in the text of this results section. **C**, example from one subject of force production from ECR muscle following stimulation at 3 x MT. The time of the first observed peak in force production is indicated by the dashed line and taken as the measure of twitch time. **D**, distribution of twitch time measured in nine subjects. **E**, average from nine subjects of H-reflex amplitude following mechanical tap to ECR tendon as conditioning stimulation at 1 x TT for 18 ISIs. **F**, average from five subjects of H-reflex amplitude (as percentage of control) conditioned by cutaneous stimulation (2 x perceptual threshold at 25 ms ISI) alone (white bar), by ECR stimulation (3 x MT at 30 ms ISI) alone (grey bar) and by ECR stimulation combined with cutaneous stimulation (black bar). * indicates significant differences. Display conventions in (A, B, E) as in Fig. 15.

An alternative hypothesis for the generation of the facilitation is that the extensor muscle twitch generates a wrist extension, which thereby stretches the wrist flexor

muscles and activates Group Ia and/or Ib afferents originating from flexors. We first investigated this by repeating the main protocol while subjects had their wrist held in a flexed position, which disengaged the FCR muscle and should have greatly reduced flexor afferent activation after the ECR twitch. There was a significant effect of ISI (ANOVA, $F_{(17, 112)} = 3.65$, $p < 0.001$). Figure 17A shows that there was still a significant facilitation at ISIs of 30 and 40 ms (t test, $p = 0.0138$ and $p = 0.0421$, respectively) and significant suppression at ISIs of 70, 100 and 200 ms (t test, all $p < 0.040$). The facilitation at 30 ms ISI was smaller than with the wrist in a neutral position, but the comparison between the two using a two-sample t-test did not reach significance ($p > 0.05$). This suggests that FCR afferents cannot be the only source of the facilitation effect.

To clarify further whether afferents activated by FCR stretch might play an important role in the facilitation, we repeated the main protocol replacing the ECR electrical stimulation by a passive extension movement of the wrist. This movement was substantially larger than the movement produced after the ECR shock at 3 x MT. We expect that the passive movement would activate flexor afferents strongly due to the muscle stretch, but cause little or no activation of extensor Ib afferents. Figure 17B shows average results across subjects. There was a significant effect of ISI (ANOVA, $F_{(17, 85)} = 2.53$, $p = 0.002$). A small but non-significant facilitation was seen for ISIs 20-60 ms, and a significant suppression for ISIs 100- 1000 ms (t test, all $p < 0.040$). Again, this result suggests that stretch activation of FCR afferents is unlikely to be the only source of the facilitation at 30 ms ISI.

Finally, we tested the effect of replacing the shock to ECR by a mechanical tap to the FCR muscle tendon, which should generate predominant activation of FCR afferents. There was a significant effect of ISI (ANOVA, $F_{(17, 68)} = 16.95$, $p < 0.001$). Figure 17C shows average results indicating significant facilitation at the ISIs 3, 3.5, 10 and 15 ms (t test, all $p < 0.050$) and significant suppression for ISIs 30-100 ms (t test, all $p < 0.030$). This implies that the facilitation can be produced by the activation of FCR afferents alone, without involvement of ECR afferents.

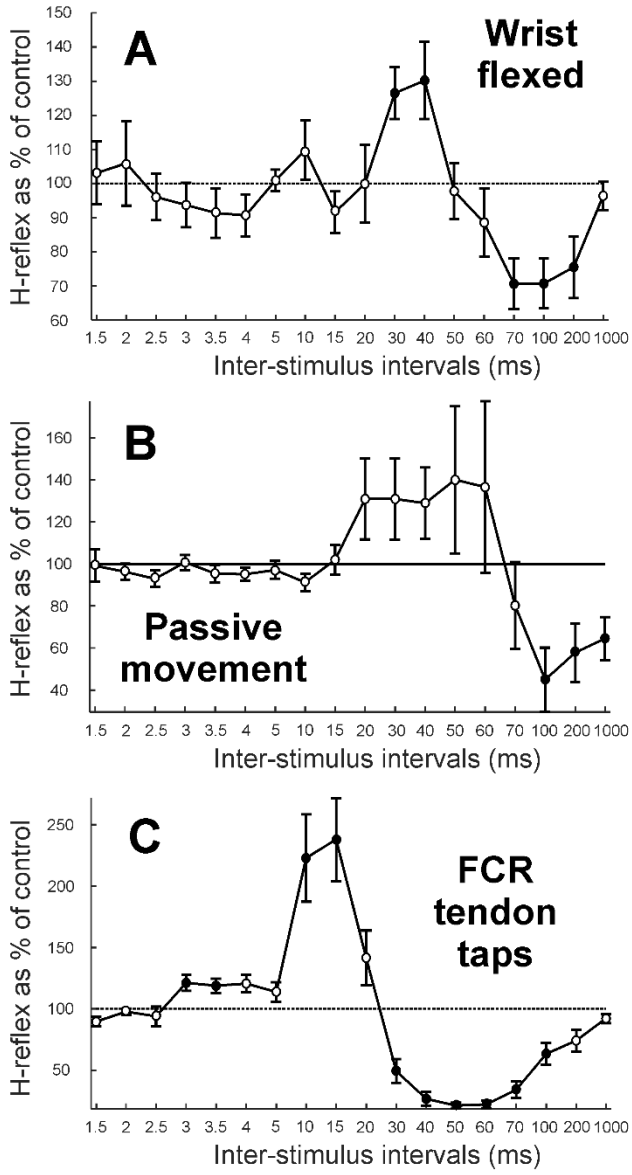

Figure 17. Studies in healthy humans probing which afferents mediate the facilitation. **A**, average from eight subjects of H-reflex amplitude with 18 ISIs between median nerve and conditioning ECR electrical stimulation at 3 x MT, as in Fig. 15, but while subjects had their wrist held in a flexed position. For one subject data from seven ISIs (up to 5 ms) are not displayed as part of the average results due to stimulus artefact contamination. **B**, average from six subjects of H-reflex amplitude with 18 ISIs between median nerve and conditioning passive wrist extension movement caused by mechanical perturbation. **C**, average from five subjects of H-reflex amplitude with mechanical tap to FCR tendon as conditioning stimulation at 1 x TT. Display conventions as in Fig. 15.

- *Monkey experiments*

We tested the main protocol in all four monkeys, conditioning the response to PT stimulation with prior stimulation of the ECR muscle (Fig. 18AB). Figure 18C shows results excluding data contaminated by stimulus artefact (ISIs up to 5 ms for monkeys PAT, PDR and TNS). There was a significant effect of ISI for all four monkeys (ANOVAs, Monkey PDR: $F_{(10, 209)} = 38.47$, $p < 0.001$; Monkey PLK: $F_{(17, 342)}$

= 13.9, $p < 0.001$; Monkey PAT: $F_{(10, 209)} = 10.46$, $p < 0.001$; Monkey TNS: $F_{(10, 209)} = 37.36$, $p < 0.001$). Although the strength and temporal extent of the effects varied between monkeys, in all cases there was a facilitation at 30 ms ISI, similar to that observed in the human studies.

We repeated the main protocol in three monkeys after cutting the ECR tendon near the wrist. In this preparation, electrical activation of afferents by the stimulus should persist, but the stimulus-evoked twitch should be prevented from activating ECR Ib afferents, or generating a wrist movement which could stimulate flexor afferents. Figure 18D shows the results in monkey PLK; the tendon cut had a significant effect on the curve (ANOVA, $F_{(1, 684)} = 25.3$, $p < 0.001$). Following the tendon cut, the facilitation for ISIs around 30 ms was lost. Results from the other monkeys in this protocol were similar. For monkey PAT a significant effect of tendon cut on the curve was observed(ANOVA, $F_{(1, 418)} = 21.1$, $p < 0.001$); after cutting the ECR tendon the facilitation at 30 ms ISI was lost and there was significant facilitation only at the ISIs 10, 15 and 20 ms, which was also present with tendon intact (all t-tests, $p < 0.050$), and significant inhibition at 70 ms ISI ($p = 0.0497$), not present with tendon intact (not shown). For monkey PDR although a visible peak at 30ms ISI was lost after cutting the ECR tendon, ANOVA on the effect of tendon cut did not reach significance, $F_{(1, 418)} = 1.99$, $p = 0.158$).

To test the hypothesis that FCR afferents were involved in the facilitation effect, we repeated the main protocol in monkey TNS after cutting the FCR tendon near the wrist and subsequently after re-attaching it. If ECR Ib afferents alone were causing the facilitation with no involvement of FCR afferents it would be expected that cutting the FCR tendon would not change the effect. Figure 18E shows that the broad facilitation around 30 ms ISI was lost, or even reversed to a suppression, following the FCR tendon cut. When the tendon was reattached to the hand, so that wrist extension once again generated muscle stretch in FCR, the facilitation was restored, although it was of lower amplitude and peaked earlier (at 20 ms ISI) than originally. The effects were significant (ANOVA, factor tendon intact/cut/reattached, $F_{(2, 627)} = 79.98$, $p < 0.001$). These results imply that FCR afferents also play an important role in the generation of the facilitation around 30 ms ISI.

To investigate whether we could see the facilitation after activating ECR afferents without involvement of flexor afferents, we reproduced the main protocol in one monkey, replacing the conditioning stimuli by strong mechanical pulls on the cut ECR tendon. There was a significant effect of ISI (ANOVA, $F_{(17, 342)} = 2.2$, $p < 0.001$).

Figure 18F shows that a significant facilitation was generated at ISIs 1.5-4 ms (t-test, $p < 0.05$). Note that for this protocol, the intervals quoted are times until the first stimulus of the train of three to the PT, instead of the last stimulus as used for other protocols; these intervals therefore correspond to 7.5-10 ms before the last (effective) PT stimulus. This indicates that a facilitation could be produced solely by ECR afferent activation.

Subsequently, to investigate which category of ECR afferents might generate the facilitation, we tested a series of different amplitude tendon pulls in the same monkey, for a fixed ISI of 2.5 ms; the result is illustrated in Fig. 18G. There was a significant effect of pull intensity (ANOVA, $F_{(19, 1980)} = 1.88$, $p = 0.010$). Significant facilitations were seen only for pulls >250 µm (t-test, $p < 0.05$). Lundberg and Winsburry (1960) reported that muscle stretches up to 100 µm activate Ia afferents exclusively, while stretches greater than 100 µm also activate Ib afferents. Our results suggest that the facilitation was not generated at intensities consistent with the activation of Ia afferents alone; only amplitudes expected to activate Ib afferents produced facilitation.

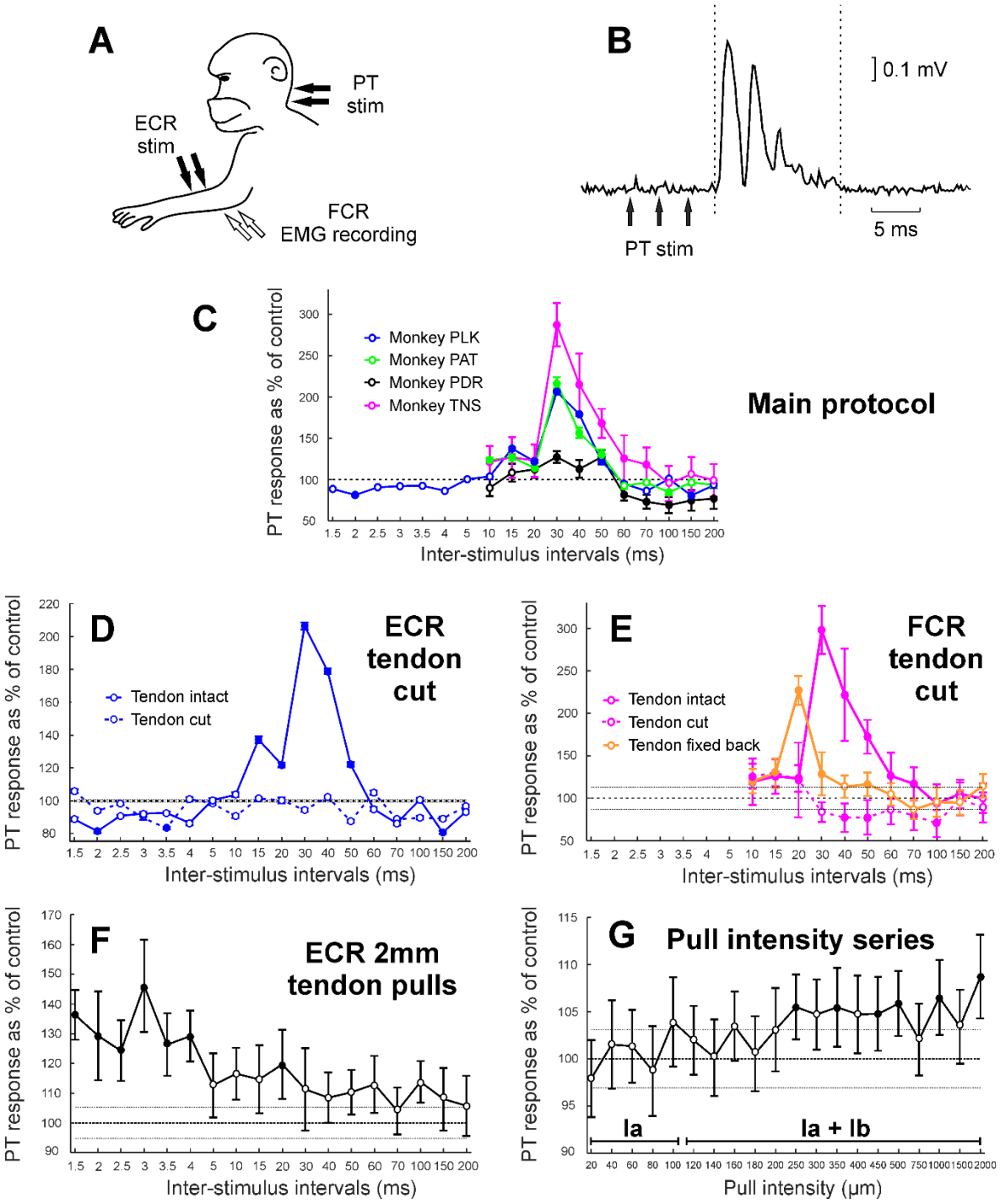

Figure 18. Monkey experiments. A, schematic representation of experimental setup. Wire electrodes for EMG recording were inserted in the FCR muscle, and for stimulation into the ECR muscle. Contralateral PT electrodes were used to evoke responses in the FCR. B, example of FCR response (rectified EMG signal) to PT stimulation from monkey PDR. Trains of 3 stimuli, 3 ms apart, were used to evoke responses in this monkey. Dashed lines indicate region used to calculate area under the curve as a measurement of PT response amplitude. C, main protocol results from monkeys PLK (blue), PAT (green), PDR (black) and TNS (pink). For each monkey average PT response amplitude is shown for 18 ISIs, using conditioning ECR electrical stimulation at 3 x MT. For monkeys PAT, PDR and TNS data from ISIs up to 5 ms are not displayed due to stimulus artefact contamination. D, results as in C, with ECR tendon intact (continuous blue line) and cut (dashed blue line). Monkey PLK. E, Results as in C, with FCR tendon intact (continuous pink line), cut (dashed pink line) and re-attached (continuous orange line). Monkey TNS. For D, E, F and G error horizontal lines around 100% (control H-reflex) represent standard error of all repetitions of the control H-reflex (with no conditioning stimulation); for D and E these error lines represent the average control H-reflex error across all data

sets displayed. F, average PT response amplitude as percentage of control for 18 ISIs, using 2 mm amplitude mechanical pulls to ECR tendon as the conditioning stimulus. Monkey PDR. Note that for this protocol responses are synchronized to the first of three shocks given to PT instead of the last shock as used in other protocols. G, average PT response amplitude as percentage of control, as a function of ECR tendon pull amplitude used as the conditioning stimulus (ISI 2.5 ms). Bar above abscissa indicates intensities expected to activate different afferent classes, based on Lundberg and Winsbury (1960). Display conventions for C-G as Fig. 15.

2.5 Discussion

In this study, we conditioned the FCR H-reflex with electrical stimulation over the ECR muscle belly and reported a reflex facilitation at 30 ms ISI. Our findings reveal novel spinal circuits, easily assessed non-invasively in humans. Some properties of these circuits are schematically illustrated in Figure 19, which may form a useful reference as individual features are described.

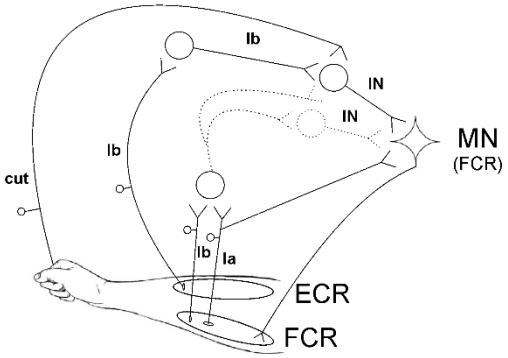

Figure 19. Schematic representation of the spinal circuits causing FCR H-reflex facilitation. Two convergent inputs excite the motoneurons (MN) of the FCR muscle, one originating from ECR Ib afferents and the other from Ib and/or Ia afferents in FCR. ECR Ib afferents synapse with Ib interneurons and subsequently with another set of interneurons (IN) (pathway described by Pierrot-Deseilligny and Burke (2012)). It is uncertain whether input from FCR afferents converge onto the same interneurons as the input from ECR Ib afferent or onto another set of interneurons. Cutaneous (cut) inputs facilitate Ib pathways.

- *Afferent Pathways Mediating Facilitation*

Several lines of evidence indicated that the facilitation was generated by the mechanical consequence of the ECR stimulus. The lack of changes in threshold intensity after prolonged vibration (Fig. 16B) argued against a contribution from electrical activation of ECR Ia afferents. Electrical activation of Ib afferents at the Golgi tendon organ was unlikely, given their location at the musculotendinous

junction far from the stimulus site, although it remains possible that these afferents could have been activated at the point where the nerve leaves the muscle. The twitch time of the muscle (Fig. 16CD) was consistent with the timing of the facilitation effect, which peaked at 30 ms ISI. The facilitation came earlier when the sluggish ECR twitch was replaced with a rapid mechanical tap or pull to the muscle (Fig. 16E, Fig. 18F). Finally, the facilitation was lost when the ECR tendon was cut (Fig, 18D), which would prevent the muscle from generating mechanical effects but leave electrical activation of afferents within the ECR unchanged.

It is well known that electrical stimulation of a muscle powerfully activates Group Ib afferents (Hunt and Kuffler, 1951). Multiple findings indicated a contribution to the facilitation from ECR Ib afferents. The facilitation was preserved when the wrist was flexed (Fig. 17A), which would tend to disengage the wrist flexor muscles and prevent activation of flexor afferents. Although the facilitation could be generated by taps or pulls to ECR (Fig. 16E, Fig. 18F), the threshold pull intensity was above that reported to activate only group Ia afferents (Fig. 18G), suggesting a requirement for Ib activation which are known to be discharged by tendon taps in humans (Burke *et al.*, 1983). Finally, the facilitation could be augmented by suitably-timed cutaneous stimulation (Fig. 16F). Cavallari et al. (1985) reported that a cutaneous shock placed 7 ms before the median nerve stimulus could facilitate putative Ib pathways; no other intervals were tested. Our study used a longer interval of 25 ms, chosen based on a pilot study to give the most robust effect. The electrically-evoked twitch would activate ECR Ib afferents with a much more dispersed time course compared with the temporally precise radial nerve stimulus used by Cavallari et al. (1985). It is therefore most likely that we accessed the same cutaneous pathway.

The second possibility which we investigated was that the ECR twitch produced a wrist extension movement, which stretched the wrist flexor muscles and activated flexor afferents. This mechanism must play some role. Tendon taps to the FCR muscle could also generate H reflex facilitation (Fig. 17C). Cutting the FCR tendon abolished the facilitation, which was restored if a connection between tendon and wrist movement was restored (Fig. 18E). Passive wrist extension by a torque motor also seemed to generate a weak facilitation (Fig. 17B), although this was heterogeneous across subjects and failed to reach significance. Group Ia afferents in flexors would be the most obvious candidates to mediate this effect, but a contribution from Ib afferents is also possible.

Other alternatives for the afferents mediating the facilitation seem improbable. The surface stimulus over ECR in human subjects would undoubtedly activate cutaneous receptors, but the facilitation was also seen in the monkey experiments using intramuscular wires, so a cutaneous origin is unlikely. Group Ia afferents in ECR are also unlikely to contribute. These afferents pause their firing after a twitch evoked by electrical stimulation, as the muscle goes slack (Hunt and Kuffler, 1951). Pulling the ECR tendon with amplitudes below 100 μm, which should activate Ia afferents exclusively, did not cause facilitation. As noted above, direct electrical activation of Ia afferents in ECR was unlikely to be the origin of the effect as the effect was lost after cutting the ECR tendon, and the threshold for the facilitation was unaltered by prolonged vibration which should raise the electrical threshold for stimulation of Group Ia fibers. Another possibility for the mediation of the facilitation effect could be group II afferents. Since spindles secondary endings, which give origin to group II afferents, are much less sensitive to vibration stimulation (Pierrot-Deseilligny and Burke, 2012), our vibration protocol does not exclude the possibility of group II afferents participation in the effect. Experiments using the cooling of the nerve as a way to selectively investigate the role of these fibres (e.g., Marque *et al.*, 2005) could be implemented in humans to further explore this possibility. Nevertheless, the monkey ECR tendon cut protocol showed that the facilitation effect was completely abolished after cutting the tendon, which allowed normal activation of muscle spindles following the ECR shock, and therefore group II afferents, making a group II contribution to the effect unlikely.

Our evidence thus suggests that both ECR Ib afferents and FCR afferents participate concurrently in producing the H reflex facilitation in FCR. It remains uncertain whether these afferents connect to common, or separate interneurons. We cannot determine definitively what central pathway generates this effect, as the dispersed time course of afferent activation after ECR stimulation precludes precise measures of central delay. One possibility is that it involves non-segmental circuits, such as C3-C4 propriospinal interneurons. However, the peak of the facilitation occurs rapidly after the peak of the twitch tension in the ECR (Fig. 16D), suggesting a short central delay which is consistent with mediation by segmental interneurons.

Work in cats has suggested that the excitatory Ib pathway is trisynaptic: the afferents excite Ib interneurons, that subsequently synapse with a further set of interneurons, which in turn excite motoneurons (Pierrot-Deseilligny and Burke, 2005). In our anesthetized monkey recordings we found that the amplitude of facilitation

produced by the same stimulus could vary between separate recordings (e.g. compare points in Fig. 18F and 18G for 2.5ms interval, 2000 μm amplitude). This is in agreement with a trisynaptic pathway, which would be expected to be especially sensitive to the fluctuations in anesthetic depth which typically occur in such studies. Our results suggest that for the primate wrist, this putative circuit receives highly converging inputs (see Fig. 19).

As well as demonstrating inputs from afferents in ECR and FCR muscles, plus cutaneous receptors in the digits, we also showed in some pilot experiments (not reported here) that a similar FCR H reflex facilitation could follow taps to the tendon of extensor carpi ulnaris and flexor carpi ulnaris. In cat lower limb, the effect of Golgi tendon organs on antagonist muscles can switch from inhibition to excitation during locomotion (Pearson and Collins, 1993; Prochazka *et al.*, 1997), providing flexible sensory feedback. How Golgi tendon organs act during voluntary movements of the human upper limb is yet to be determined, but we assume that the pathway which we describe plays an important role. With wrist flexed, the H reflex facilitation should be mediated primarily by ECR Ib rather than FCR afferents. This posture might therefore be used to maximize the specificity of our protocol for non-invasive assessment in humans.

The monkey and human experiments differed in several important regards, even though motor circuits in these species are very similar. The monkeys were anaesthetized, whereas the human volunteers were awake and at rest. Anesthesia will suppress central circuits, although our experience with microelectrode recordings under this anesthetic combination is that spinal interneurons remain highly active. Different test stimuli were used in the two species, but both will generate monosynaptic inputs to FCR motoneurons, giving an assessment of motoneuron excitability. Non-monosynaptic input pathways may also contribute, although only minimally for PT stimulation, where such circuits are dominated by feedforward inhibition (Maier *et al.*, 1998; Alstermark *et al.*, 1999). Synaptic input from Ia afferents is subject to pre-synaptic inhibition (Rudomin and Schmidt, 1999), but corticospinal input is not (Nielsen and Petersen, 1994; Jackson *et al.*, 2006). Despite these differences, remarkably similar facilitations following ECR stimuli could be seen in human and monkey data (compare Fig. 14C and 15 vs Fig. 18C). This suggests that both facilitations largely reflect post-synaptic increases in motoneuron excitability, rather than pre-synaptic or upstream effects.

- *Comparison with Effects of Conditioning Stimuli to the Radial Nerve*

When the FCR H reflex is conditioned by stimulation of the radial nerve at the spiral groove, three phases of reflex suppression are typically seen (Day *et al.*, 1984). The short latency effect (intervals -1 to +3 ms) is suggested to arise from disynaptic inhibition caused by either group Ia or Ib extensor afferents (Day *et al.*, 1984; Wargon *et al.*, 2006). We also found evidence for a suppression at short intervals by ECR stimulation (3-5 ms, Fig. 15), which could be mediated by the same pathway – the slightly longer latency is compatible with the more distal location of the ECR stimulation site compared with the radial nerve in the spiral groove. The suppression was smaller than previously reported using radial nerve stimulation – less than a 20% reduction (Fig. 15), and was not consistently observed in all subjects (Fig. 14C). Stimulation of the radial nerve at short intervals reduces the H reflex by ~75% (Day *et al.*, 1984). This may be because fewer afferents were stimulated within the single muscle compared with the whole nerve. Additionally, intramuscular stimulation may be more likely to activate Group Ia than Ib afferents directly, given the location of muscle spindles within the muscle belly compared to Golgi tendon organs at the musculo-tendon junction (Matthews, 1972). It has been suggested that short-latency disynaptic inhibition at the wrist is predominantly dependent on Ib afferents (Wargon *et al.*, 2006), which could also explain why smaller effects at short latency were seen in our studies.

Two later phases of suppression following radial nerve stimulation, at 5-50 ms and 50-1000 ms, are referred to as D1 and D2 inhibition (Mizuno *et al.*, 1971). D1 inhibition most likely arises from pre-synaptic inhibition of the FCR group Ia afferents (Berardelli *et al.*, 1987); the origin of D2 inhibition is less certain, although may also be pre-synaptic (Lamy *et al.*, 2010). We found a clear long-lasting suppression which peaked around 70 ms ISI; this could be comparable to the previous reports of D2 inhibition, although it is beyond the scope of the current report to investigate this further.

One intriguing question is why we observe reflex facilitation at ISIs around 30 ms when conditioning using ECR stimulation, whereas stimulating the radial nerve generates a D1 suppression at these intervals. It is possible that this reflects a difference in relative proportions of different afferents activated. Although intramuscular stimulation can activate group I afferents directly (Muir and Lemon, 1983), our results after prolonged vibration suggest that electrical activation of Ia afferents contributes little to the facilitation at 30 ms. The ECR muscle twitch likely

produces a very powerful Ib afferent activation (Hunt and Kuffler, 1951). The different effects at 30 ms ISIs between radial nerve and ECR stimulation may therefore reflect a dominance of activation of Group Ia (producing D1 suppression) or Group Ib afferents (producing facilitation) respectively. However, in conflict with this argument is the observation that a tap delivered to the ECR tendon also produced a facilitation (Fig. 16E); we would expect a tendon tap to activate Group Ia afferents more powerfully than Ib (Burke *et al.*, 1983). One important factor may be that both ECR tendon taps and ECR twitch are likely to produce repetitive afferent discharge (Hunt and Kuffler, 1951; Burke *et al.*, 1983), which may alter the relative balance between suppression and facilitation. It is known, for example, that pre-synaptic inhibition is weaker if measured using a tendon tap reflex than an electrically-evoked H reflex, presumably reflecting a difference between effects on repetitive versus single spike discharge (Morita *et al.*, 1998).

In summary, we have described a spinal circuit with converging input from wrist flexor afferents and extensor Ib afferents onto the wrist flexors (Fig. 19). This circuit can be easily assessed non-invasively in humans with the measurement of the FCR H-reflex conditioned by ECR stimulation. Such a finding represents a contribution to our knowledge of human spinal cord circuitry as well as having potential clinical relevance in aiding the understanding of changes occurring after damage, such as following stroke and spinal cord injury.

Chapter 3.
Effect of central lesions on a spinal circuit facilitating human wrist flexors

3.1 Abstract

Introduction: A putative spinal circuit with convergent inputs facilitating human wrist flexors has been recently described. This study investigated how central nervous system lesions may affect this pathway. **Methods**: We measured the flexor carpi radialis H-reflex conditioned with stimulation above motor threshold to the extensor carpi radialis at different intervals in fifteen stroke and nine spinal cord injury patients. **Results**: Measurements from stroke patients revealed a prolonged facilitation of the H-reflex, which replaced the later suppression seen in healthy subjects at longer intervals (30-60 ms). Measurements in patients with incomplete spinal cord injury at cervical level revealed heterogeneous responses. **Discussion**: Results from stroke patients could represent either an excessive facilitation or a loss of inhibition, which may reflect the development of spasticity. Spinal cord injury results possibly reflect the varied nature of the injuries and damage to the segmental interneuron pathways.

3.2 Introduction

A number of non-invasive techniques have been described in the literature to assess the function of different spinal circuits in humans – including pre-synaptic inhibition, reciprocal inhibition, amongst others (Bussel and Pierrot-Deseilligny, 1977; Day *et al.*, 1984; Berardelli *et al.*, 1987) – representing an important contribution to the understanding of human spinal circuitry. Recently, a novel spinal circuit has been described in which both wrist flexor afferents and wrist extensor Ib afferents (from Golgi tendon organs) facilitate wrist flexors in healthy humans. This circuit can be easily assessed non-invasively by conditioning the flexor carpi radialis (FCR) H-reflex with stimulation above motor threshold (MT) of the extensor carpi radialis (ECR). At

an interval of 30 ms between stimuli a clear facilitation is observed as a consequence of convergent excitatory inputs to the wrist flexor. A later inhibition at 70 ms interval is also observed but the pathways involved are still unclear. Although the description of the circuit in healthy subjects was important, it is still unknown how central nervous system lesions may be related to the circuit and could affect the observed results of the assessment. The purpose of this study is to explore how central lesions may affect this spinal circuit.

In this study we tested the spinal circuit described by Aguiar and Baker (2018), with converging input from flexor afferents and extensor Ib afferents to the wrist flexor, in stroke and spinal cord injury patients to investigate the effect of central lesions to this circuit. We found a prolonged facilitation of the flexor H-reflex at long intervals in stroke patients, which could reflect either excessive facilitation or loss of inhibition and heterogenous responses in spinal cord injury patients possibly reflecting the varied nature of the injuries and damage to segmental interneuron pathways.

3.3 Methods

Fifteen stroke patients, 32 to 73 years of age (ten male and five female) and nine spinal cord injury patients, 28 to 73 years of age (eight male and one female) participated in this study. Tables 1 and 2 show relevant information about stroke and spinal cord injury patients and their lesions, respectively. All procedures in stroke patients were approved by the Ethical Board of the Institute of Neurosciences Kolkata, India, where these were conducted, and all procedures in spinal cord injury patients were approved by the Ethical Committee of the University of Miami, where these were conducted. All subjects signed a written consent form prior to participation. The Ashworth scale was used to quantify the level of spasticity in stroke and spinal cord injury patients. Stroke patients were classified within spasticity levels 0 (n=2), 1 (n=3), 1+ (n=3), 2 (n=6) and 3 (n=1), and they were a mixture of hemorrhagic and ischemic strokes; time after stroke varied from 3 months to 10 years. The arm tested in stroke patients was the one corresponding to the most affected side of the body. Spinal cord injury patients were classified within spasticity levels 0 (n=3), 1 (n=1), 2 (n=3) and 3 (n=2); time post-lesion and level of damage

varied from 1 to 32 years and from C3 to C7, respectively. The right arm was tested for all spinal cord injury patients.

Table 1. General information about stroke patients and their lesions.

Patient	Gender	Age (years)	Time of lesion (months)	Spasticity level (Ashworth Scale)
PSB	Male	64	11	0
SPS	Male	34	19	1
SG	Male	51	125	1+
NS	Male	69	36	2
NRN	Female	73	14	0
NC	Female	34	21	1
AK	Male	54	16	1
MP	Female	35	3	1+
SK	Male	54	5	1+
NKM	Male	57	26	2
BM	Male	44	58	2
AB	Male	68	7	2
SWB	Female	48	23	2
SPP	Male	49	21	2
ND	Female	52	10	3

Table 2. General information about spinal cord injury patients and their lesions (ROM = range of movement).

Patient	Gender	Age (years)	Time of lesion (months)	Level of lesion	Spasticity level (Ashworth Scale)	Function of upper limbs
AM	Male	74	264	C4	0	Full ROM
LM	Female	56	107	C4-C5	0	Full ROM
HF	Male	28	97	C5-C6	0	Good arm and minimal hand function
JB	Male	70	381	C5-C7	2	Good arm and hand function
PG	Male	42	240	C5-C6	1	Full ROM on arms, minimal hand function

DB	Male	57	151	C5-C6	3	Full ROM in arms, no abduction in hands
PL	Male	62	96	C5-C6	2	Able to grip
GM	Male	60	12	C5	3	Full ROM
JH	Male	45	276	C3-C4	2	No hand and arm function

Stroke and spinal cord injury patients were submitted to the main protocol described for healthy humans in (Aguiar and Baker, 2018), including all procedures and statistical analysis. Briefly, the experimental procedure was the measurement of the H-reflex in the FCR muscle, evoked by median nerve stimulation, conditioned by electrical stimulation of the ECR muscle at 3 x MT. Eighteen different inter-stimulus intervals (ISIs) between median nerve and ECR stimulation were tested.

Median nerve and ECR stimulation used intensities up to 12.7 mA and 49.8 mA, respectively, for stroke patients and 18.8 mA and 42 mA, respectively, for spinal cord injury patients. We also measured the correlation between spasticity level and H-reflex amplitude at 30 ms and 70 ms ISIs.

3.4 Results

Figures 20A and C show overlain individual results for the main protocol in 15 stroke and nine spinal cord injury human patients (coloured lines), compared to 17 healthy adults (black). Stroke patients are classified according to their spasticity level on the Ashworth scale, using different coloured lines. Figures 20B and D show average results across each population. Results displayed for healthy adults duplicate results previously published in Aguiar and Baker (2018) to allow comparison with the patient data.

In stroke patients (Figures 20A and B) a similar facilitation at 30 ms was seen as previously described for healthy subjects (Aguiar and Baker, 2018), but this was greatly prolonged, and the suppression normally seen in healthy adults at later intervals was lost. The level of facilitation did not correlate significantly with spasticity as measured by the Ashworth scale, at ISIs of 30 or 70 ms ($R = -0.19$ and $R = 0.03$, respectively; both $p > 0.05$). In spinal cord injury patients (Figures 20C and D) no

significant facilitation or suppression was seen in the averaged results at any of the ISIs tested. This reflected the highly heterogeneous nature of the individual datasets. In spinal cord injury patients the H-reflex amplitude also did not correlate significantly with spasticity as measured by the Ashworth scale, at ISIs of 30 or 70 ms (R = 0.28 and R = -0.06, respectively; both p > 0.05).

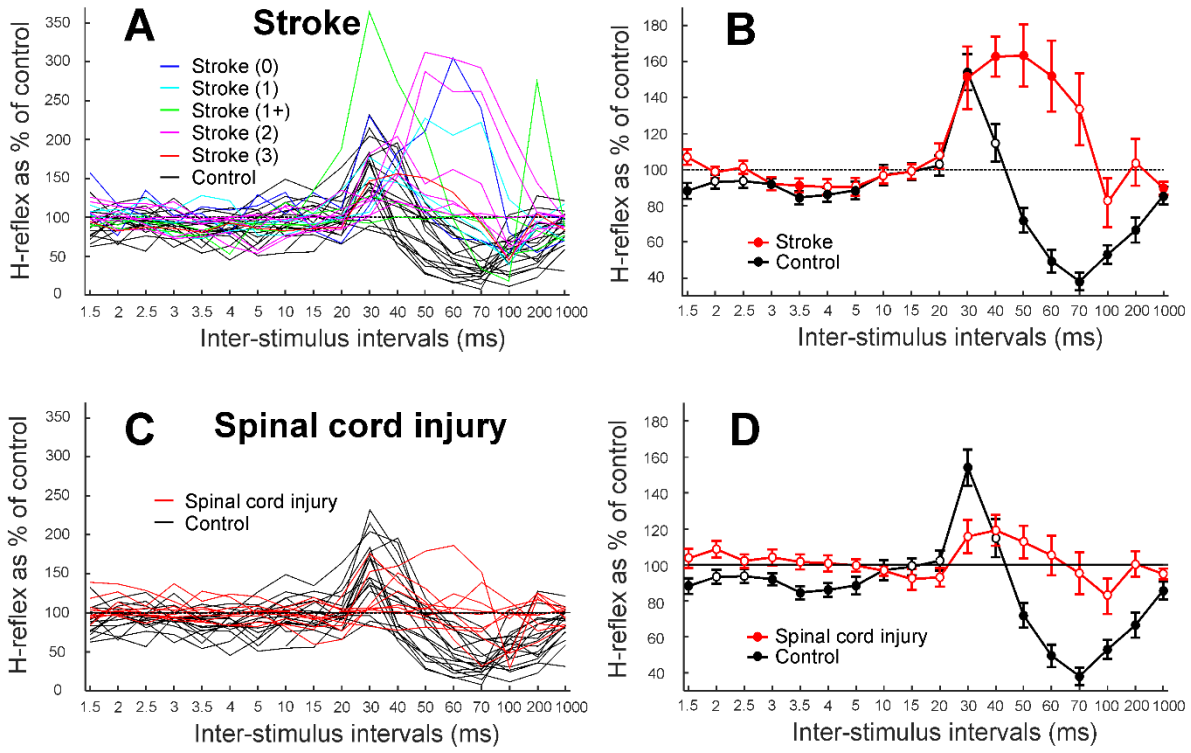

Figure 20. A, individual results from 17 healthy volunteers (black lines) and 15 stroke patients (colored lines). Different colors represent different levels of spasticity assessed by the Ashworth scale, as shown in the inset key. **B**, average data from (A). **C**, individual results from 17 healthy volunteers (black) and nine spinal cord injury patients (red). **D**, average data from (C). For A, B, C and D H-reflex amplitude is shown as a percentage of its control amplitude for 18 ISIs between median nerve and conditioning ECR electrical stimulation at 3 x MT. For B and D filled circles represent responses significantly different from control and error bars represent standard error. Data from healthy volunteers is duplicated from data previously published in Aguiar and Baker (2018) for comparison.

3.5 Discussion

In this study we tested a spinal circuit mediated by converging input from FCR afferents and ECR Ib afferents to the wrist flexor in stroke and spinal cord injury patients to explore the effects of central lesions to the circuit. We found a prolonged facilitation of the flexor H-reflex at long intervals in stroke patients, reflecting either excessive facilitation or loss of inhibition. Heterogenous responses in spinal cord

injury patients possibly reflecting the varied nature of the injuries and damage to segmental interneurons.

In stroke patients the facilitation at 30 ms ISI was similar to healthy adults, but it was prolonged to later ISIs which normally show suppression. One possibility is that even in healthy individuals, both facilitation and suppression processes occur concurrently, with suppression normally dominating around 70 ms ISI. In this case, the abnormal switch to facilitation could represent an increase in facilitation, or a loss of inhibition. Loss of inhibition related to changes in KCC2 function has been demonstrated to contribute to spasticity after both stroke and spinal cord injury (Boulenguez *et al.*, 2010; Toda *et al.*, 2014). Therefore, although no correlation was observed between spasticity levels and H-reflex amplitude at 70 ms ISI, spasticity might play a role in the observed results in stroke patients. While the spinal circuits involved in the 30 ms facilitation have been described (Aguiar and Baker, 2018), the pathways involved in the later inhibition at 70 ms are still unclear. Further work is required to understand this pathway and to uncover the mechanisms underlying the reported changes in stroke survivals. Understanding the abnormalities in these responses might help to understand, and possibly treat, spasticity.

In spinal cord injury patients highly heterogenous conditioning curve patterns were observed, including subjects with results similar to healthy humans, similar to stroke patients and subjects with no modulation of the H-reflex for any of the ISIs tested. These different curve patterns presented no evident correlation with the level of lesion. We suggest that variation in the extent of damage to spinal segmental circuitry may lead to such a high diversity, compared to the more homogenous results in stroke. Since this is a spinally mediated response which might be influenced by descending control is perhaps not unexpected that stroke survivals will show similar curve patterns resulting from corticospinal tract loss alone, whereas spinal cord injury leads to more diverse findings reflecting the variable damage to spinal segmental circuitry.

Although further work is necessary to uncover the specific spinal circuits mediating the later suppression seen at 70ms interval, Aguiar and Baker (2018) suggest this could represent the D2 inhibition, possibly of pre-synaptic origin, reported by Berardelli and colleagues when using radial nerve stimulation as opposed to the ECR stimulation used in this study (Berardelli *et al.*, 1987). Pre-synaptic inhibition at the spinal level seems to be in line with our results showing heterogeneous curve patterns for spinal cord injury patients, who have variable

spinal lesions affecting different spinal levels, causing variable damage to spinal interneurons, and loss of descending control. The high variability on the detrimental effect of these lesions at the spinal level would explain therefore the highly heterogeneous results found in spinal cord injury patients. Meanwhile, this spinal mediated response was affected in a very consistent manner in stroke survivals, whose lesion damage limits to loss of descending control alone.

Another important characteristic of this 70ms inhibition circuit is that it receives inhibitory input from the corticospinal tract, as evidenced by TMS protocols (Aguiar and Baker, submitted). Authors suggest inhibition from the corticospinal tract might take place directly at the FCR motorneurons, pre-synaptically at the Ia terminals from FCR, at the Ib interneurons activated by Ib afferents from the extensor muscle, or pre-synaptically at the Ib terminals of ECR which subsequently synapse with these same Ib interneurons (Aguiar and Baker, submitted). Once again the variable loss of descending control caused by the incomplete and variable spinal lesions of the spinal cord injury patients seems in line with the more heterogeneous responses from these patients when compared to stroke survivors, who present similar lesion affecting descending control only. Unfortunately, since this is a novel spinal circuit described recently insights are not available in the literature to evaluate more specific components of the circuit. Future work is necessary to reveal the specific mechanisms through which such inhibition takes place. The long delay of the effect certainly makes this task more challenging since it provides enough time for a larger number of synapses and neural components to be involved and every single one of these elements needs to be unravelled.

Chapter 4.
Descending inputs to spinal circuits facilitating and inhibiting human wrist flexors

4.1 Abstract

Recently we reported in humans that electrical stimulation of the wrist extensor muscle extensor carpi radialis (ECR) could facilitate or suppress the H reflex elicited in flexor carpi radialis (FCR), for inter-stimulus intervals of 30 ms or 70 ms respectively. The facilitation at 30 ms may be produced by both flexor afferents and extensor Ib afferents acting on a spinal circuit; the origin of the suppression at 70 ms is less certain. In this study, we investigated possible descending inputs to these systems. We used magnetic stimulation of the contralateral primary motor cortex, and click sound stimulation, to activate the corticospinal and the reticulospinal tracts respectively, and measured the effects on the H reflex conditioned by ECR stimulation. Corticospinal inputs reduced both the 30 ms facilitation and 70 ms suppression, indicating corticospinal inhibition of both circuits. By contrast, we failed to show any effect of clicks, either on the H reflex or on its modulation by ECR stimulation. This suggests that reticulospinal inputs to these circuits may be weak or absent.

4.2 Introduction

Although assessing the function of spinal circuits non-invasively in humans can be a challenging task, several spinal circuits as well as ways of assessing them have been described in the literature – e.g. reciprocal inhibition (Day *et al.*, 1984), recurrent inhibition (Bussel and Pierrot-Deseilligny, 1977), cutaneomuscular reflexes (Jenner and Stephens, 1982), amongst others. The investigation of spinal circuitry is crucial not only to understand function but to explore and possibly treat pathology. Despite the great progress achieved, one important gap was assessment of Ib pathways in human upper limb. Recently, however, we described an approach which

allows a straightforward and easy assessment of Ib function in humans (Aguiar and Baker, 2018). The assessment consists of the measurement of the flexor carpi radialis (FCR) H-reflex conditioned by electrical stimulation of the extensor carpi radialis (ECR) muscle. At a 30 ms interval (ECR stimulation preceding median nerve), the FCR H-reflex is facilitated, with contributions from both wrist flexor and extensor Ib afferents via a putative spinal circuit. With a 70 ms interval, the FCR H-reflex is inhibited, but the specific components of the circuit generating this inhibition are still to be uncovered (Aguiar and Baker, 2018).

It is known that many spinal cord interneurons receive convergent inputs from major descending systems such as the corticospinal and reticulospinal tracts, although some interneurons have input from only one of these pathways (Riddle and Baker, 2010). In this study, we investigated whether the circuits producing facilitation and suppression of the FCR H-reflex following stimulation of the ECR muscle receive descending input. We used loud click sounds to activate the reticular formation (Fisher *et al.*, 2012a), and found no effect on either the circuit responsible for FCR facilitation or suppression. By contrast, TMS to primary motor cortex appeared to reduce both the facilitation and suppression of FCR generated by ECR stimulation, suggesting that both of these circuits are inhibited by corticospinal input.

4.3 Methods

Fifteen healthy adults, 18 to 56 years of age, participated in this study (12 female, 3 male). This study was carried out in accordance with the recommendations of the ethics guidelines, Ethical Committee of the Medical Faculty, Newcastle University. The protocol was approved by the Ethical Committee of the Medical Faculty, Newcastle University. All subjects gave written informed consent in accordance with the Declaration of Helsinki.

The FCR H-reflex in the right arm was measured, evoked by stimulation of the median nerve at the cubital fossa (monophasic pulse, intensities up to 9.5 mA, 500 μs pulse width), and conditioned by electrical stimulation of the ECR muscle at 3 x motor threshold (MT) (monophasic pulse, intensities up to 24 mA, 1 ms pulse width). All procedures were as described previously, including electrode placement, and equipment for EMG recording and muscle and nerve electrical stimulation (Aguiar

and Baker, 2018). Two intervals between ECR conditioning stimulation and median nerve shock (ECR-Median nerve interval) were used in the study, 30 and 70ms (ECR preceding median nerve). The FCR H-reflex conditioned by ECR stimulation was further conditioned by either TMS or click sounds, in two separate set of experiments.

- *TMS experiments*

For TMS experiments, we used a Magstim 2002 stimulator with figure of eight coil (7 cm outer winding diameter; The Magstim Company Ltd, UK), and first located the optimal site over left primary motor cortex to elicit a motor evoked potential (MEP) in the FCR muscle. Coil orientation was at a 45° angle to the midline, with the handle directed posteriorly; this produces current in the brain in a posterior-anterior direction. We then measured the passive threshold, defined as the minimal TMS intensity capable of producing a MEP in the FCR muscle in 5 out of 10 measurements with the muscle at rest (4s inter-stimulus interval). TMS intensity was set as 90% of this passive threshold. Such intensity was chosen as a way to provide stimulation of the corticospinal tract strong enough to make it possible to detect inputs from this tract to the response measured, but at the same time trying to avoid possible motor responses (MEPs) to contaminate the H-reflex measurements. Different inter-stimulus intervals (ISIs) between TMS and median nerve stimulation were tested. Ten repetitions of each ISI were recorded with and without ECR conditioning stimulation. Twenty repetitions were recorded of the control H-reflex, with no conditioning stimulation, and 20 repetitions were also recorded of the H-reflex conditioned by ECR stimulation alone (with no TMS). H-reflex amplitudes were expressed as percentages of control H-reflex (with no conditioning stimulation). Intervals of 4s were used in between H-reflex measurements to control for homosynaptic depression. This entire procedure was repeated for each ECR-Median nerve interval tested (30 and 70 m) in random order. The ISIs tested with 30ms ECR-Median nerve interval were -4, -3, -2, -1, 0, 1, 2, 3, 4 and 5 ms, and for the 70ms ECR-Median nerve interval were -3, -2, -1, 0, 1, 5, 10, 15, 20, 25, 30, 35, 40 and 45 ms (negative intervals correspond to median nerve preceding TMS). Such ISIs were chosen so that our protocols would be able to detect the earliest and longest effects TMS might have on the H-reflex conditioned by ECR stimulation based on the delays for corticospinal tract activation through TMS shown in the literature (Baldissera and Cavallari, 1993; Mercuri *et al.*, 1997); longer intervals are used for the 70ms inhibition protocol since there are longer delays involved in this spinal pathway. For the 30ms

ECR-Median nerve interval, which causes facilitation of the FCR H-reflex, we decreased the intensity of median nerve stimulation so that the amplitude of the H-reflex + ECR matched the amplitude of the control H-reflex, with no conditioning stimulation. For the 70ms interval, which causes FCR H-reflex inhibition, we increased the intensity of the median nerve shock so that the amplitude of the H-reflex + ECR matched the amplitude of the control H-reflex, with no conditioning stimulation. This size matching was confirmed through t-tests comparing the 20 repetitions of the control H-reflex, with no conditioning stimulation, and the 20 repetitions of the H-reflex conditioned by ECR stimulation alone (with no TMS). Only data sets in which no significant difference was detected in the t-tests were considered for analysis. The reason for the implementation of this normalization of the sizes of the H-reflex conditioned by ECR stimulation (at both 30 and 70ms intervals) was to better detect possible TMS and/or click effects on the size of the H-reflex conditioned by ECR stimulation. Since the 30ms ECR interval causes a significant increase in the H-reflex amplitude, a possible further facilitation caused by TMS and/or clicks might not have been possible to detect without this normalization due to saturation of the response, which could not increase any further. The same rationale applies for the 70ms ECR interval. The significant suppression caused by ECR alone could reach values close to 0%, leaving no space for the detection of a further suppression that could be caused by TMS and/or click stimulation.

The peak-to-peak size of the H reflex was measured in each condition. Measurements of H reflex conditioned by TMS were expressed as a percentage of the unconditioned H reflex amplitude. Measurements of the H reflex conditioned by ECR stimulation and TMS were expressed as a percentage of the amplitude of the H reflex conditioned by ECR stimulation alone.

Nine subjects in total participated in the 30ms ECR-Median nerve interval protocol. Given the fine-grain resolution of ISI for this protocol, we expressed the ISIs relative to the first ISI which showed a significant effect of TMS on the H-reflex. The interval of this first effect was described as 0 ms for all subjects and previous and subsequent intervals were adjusted accordingly and named early facilitation delays (EFDs). This meant that a different number of subjects contributed to each one of the intervals (EFDs). In the figures, we display data with EFDs -5, -4, -3, -2, -1, 0, 1, 2, 3, 4, 5, 6, 7, 8 and 9 ms. The 0ms EFD represents therefore the interval in which the earliest arriving synaptic input from the descending corticospinal volley produced by TMS excites the FCR motorneurones facilitating the H-reflex. This interval was

chosen based on statistical analysis in which t-tests were performed comparing the amplitude of the H-reflex alone and the H-reflex conditioned by TMS separately for each of the ISIs used in the study. The first ISI which showed significant effect of TMS on the H-reflex amplitude was considered the 0ms EFD. After this synchronization, statistical analysis was conducted across subjects. The first analysis had the purpose of investigating the effects of TMS alone on H-reflex measurements. This analysis therefore used only sweeps with no conditioning ECR stimulation. We first performed a two-way ANOVA with factors subjects and ISIs to investigate if TMS at different ISIs had any effect on H-reflex measurements. If the ANOVA showed a significant effect of ISI we then computed t-tests with the reference value of 100% (control H-reflex) to show which ISIs were affected by TMS. The second analysis aimed to compare results with TMS alone and with TMS + ECR conditioning stimulation. We first performed a three-way ANOVA with factors subjects, ISIs and with/without ECR conditioning stimulation to investigate if both the ISIs and the ECR conditioning stimulation had any effect on the H-reflex measurements. If the ANOVA showed significant effect of ECR conditioning stimulation and ISIs, we then used t-tests comparing the results from all subjects on each ISI with and without ECR stimulation. For ANOVA and t-tests the significance limit was set at $P<0.05$.

For the protocol with ECR-Median nerve interval of 70 ms, we averaged results from nine subjects in each ISI. No synchronization was applied for this protocol given the longer ISIs tested, which dwarfed the small variations in EFD across subjects. Statistical analysis was conducted as described for the 30 ms ECR-Median nerve interval, to analyse both the effect of TMS alone on the H-reflex and the effect on ECR conditioning stimulation.

Findings from a single subject are illustrated in Results; statistical analysis of these data used measurements of H-reflex amplitude taken from single sweeps (rather than averages), and applied the same statistical tests as described above, except that ANOVA without the factor ‘subjects’ was used.

- *Click experiments*

Click sounds were generated by delivering a 0.1-ms-wide, square excitation pulse into headphones, with a Z-weighted intensity AZ of 125 dB SPL (amplifier Topaz SR20, Cambridge Audio, UK, driven with 5V input pulses with volume turned to maximum). Click sound stimulation was given to the left ear while responses were recorded from the FCR muscle in the right forearm. Similar to TMS experiments we

also tested the same two ECR-Median nerve intervals of 30 and 70ms and different ISIs between click sound and median nerve stimulation. The ISIs tested with 30ms ECR-median nerve interval were -1, 0, 1, 2, 3, 4, 5, 6, 7, 8, 9, 10 and 11 ms, and for the 70ms ECR-median nerve interval were -1, 0, 1, 2, 5, 10, 15, 20, 25, 30, 35, 40 and 45 (negative intervals correspond to median nerve preceding click). Once again such ISIs were chosen so that our protocols would be able to detect the earliest and longest effects click sound stimulation might have on the H-reflex conditioned by ECR stimulation based on the delays for reticulospinal activation through clicks shown in the literature (Fisher *et al.*, 2012a); longer intervals are used for the 70ms inhibition protocol since there are longer delays involved in this spinal pathway. The number of repetitions in each ISI, control H-reflex and H-reflex conditioned by ECR stimulation alone was also the same used for TMS experiments. The matching of the sizes of H-reflex control and H-reflex conditioned by ECR alone (at both 30 and 70ms ECR-Median nerve intervals) was conducted exactly as for TMS experiments. Statistical analyses were also conducted in the same way as for TMS experiments, except that no synchronization of ISIs relative to EFD was applied. Six and eight subjects participated in the 30 and 70ms ECR-Median nerve interval protocols, respectively.

4.4 Results

- *TMS experiments*

Figure 21 shows results from a single subject who participated in the TMS experiment. Figure 21A shows how the H reflex was facilitated by TMS in this subject at different ISIs. There was a significant effect of ISI (ANOVA, $p < 0.001$). Post hoc t-tests showed that TMS caused facilitation of the H-reflex at ISIs -4, -3, -1, 0, 1, 2, 3, 4 and 5 ms (all $p < 0.002$; shown with filled circles in Fig. 21A). Figure 21B shows, for the same subject, the difference between the effect of TMS on the H reflex conditioned by ECR stimulation with a 30 ms interval, and TMS on the H reflex alone. There was a significant effect of both ISI and ECR conditioning stimulation (ANOVA, both $p < 0.001$). T-tests showed that the effect of TMS on the H-reflex conditioned by ECR stimulation was significantly smaller than the effect of TMS on the H reflex alone at ISIs 0-5ms (all $p < 0.05$, Fig. 21B).

Figure 21C shows the effect of TMS on the H reflex in a different subject. Again, there was a significant effect of ISI (ANOVA, $p < 0.001$), and post-hoc t-tests showed that TMS facilitated the H-reflex at ISIs -2, -1, 0, 1, 5, 10 and 15ms (all $p < 0.005$). Figure 21D shows, in this subject, the difference between the effect of TMS on the H reflex and on the H reflex conditioned by ECR stimulation at a 70 ms interval (ECR precedes median nerve). Once again, there was a significant effect of ISI and ECR stimulation (ANOVA, all $p < 0.007$). Post-hoc t-tests indicated that TMS significantly increased the H-reflex conditioned by ECR stimulation more than the H reflex alone at ISIs 40 and 45ms (all $p < 0.009$, Fig 21D).

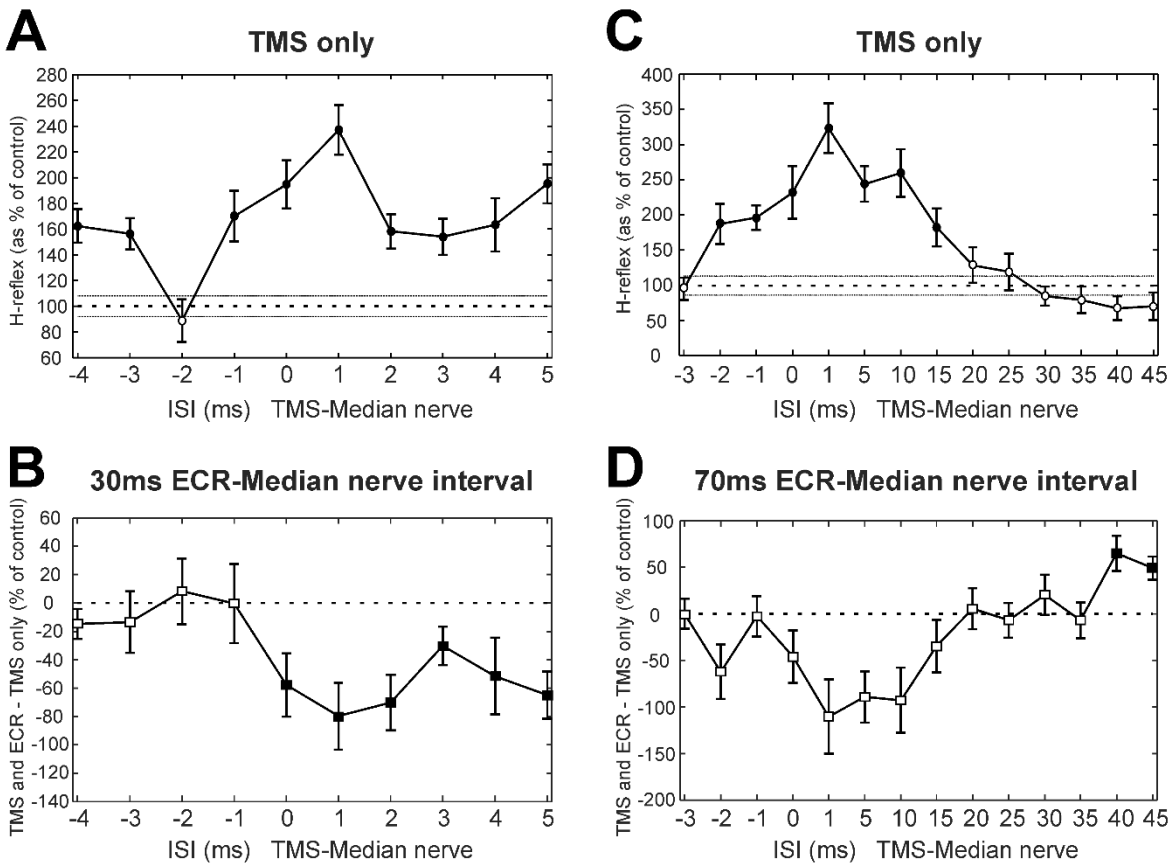

Figure 21. TMS results from single subjects. **A**, effects of TMS on the FCR H-reflex at different ISIs from a single subject. **B**, difference between the effect of TMS on the H reflex, and the effect of TMS on the H reflex conditioned by ECR stimulation 30 ms before the median nerve shock. Same subject as (A). **C**, effects of TMS on the FCR H-reflex, for different ISIs and a different subject from (A). **D**, difference between effect of TMS on H reflex, and on H reflex conditioned by ECR stimulation 70 ms before the median nerve shock. Same subject as (D). In (A) & (C), the peak-peak amplitude of the H reflex is plotted as a function of inter-stimulus interval, as a percentage of the size of the unconditioned H reflex. Filled symbols show points significantly different from 100% (A,C) or 0% (B,D). Error bars indicate standard error of the mean.

Results averaged across subjects for the TMS experiment are displayed in Figure 22, following a similar layout to the single subject plots of Fig. 21. Figure 22A shows how TMS affected the H reflex. The abscissa here is plotted as early facilitation delay (EFD). As expected, the H reflex for ISIs before 0ms EFD showed no modulation, but after this interval there was facilitation (significant effect of ISI, ANOVA $p = 0.038$; post-hoc t-tests showed significant facilitation at 0, 3-7 ms, all $p < 0.047$, filled symbols in Fig. 22A). The 0 ms EFD occurred at ISIs -4 to 1 ms in the nine subjects tested (-2.1 ± 1.5 ms, mean ± SD). Figure 22B shows the difference between the effect of TMS on the H reflex alone and on the H reflex conditioned by ECR stimulation 30 ms before the median nerve stimulus. ANOVA showed an effect of factors EFD and ECR conditioning stimulation (all $p < 0.002$). Post-hoc t-tests indicated that TMS had a significantly smaller effect on the H-reflex conditioned by ECR stimulation than on the H reflex alone, for EFDs 6 and 7ms (all $p < 0.045$, filled symbols, Fig. 22B).

Figures 22C and D show TMS results for the 70ms ECR-Median nerve interval; in this case, the abscissa shows raw TMS-median nerve interval, uncorrected for EFD. TMS produced a broad facilitation of the H reflex (Fig. 22C; ANOVA significant effect of ISI, $p < 0.001$; post-hoc t-tests indicated facilitation at ISIs -2, -1, 0, 5, 10 and 15ms, all $p < 0.031$). Figure 22D shows the difference between the effect of TMS on the H reflex alone, and on the H reflex conditioned by ECR stimulation 70 ms before the median nerve shock. ANOVA showed an effect of ISI and ECR conditioning stimulation (all $p < 0.001$). Post-hoc t-tests indicated that TMS had a significantly greater effect on the H-reflex conditioned by ECR stimulation than on the H-reflex alone, for ISIs 25 and 40ms (all $p < 0.032$, Fig 22D).

In summary, with appropriate timing TMS can significantly decrease the facilitation of the H-reflex by stimulation of the ECR 30 ms before the median nerve shock. TMS is also capable of reducing the suppression of the H-reflex following ECR stimulation 70 ms before the median nerve shock. This suggests that both circuits mediating effects of ECR stimulation on the H reflex are inhibited by corticospinal output activated by TMS.

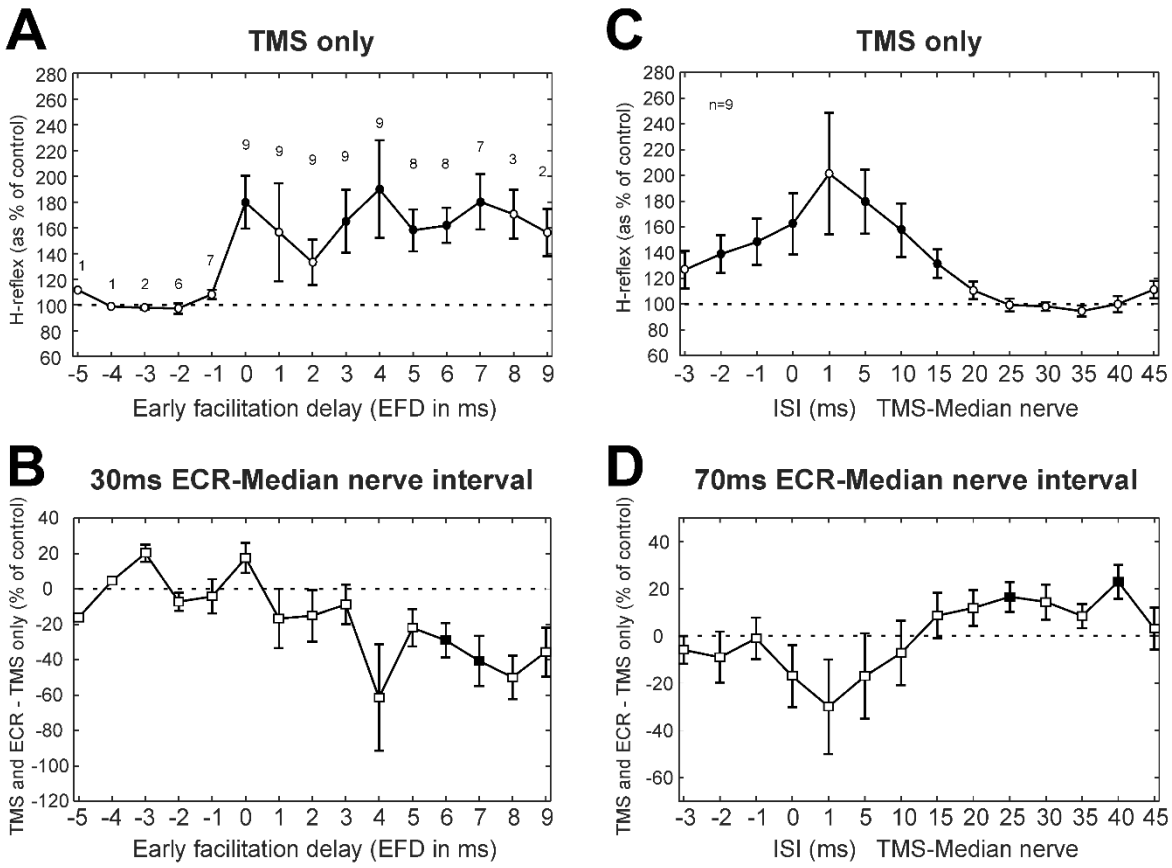

Figure 22. TMS results averaged across subjects. **A**, effects of TMS on the FCR H-reflex at different early facilitation delays (EFD). Numbers above each result display the number of subjects contributing to each data point. **B**, difference between the effect of TMS on the H reflex, and the effect of TMS on the H reflex conditioned by ECR stimulation 30 ms before the median nerve shock. Numbers of subjects contributing at each interval are as in (A). **C**, effects of TMS on the FCR H-reflex at different ISIs. **D**, difference between effect of TMS on H reflex, and on H reflex conditioned by ECR stimulation 70 ms before the median nerve shock. Filled symbols show responses significantly different from 100% (A,C) or 0% (B,D). Error bars indicate standard error of the mean. C and D are both averaged over n=9 subjects.

- *Click experiments*

Figure 23 shows results from clicks, averaged across subjects. Clicks did not produce a significant change in the H-reflex amplitude (no effect of ISI, ANOVA $p > 0.05$; Fig. 23A). Likewise, clicks did not produce significantly different effects on the H reflex conditioned by ECR stimulation at 30 ms interval compared with H reflex alone (ANOVA, $p > 0.05$ for both ISI and ECR conditioning, Fig 23B).

Figures 23C and D show results for the 70ms ECR-Median nerve interval, in a similar format. For the longer intervals used in this experiment, clicks also did not exert a significant effect on the H reflex (ANOVA, no effect of ISI, $p > 0.05$, Fig. 23C). There was no significant difference between the effect of clicks on the H reflex or on

the H reflex conditioned by ECR stimulation (ANOVA, no effect of ISI or ECR conditioning stimulation, $p > 0.05$, Fig 23D).

Although no significant effects were observed, we were concerned that we might have failed to detect small effects due to statistical thresholding. In particular, it appeared that both Fig. 23B&D had groups of points which lay consistently above 100%, even though the error bars were large. To check for this, we repeated the analysis by grouping together sets of three ISIs, with the aim of decreasing the variability and increasing the chances of obtaining significant differences. Yet even with this manipulation, there were no significant differences between the effects of clicks on the H reflex and on the H reflex conditioned by ECR stimulation, for either the 30 ms or 70 ms intervals ($p>0.05$). Although it is impossible to demonstrate that there is no effect of a particular pathway, any effects must be very weak, failing to be detected even with additional data averaging. We therefore conclude that pathways activated by clicks provide negligible inputs to the circuits mediating facilitation or suppression of the FCR H-reflex following ECR stimulation.

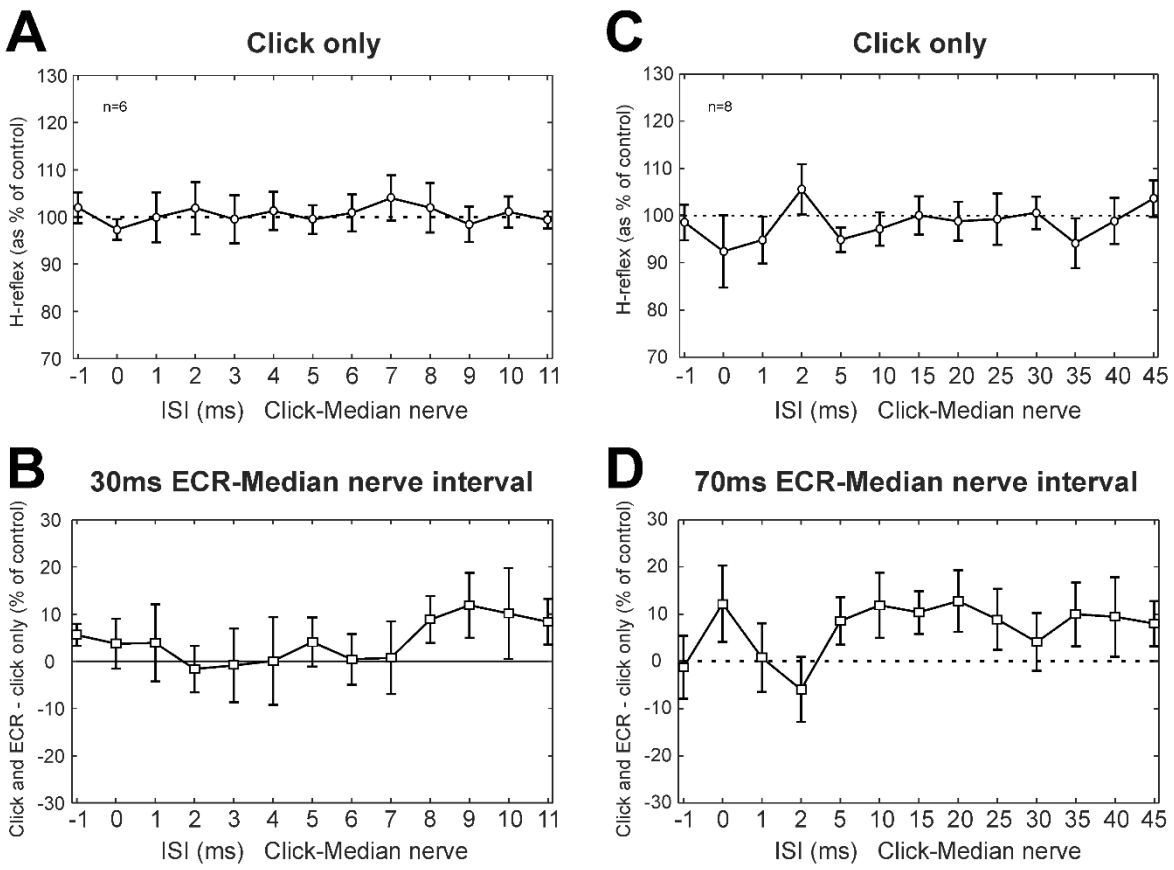

Figure 23. Clicks results averaged across subjects. **A**, effects of clicks on the FCR H-reflex at different ISIs. **B**, between the effect of click on the H reflex, and the effect of click on the H reflex conditioned by ECR stimulation 30 ms before the median nerve shock which elicited the H reflex. A,B, averaged over n=6 subjects. **C**, effects of clicks on the FCR H-reflex at different ISIs (note different time scale from

A). **D**, difference between effect of click on H reflex, and on H reflex conditioned by ECR stimulation 70 ms before the median nerve shock. C,D, averaged over n=8 subjects. In no cases in any plot were responses significantly different from control. Error bars indicate standard error of the mean.

4.5 Discussion

The purpose of this study was to investigate possible descending inputs, from the corticospinal and reticulospinal tracts, to the spinal circuits generating facilitation of the FCR H-reflex at 30ms and suppression at 70ms ECR-median nerve interval. Our results suggest that there is negligible input to both circuits from reticulospinal pathways activated by clicks. By contrast, corticospinal circuits activated by TMS appear to inhibit both the facilitation at 30ms and the suppression at 70ms ECR-median nerve intervals.

- *Corticospinal tract*

The facilitation caused by ECR stimulation 30 ms before the median nerve shock was significantly reduced by TMS at 6 and 7 ms EFDs. Figure 24A shows a schematic representation of the spinal circuit described by Aguiar and Baker (2018) with the addition of corticospinal tract input to the circuit, which would explain our experimental findings. ECR Ib afferents synapse with Ib interneurons which ultimately excite FCR motorneurons. Although this is shown in Fig. 24A as a monosynaptic connection, we cannot tell definitively how many interneurons are involved, or whether this circuit is confined to the spinal segment or includes a non-segmental pathway. However, the earliest effect of TMS was detected at an EFD of 6 ms (Fig. 22B). It has been suggested that Ib extensor afferents facilitate flexor motoneurons via a trisynaptic pathway, i.e. with two interposed interneurons (Eccles *et al.*, 1957; Pierrot-Deseilligny and Burke, 2005). The longer effective conditioning interval using TMS is consistent with this, and may indicate that corticospinal inhibitory input is provided to the first, but not the second, of the two interneurons. Another possibility that cannot be ruled out is a corticospinal inhibitory connection to Ib terminals pre-synaptically (as suggested in option c of Figure 24B for the 70 ms inhibition circuit), which would reduce input to the interneurons.

Figure 22A shows that the TMS alone first facilitatory effect on the FCR H-reflex (0ms EFD) is followed by a 2ms period of no facilitation, followed by a longer phase of facilitation from 3ms onwards. Such results corroborate the findings of other

studies showing the TMS effect on the H-reflex is biphasic. The first facilitation phase is believed to originate from a monosynaptic corticospinal volley, due to its short latency, while the second phase can arise from disynaptic EPSPs mediated through propriospinal neurones (Gracies *et al.*, 1994). The intermediate period in between these two phases showed no significant facilitation in our results, but other studies have shown a weaker but still significant facilitation instead (Gracies *et al.*, 1994). This might be explained by differences in methodological details such as the sample size and the variability of the responses measured.

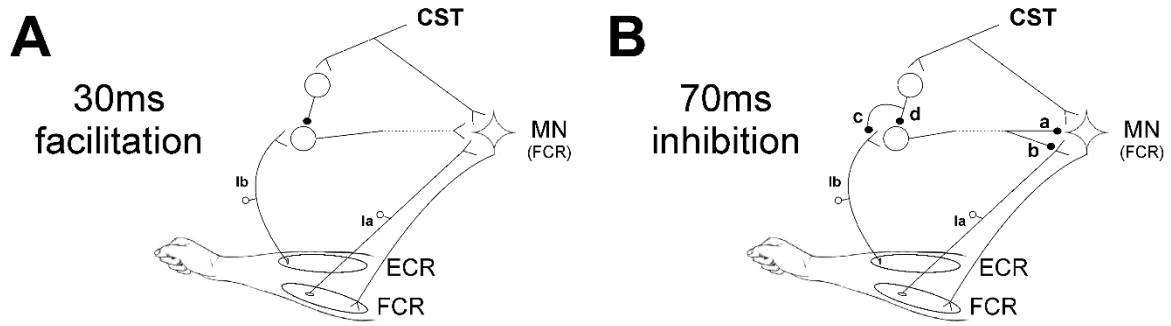

Figure 24. Schematic representation of spinal circuits. **A**, corticospinal tract (CST) input to spinal circuit generating facilitation of the FCR H-reflex at 30ms ECR-Median nerve interval. The CST inhibits Ib interneurons which excite FCR motorneurons (MNs). **B**, CST input to spinal circuit generating suppression of the FCR H-reflex at 70ms ECR-Median nerve interval. The components of this circuit are uncertain, and several possibilities are shown. The interneuron excited by Ib afferents may inhibit the FCR motorneurons post-synaptically (a) or pre-synaptically (b). The CST may inhibit this interneuron either via pre-synaptic inhibition to its Ib inputs (c) or via post-synaptic inhibition of the interneuron (d).

The pathway producing inhibition at 70ms ECR-Median nerve interval is more uncertain. We have previously speculated (Aguiar and Baker, 2018) that the origin of this suppression might be pre-synaptic at the FCR Ia afferent terminals, comparable to the D2 inhibition seen when conditioning the FCR H-reflex with radial nerve stimulation at intervals of 50-1000 ms (Berardelli *et al.*, 1987). In Fig. 24B a schematic representation of the possible spinal circuits generating inhibition is presented, including where corticospinal tract inputs could contribute. Our results showed that the corticospinal input to the circuit reduces the suppression seen at 70ms ECR-Median nerve interval when TMS is applied with ISIs of 25 and 45ms. Figure 24B shows that inhibition of the FCR response could occur either post-synaptically (synapse labelled ‘a’ in the figure) or pre-synaptically (‘b’). The

interneuron responsible for either pathway must be inhibited by the corticospinal tract, either pre- (‘c’) or post-synaptically (‘d’).

The possibility of pre-synaptic inhibition mediating the 70ms inhibition (‘b’ in Fig. 24B) could be in line with our observation that this 70ms inhibition is weak or absent in stroke survivors (Aguiar, Choudhury, Kumar, Perez & Baker, unpublished observations). Loss of inhibition related to changes in KCC2 function are present in spasticity, which is a common consequence of stroke (Toda *et al.*, 2014). We showed weak or absent inhibition at 70ms ECR-Median nerve interval in 17 stroke patients with spasticity levels 0 to 3 in the Ashworth scale, although no significant correlation was found between response size and spasticity level (Aguiar, Choudhury, Kumar, Perez & Baker, unpublished observations). Reduced pre-synaptic inhibition of FCR Ia terminals has been previously demonstrated in hemiplegic patients after stroke (Nakashima *et al.*, 1989). The corticospinal tract has been shown both to facilitate and suppress pre-synaptic inhibition of Ia terminals (Meunier and Pierrot-Deseilligny, 1998; Meunier, 1999). Our results indicate that the suppression following ECR stimulation is reduced by TMS, indicating an inhibitory input to this circuit activated from the corticospinal tract.

Several other systems generating inhibition have been described in the literature; any of these could be related to the 70ms inhibition caused by ECR stimulation. Jenner and Stephens (1982) reported the cutaneomuscular reflex responses following digital nerve stimulation. There is an inhibitory component to this reflex (referred to as the I1 reflex); this appears to be generated by a spinal pathway under descending control, as the I1 is absent in patients with motor cortical damage. The D2 inhibition already described above is another inhibitory system of the motor system, probably of pre-synaptic origin (Berardelli *et al.*, 1987). Other important inhibitory systems include short- (SAI) and long-latency afferent inhibition (LAI), although current knowledge about these circuits is still insufficient, especially in the case of LAI (Turco *et al.*, 2018). The inhibition described here at 70ms ECR-Median nerve interval might be related to one or more of these previously-described inhibitory systems, including cortical components and afferent inputs. Further work is necessary to uncover the mechanisms involved in this inhibition.

One possible limitation of our study is the fact that some of the individual results showed facilitation of the FCR H-reflex with the earliest ISI tested (-4ms, as in the example illustrated in Fig 21A). This raises the possibility that the earliest facilitation of the H-reflex actually occurred even earlier, at an interval which we did not test.

However, this is unlikely; in the literature, the earliest effect of TMS on the FCR H-reflex is not shorter than -4ms (Baldissera and Cavallari, 1993; Gracies *et al.*, 1994; Mercuri *et al.*, 1997); shorter intervals would be hard to reconcile with the known conduction delays.

- *Reticulospinal tract*

Results from experiments using clicks failed to show any significant effects. Firstly, click sounds alone did not change the FCR H-reflex at any of the ISIs investigated in our experiments. Although there are known reticulospinal inputs to forearm flexor motoneurons in primates, they have an amplitude around five times smaller than inputs from the corticospinal tract (Riddle *et al.*, 2009). In addition, part of the reticulospinal input comes via a disynaptic pathway, raising the possibility that it may be gated out in the resting conditions tested in our study (Schepens and Drew, 2006). The study of Fisher et al. (2012a) reported late responses to TMS in reticular formation cells which seemed to be mediated by the click sound generated by the coil discharge. However, out of eight reticulospinal cells, only three responded at the latency consistent with being generated by clicks. It is thus perhaps unsurprising that no statistically significant effects on the H reflex were observed from the partial activation of an already weak input.

Secondly, we could not detect an effect of the click-evoked activity on either the facilitation or suppression generated by ECR stimulation. Once again, this could be because inputs were too weak to be detected. However, Riddle and Baker (2010) reported that 66% vs 54% of cervical spinal cord interneurons responded to a train of three corticospinal vs reticulospinal stimuli, with 0.48 vs 0.67 extra spikes elicited per stimulus respectively. The strength of inputs from the two descending pathways to interneurons in general is therefore not greatly different. The fact that no inputs could be detected to the circuits tested may suggest that there is a genuine difference here, and that these circuits receive corticospinal, but no reticulospinal inputs. This is possible given the data of Riddle and Baker (2010), who found that of cells which responded to at least one of the descending inputs tested, 15% responded only to stimulation of the medial longitudinal fasciculus (which contains mainly reticulospinal fibres).

Since reticulospinal cells receive input from neck proprioceptors and are therefore influenced by posture (Baker, 2011; Baker *et al.*, 2015), one possible limitation of our study could be that the posture used here might not have been the

most appropriate to activate the reticulospinal tract using the click sounds strongly. Testing the protocol with different postures using neck rotations might be appropriate to investigate this possibility further (Ziemann *et al.*, 1999; Tazoe and Perez, 2014).

Another important aspect of our results is that it is uncertain which parts of the reticular formation is activated by the click sounds used in our experiments. Fisher and colleagues (2012a) recorded click responses from cells in the primate nucleus gigantocellularis, which is an important source of the reticulospinal tract (Sakai *et al.*, 2009). In humans, loud clicks comparable to the ones applied here were used in a paired-pulse plasticity protocol, with results consistent with activation of the reticular formation (Foysal *et al.*, 2016), although the exact nucleus involved could not be determined. It remains possible, therefore, that there may be an input from reticulospinal fibres to the circuits investigated here, but that they originate from a region which is not activated by clicks.

Chapter 5.
Spasms after spinal cord injury show low-frequency intermuscular coherence

5.1 Abstract

Intermuscular coherence allows the investigation of common input to muscle groups. Although beta-band (15-30 Hz) intermuscular coherence is well understood as originating from the cortex, the source of intermuscular coherence at lower frequencies is still unclear. Here we used a wearable device which recorded EMG signals during a 24-period in four lower limb muscles of seven spinal cord injury patients (American Spinal Cord Injury Association impairment scale A or B) while they went about their normal daily life activities. We detected natural spasms occurring during these long-lasting recordings and calculated intermuscular coherence between all six possible combinations of muscle pairs. There was significant intermuscular coherence at low frequencies, between 2 and 13 Hz. The only possible source for this was the spinal cord since the spinal lesions in these patients interrupt connections to supraspinal structures. This is the first report to demonstrate that the spinal cord is independently capable of producing low frequencies intermuscular coherence.

5.2 Introduction

Intermuscular coherence is an important and useful tool in motor control studies. It can be used to investigate muscle groups receiving common input from parts of the nervous system (e.g., Nazarpour *et al.*, 2012), to assist in the diagnosis of postural tremor (van der Stouwe *et al.*, 2015) and upper motor neuron dysfunction in motor neuron disease (Fisher *et al.*, 2012b), and when combined with corticomuscular coherence can differentiate between pathways converging onto spinal motoneurons (Boonstra, 2013). Since intermuscular coherence requires only the use of surface electromyography (EMG) recordings it can be measured straightforwardly and non-

invasively in humans. Analysis of coherence detected at different frequencies provides important information on how the nervous system works to control muscle activity during different tasks.

Intermuscular coherence in the beta band (15-30 Hz) is accepted to have a cortical origin. Corticomuscular coherence can also be observed in this frequency band (e.g., Conway *et al.*, 1995; Baker *et al.*, 1999); the common cortical drive to multiple muscles leads to intermuscular coherence (e.g., Kilner *et al.*, 1999; Power *et al.*, 2006). Beta oscillations are carried down the corticospinal tract (Baker *et al.*, 2003), and damage to this pathway leads to loss of beta-band intermuscular coherence (Fisher *et al.*, 2012b). This may have substantial clinical relevance to assist in the early diagnosis of upper motor neuron dysfunction in motor neuron disease.

Although intermuscular coherence in the beta band is well understood, the mechanisms and origin of intermuscular coherence at lower frequencies are still under debate. Boonstra and colleagues (2009b) argue for a non-cortical origin for EMG synchronization around 10 Hz, which has been observed on a number of different motor tasks in healthy humans (e.g., Evans and Baker, 2003; Halliday *et al.*, 2003; Boonstra *et al.*, 2007). The lack of corticomuscular coherence around this frequency provides support for this argument (Boonstra *et al.*, 2009b); indeed, it has been proposed that specific spinal circuits act to minimize cortico-muscular coupling in this band (Williams and Baker, 2009; Williams *et al.*, 2010; Kozelj and Baker, 2014). It remains to be determined which sub-cortical neural structure generates low-frequency rhythmic activity. One possibility is the brainstem (e.g., Grosse and Brown, 2003; Boonstra *et al.*, 2009b), as invasive recordings from the reticular formation in monkey show clear synchronization with peripheral oscillations in this band (Williams *et al.*, 2010).

After spinal cord injury, patients commonly experience involuntary muscle spasms; these can affect patient's lives to varying degrees (Thomas *et al.*, 2014b). Spasms can be classified into different types including tonic EMG activity, clonus and unit firing (Winslow *et al.*, 2015). After spinal cord injury the contribution of afferent input to motoneuron output may increase: in some cases a spasm can easily be evoked by stimuli such as light touch and small postural adjustments. Other contributors to spasm generation may be changes in intrinsic motoneuron properties such as a reduction in the spiking threshold, and a reduction in post-synaptic inhibition (Thomas *et al.*, 2014a).

Recent advances in technology have allowed long-term recording of EMG activity outside the laboratory (Brown *et al.*, 2016; Zaaimi *et al.*, 2018). Such recordings have allowed quantitative characterization of types and incidence of spasms after spinal cord injury (Thomas *et al.*, 2014b), providing data on many more instances of spasms than is possible in a brief laboratory visit. In this report, we use such recordings to explore shared drive to muscles using inter-muscular coherence. We find clear evidence for coupling at 2-13 Hz. Since these patients had spinal lesions, only the spinal cord can be generating this rhythmic activity.

5.3 Methods

This report uses EMG data reported in a previous study which developed methods for detection and classification of spasms (Winslow *et al.*, 2015). Seven spinal cord injury volunteers, 28 to 66 years old (5 male, 2 female) took part in the study. Level and time of lesion varied from C3 to C7 and from 5 to 28 years, respectively. The American Spinal Cord Injury Association Impairment scale was A, B or C. Relevant information about participants and their lesions is presented in Table 3. All participants signed a written consent form and all procedures were approved by the University of Miami Investigational Review board.

Table 3. General information about spinal cord injury patients and their lesions.

Patient	Gender	Age (years)	Time of lesion (months)	Level of lesion	ASIA	Cause of injury
OA	Male	61	72	C5	A	Sports – hockey accident
KA	Female	39	288	C5	B	Motor vehicle accident
RB	Male	40	60	C4	B	Motorcycle accident
JB	Male	66	336	C6	B	Fall from roof
RC	Female	34	192	C7	A	Motor vehicle accident
JH	Male	41	228	C3	C	Sports – Karate, landed on head
RV	Male	28	132	C7	A	Motor vehicle accident

EMG was recorded from four muscles – right medial gastrocnemius (MG), tibialis anterior (TA), hamstrings (HM) and vastus lateralis (VL) – over 24 hours for each participant using a data logger. This portable device was connected to surface electrodes placed over each muscle, and recorded involuntary spasms that occurred while subjects went about their normal daily life activities. EMG signals were sampled at 1 kHz and filtered (30 Hz–1 kHz). We first used the previously-reported algorithm to mark periods in each muscle where tonic spasms occurred. This is illustrated in Fig. 25, where the dotted vertical lines mark the detected onset and offset of the spams in each muscle shown. Intermuscular coherence was calculated for all six possible combinations of muscle pairs. For a given muscle pair, coherence calculation used full-wave rectified EMG from periods where both muscles had coincident spasms, with 1.024 s-long windows. These windows are shown in Fig. 25. Further details about the recording device and algorithm for classification of tonic spasms are described by Winslow and colleagues (2015).

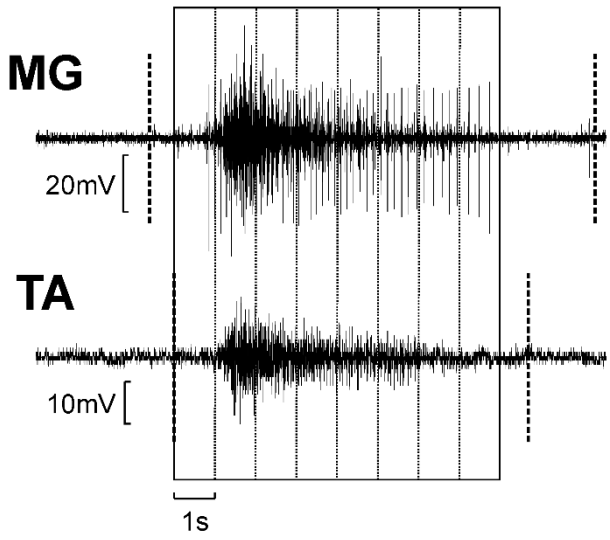

Figure 25. Method to calculate intermuscular coherence: example of EMG signals from one muscle pair (MG-TA). First, the beginning and end of tonic spasms in both muscles were detected (thick dashed vertical lines). Second, data were selected only from periods where both muscles showed spasm activity simultaneously. Third, recordings were separated into 1.024s-windows, ignoring any remaining spasm activity which could not fill a whole window. These windows were then used for the intermuscular coherence calculation.

Power spectra, coherence and the significance limit for coherence were calculated via the methods described in our previous work (Baker *et al.*, 2006), using a Fourier transform window size of 1024 sample points, corresponding to a frequency

resolution of 0.98 Hz. The number of windows used to calculate coherence varied from 271 to 6808 across the different muscle pairs and subjects.

We took two approaches to assessing the consistency of findings across subjects and muscle pairs. Firstly, coherence spectra for a given muscle pair were averaged across all seven subjects; the significance limit ($p<0.05$) for the average was calculated as described by Evans and Baker (2003). This provided a visual display of the average finding. Secondly, for an individual subject and muscle pair we determined whether coherence was above the significance limit for a given frequency bin. The number of significant values was summed over all six muscle pairs and seven subjects, providing a maximum of 42 counts if significant coherence at that frequency was a universal finding. To assess significance on these plots, we used a binomial distribution to determine that a count of 6 would not be exceeded by chance more than 5% of the time, given that the probability of a single count was $p=0.05$ on the null-hypothesis of no coherence.

5.4 Results

Figure 26 shows results from a single subject. Significant intermuscular coherence was observed at lower frequencies (2-13 Hz, grey shading) for most muscle pairs (Fig. 26B). For some muscle pairs, peaks in coherence at low frequencies corresponded to peaks in power spectra of the two muscles analyzed (Fig. 26A).

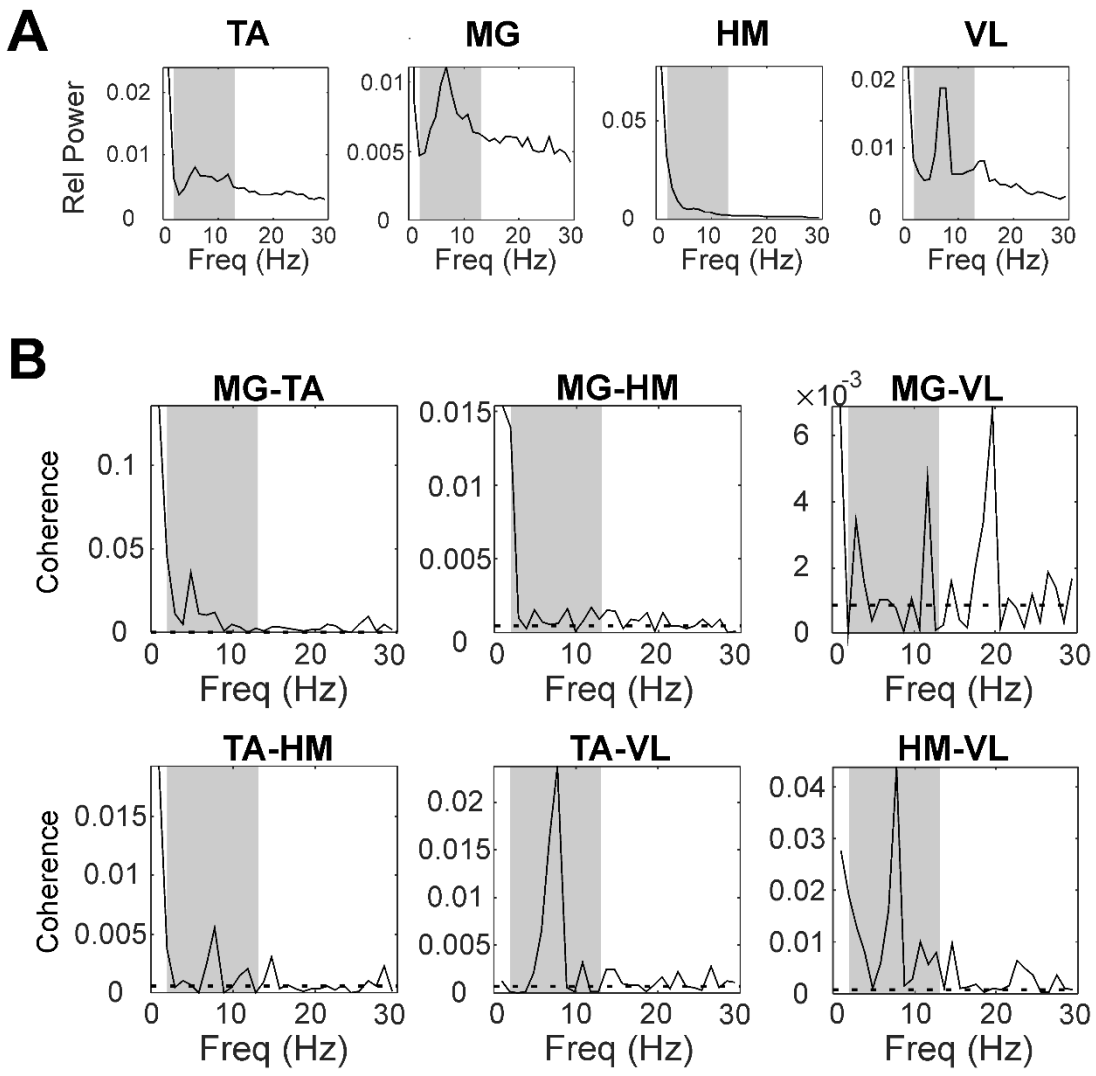

Figure 26. Results from a single subject. **A**, power spectra for the four recorded muscles, expressed as relative power (i.e., power divided by sum of power from 0 to 500 Hz). **B**, intermuscular coherence spectra for all six muscle pairs. Dashed horizontal lines represent significance limit ($p<0.05$). In A and B, highlighted grey areas show 2-13 Hz frequency band.

Average results are presented in Fig. 27. Significance intermuscular coherence at low frequencies (2-13 Hz, grey shading) was present in all six muscle pairs (Fig. 27A) and in the average across all muscle pairs (Fig. 27B). In some cases peaks in coherence appeared on top of a decay in coherence values at low frequencies, which can be seen in average results from muscle pairs MG-TA and MG-HM (Fig. 27A). This provides confidence that there was a genuine oscillatory phenomenon, rather than just a band-limited non-oscillatory process.

Figure 27C shows the number of data points above significance across all subjects and all muscle pairs. Around half of all spectra available showed significant

coherence up to 15 Hz, demonstrating that coupling at these frequencies was a robust finding. Figure 27D shows the number of peaks in coherence above significance across all subjects and all muscle pairs. Peaks in coherence were clearly seen at low frequencies. Peaks were also present at higher frequencies (15-30 Hz) although they had a smaller magnitude as assessed by the coherence traces shown in Fig. 27A and B.

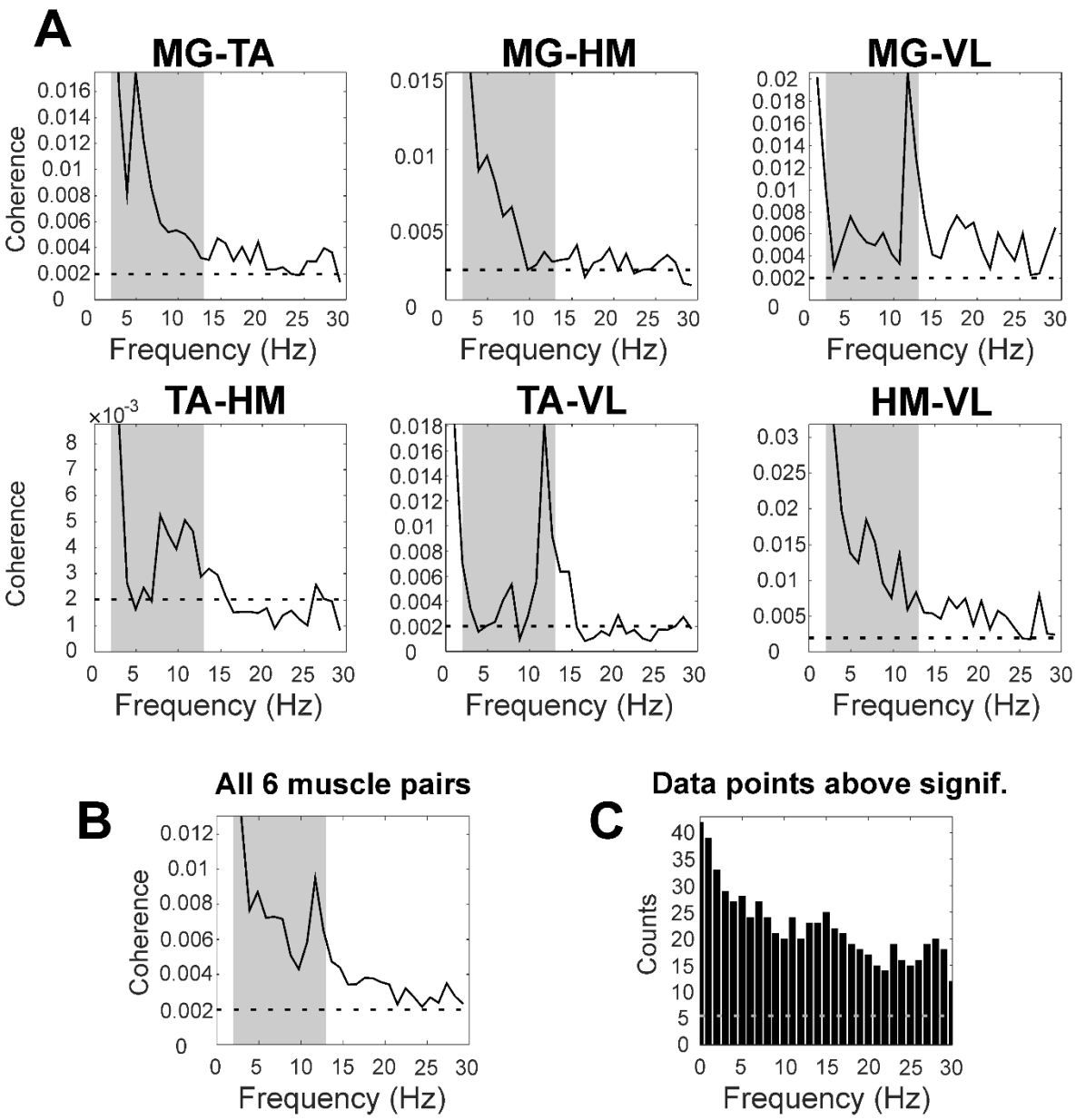

Figure 27. Average results. **A**, average coherence results from seven spinal cord injury patients for all six muscle pairs. **B**, average coherence across six muscle pairs and seven subjects. **C**, histogram showing the number of coherence measures above the significance limit summed over all seven subjects and six muscle pairs. For A and B, highlighted grey areas show 2-13 Hz frequency band. For A-C, dashed horizontal lines represent significance limit ($p<0.05$).

5.5 Discussion

Although intermuscular coherence in the beta-band (15-30 Hz) is well understood as having a cortical origin, the source of intermuscular coherence at lower frequencies is still under debate. Here we demonstrated significant intermuscular coherence at low frequencies (2-13 Hz) during spontaneously-occurring spasms in spinal cord injury patients. As these patients had a disconnected cord, lacking supraspinal input, we conclude that the spinal cord alone is capable of producing intermuscular coherence in the 2-13 Hz range.

One previous study used intermuscular coherence to analyse spasms in spinal cord injury. In a single paraplegic patient, Norton and colleagues (2004) found an isolated peak in inter-muscular coherence at 16 Hz. Noting that this is a frequency typically associated with orthostatic tremor, these authors suggested that a spinal circuit may be responsible for the pathology of orthostatic tremor. Our results did not reveal a clear 16 Hz coherence peak, although peaks at slightly lower frequencies were seen for muscle pairs MG-VL and TA-VL (Fig. 27A). These may correspond to the previous finding. However, the appearance in only a limited sub-set of muscle pairs suggests that this was not the primary oscillatory mode generated by the isolated spinal cord. By contrast, coherence at lower frequencies (2-13 Hz) was a common observation.

The absence of corticomuscular synchronization at around 10 Hz suggests that intermuscular coherence around this frequency does not originate from the cortex (Boonstra *et al.*, 2009b), and points instead to a sub-cortical origin. In healthy subjects, the brainstem is one possible candidate. We know that the reticular formation makes connections to a wide range of motoneurons innervating both upper and lower limb (Peterson, 1979; Riddle *et al.*, 2009). However, in the spinal cord injury subjects which we studied, brainstem descending systems were damaged as well as the corticospinal tract. The only remaining possibility to generate these oscillations is thus the spinal cord itself.

Intermuscular coherence at low frequencies has been observed in healthy adults during tasks involving bimanual coordination (5-12 Hz, de Vries *et al.*, 2016), in-phase finger movements (~8 Hz, Evans and Baker, 2003), bilateral precision grip (7-13 Hz, Boonstra *et al.*, 2009b), walking (8-15 Hz, Halliday *et al.*, 2003), and balance

(6-11 Hz, Boonstra *et al.*, 2009a). We speculate that these tasks could involve similar spinal circuitry to that recruited during spasms after spinal cord injury. Interestingly, bilateral synchronization is a common finding in the literature on this frequency band. The spinal cord is known to contain populations of commissural interneurons, which can mediate coupling between the two sides (Bannatyne *et al.*, 2003; Jankowska *et al.*, 2009). These have also recently been demonstrated in primate cervical cord (Soteropoulos *et al.*, 2013), so that a spinal contribution to bilateral synchronization at low frequencies is plausible even for tasks involving bimanual action.

Intermuscular coherence at 3-10 Hz has also been reported in myoclonus dystonia, which is a movement disorder with a genetic basis (Grosse *et al.*, 2004; Foncke *et al.*, 2007; van der Meer *et al.*, 2010). Similar to the spasms investigated here, this is characterized by involuntary muscle contractions. These tend to be prolonged and cause twisting movements, possibly accompanied by myoclonic jerks (Grosse *et al.*, 2004). Intermuscular coherence at low frequencies in these patients correlates with the presence of dystonia (Foncke *et al.*, 2007). Dystonia is believed to occur due to basal ganglia dysfunction, which results in decreased cortical inhibition (Morgante and Klein, 2013). This would alter descending input to the cord, possibly providing a common pathway for the generation of this pathological activity with spinal cord injury.

One unanswered question is the extent to which low frequency oscillations can be generated solely by the isolated spinal cord, or whether they require intact sensory input. In myoclonus-dystonia, van der Meer and colleagues (2010) used external perturbations to explore the role of sensory feedback, and concluded that it probably played a minimal role in low-frequency drive. Previous work from this laboratory showed that sensory input to the cord is configured to produce phase cancellation around these frequencies with descending input from the cortex (Kozelj and Baker, 2014). This suggests the possibility of a subtle interplay between central and peripheral circuits which can either cancel, or possibly generate, low-frequency activity. This would be similar to the situation for the spinal central pattern generator circuits which operate at much lower frequencies to generate locomotor activity. Whilst these can generate rhythmic alternation of activity in an isolated spinal cord ('fictive locomotion'), in the intact animal sensory input is integrated into the rhythm generation, allowing for example adjustment of walking speed to match the speed of a treadmill (Frigon, 2017).

The specific spinal circuits generating oscillatory activity in the 2-13Hz frequency band found here are still to be uncovered. Work on myoclonus dystonia, which is a condition that generates similar involuntary contractions as the spasms observed in spinal cord injury as well as similar loss of descending control, suggests sensory input does not drive such oscillations (van der Meer *et al.*, 2010). The suggestion that locomotor spinal circuits are involved in producing these oscillations seems in line with the fact that they were found in lower limb muscles and in patients with lost connection between spinal cord and higher centres since the spinal cord alone is capable of producing locomotor rhythmicity in decerebrate animals, although the frequency of the CPGs responsible for this activity is lower than the ones observed here (Frigon, 2017; Minassian *et al.*, 2017). Therefore, the low-frequency oscillations reported here during involuntary spasms might play an important role in human spinal locomotor circuitry. The fact that such oscillations were shown during natural spasms could have interesting implications for the proposition of plasticity protocols or other forms of interventions aiming at strengthening connections in the circuits responsible for such oscillations with the final goal of recovering function after a spinal cord lesion.

In summary, this is the first report to demonstrate that intermuscular coherence at low frequencies (2-13 Hz) can be produced entirely by the spinal cord. Whilst we cannot rule out a contribution from supra-spinal structures in the intact nervous system, it is likely that at least part of the synchronous activity in this frequency range observed in healthy subjects also has a spinal origin.

Chapter 6.
Enhancing spinal circuits for tremor reduction with non-invasive peripheral nerve stimulation

6.1 Abstract

Tremor is an involuntary oscillation of a limb segment. While physiological tremor is present in healthy people and does not affect the performance of individuals' daily life activities, pathological tremor can severely compromises one's abilities to perform even very simple routine motor tasks. The amplitude of physiological tremor is small because oscillations at tremor frequency in primary motor cortex (M1) and spinal cord are opposite in phase to each other, resulting in phase cancellation at the motoneuron level. Synaptic strength can be altered by temporally precise stimulation, following the principles of spike-timing dependent plasticity (STDP). It is hypothesized here that peripheral nerve stimulation given at the correct phase could induce plasticity in interneurons in the spinal cord strengthening connections to optimize phase cancellation between M1 and spinal cord. We carried out experiments assessing tremor before and after a stimulation intervention both (1) using a wearable device that subjects wore for long periods as they went about their normal daily life activities whilst receiving stimulation, and (2) in a lab-based protocol in which stimulation was given at a much higher rate inside the lab while the subject performed a tremor-inducing task. In both cases stimulation was given at different phases of ongoing tremor with the purpose of testing the ability of the stimulation protocol to produce plastic effects to cause phase-dependent modulation of tremor. Results from the first experiments using the wearable device showed only modest evidence for tremor increase in the 45° phase. In addition, the control condition with no stimulation caused tremor reduction, which was likely to be attributed to a placebo effect since this was the first condition tested for all subjects. Results from the second set of experiments, with a lab-based short version of stimulation intervention, showed reduction in tremor in the control condition with no stimulation and no clear phase-dependent modulation of tremor after stimulation. In conclusion, these studies showed that the tremor assessment was adequate to evaluate possible changes in tremor after stimulation and the algorithm used was efficient in detecting tremor

oscillations in the EMG signal on real time and triggering stimulation at specific phases of ongoing tremor. However, no clear phase-dependent modulation of tremor was observed on all protocols. Future studies can now use the progress achieved with the tremor assessment and stimulation protocol to improve methodology and continue to explore the potential of non-invasive peripheral nerve stimulation to reduce pathological tremor through plastic changes in connectivity at the spinal cord level.

6.2 Introduction

6.2. 1 Tremor

Tremor is an involuntary oscillation of a limb segment. It can be either physiological or pathological. Physiological tremor occurs in the 8-12 Hz frequency band, is present in healthy humans to varying degrees and has little or no effect on daily life activities. Three principal components are thought to drive physiological tremor: mechanical oscillations at the limb resonant frequency, oscillations around reflex feedback loops and centrally generated rhythmic motor output (Elble and Koller, 1990).

Pathological tremor, on the other hand, can severely compromises one's ability to perform trivial tasks, and is the most common movement disorder encountered in adults (e.g., Fasano and Deuschl, 2015). The most common forms of pathological tremor include essential tremor, Parkinsonian tremor, cerebellar tremor, amongst others. These types of tremor vary in the frequency band in which they manifest as well as in their origin and behavioural outcome (e.g., resting tremor, tremor during movement, etc).

- *Physiological tremor: phase cancellation between oscillations in M1 and spinal cord*

Recent work has provided insight into why physiological tremor is of such small amplitude as not to interfere significantly with the execution of daily life motor tasks. The fact that even though M1 presents oscillations at 10 Hz, which is the tremor frequency range, those are usually not coherent with muscular activity, led authors to

speculate on the existence of a neural system, possibly in the spinal cord, that 'filters' 10 Hz oscillations to motoneurons (Williams and Baker, 2009). Work with a computational model demonstrated that Renshaw cells are one type of spinal system serving such a purpose, reducing muscle activity and corticomuscular coherence at 10 Hz via recurrent inhibition. The authors emphasized however that this is not the only spinal system responsible for reduction in 10 Hz activity at the motoneuron level, and consequently reduction of tremor, since recurrent inhibition from Renshaw cells could decrease but not completely abolish 10 Hz corticomuscular coherence (Williams and Baker, 2009). Williams, Soteropoulos and Baker (2010) demonstrated in monkeys that oscillations in the spinal cord intermediate zone at around 10 Hz are actually anti-phase to 10 Hz oscillations in M1 (Figure 28A). The phase cancellation that results from that is the reason why 10 Hz activity at the motoneuron level is small and consequently so is physiological tremor amplitude. The function of spinal circuits would be therefore to amplify cortical commands so motoneurons would get closer to firing threshold but also phase-invert those commands at 10 Hz cancelling this frequency in motoneurones (Figure 28B).The authors conclude that fluctuations in tremor amplitude occur due to the limited capacity of spinal circuits to adjust the amplitude of its oscillations to changes in amplitude of cortical oscillations at around 10 Hz (Williams *et al.*, 2010). This important finding forms the basis for the hypothesis of this study. Subsequently, Kozelj and Baker (2014) demonstrated that the phase difference between oscillations at tremor frequency in M1 and spinal cord results in large part from different responses to afferent input oscillations.

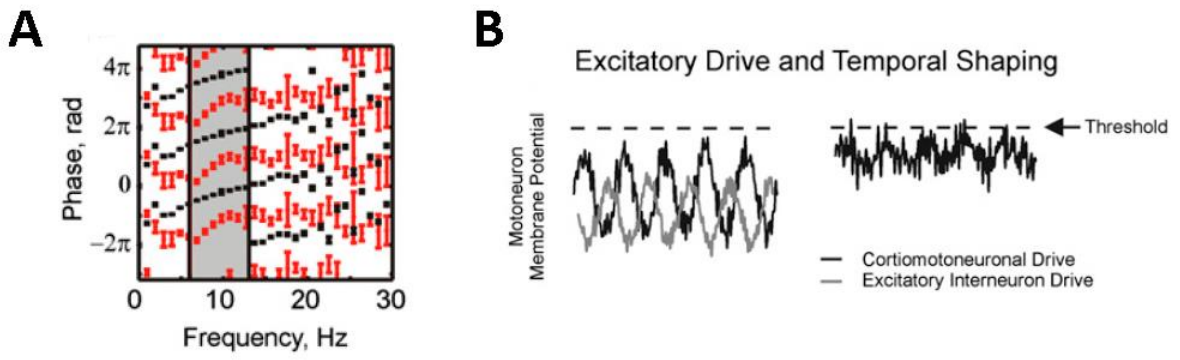

Figure 28. **A**, Phase of coherence between tremor measured with accelerometry and local field potentials recorded in spinal cord intermediate zone (red points) and in primary motor cortex (M1, black points) obtained from two monkeys during a slow finger movements task which induces tremor. **B**, Anti-phase relationship between spinal cord and M1 will increase membrane potential of motoneurons approximating it to firing threshold and also promote cancellation of tremor frequency. From WIliams et al. (2010).

6.2. 2 Spike timing-dependent plasticity (STDP)

One of the reasons for the remarkable capabilities of the human brain in generating movement is the fact that the nervous system is capable of adapting and modifying neural connections on the basis of experience. This process has been termed plasticity and great progress has been achieved in the past few decades in understanding the mechanisms underlying such changes in connectivity (Markram *et al.*, 2011). Specifically, long-lasting strengthening and weakening of synapses based on patterns of activity have been documented and named long-term potentiation (LTP) and depression (LTD), respectively. The precise timing and order of spikes from pre- and post-synaptic elements have shown to be crucial for inducing LTP or LTD, giving rise to what is called spike-timing dependent plasticity (STDP). Figure 29 is a classical representation of the general rules governing this process and shows the magnitude and type of synaptic change according to different intervals of pre and post synaptic action potentials for experiments in hippocampus (Abbott and Nelson, 2000).

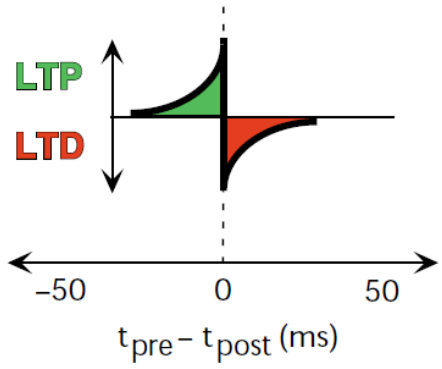

Figure 29. Magnitude and type of synaptic change according to different intervals of pre and post synaptic action potentials. From Abbott and Nelson (2000).

In typical Hebbian STDP when the presynaptic EPSP occurs before the postsynaptic spike LTP is induced, i.e., the EPSP magnitude is increased; when postsynaptic spike occurs before presynaptic EPSP LTD is induced, i.e., the EPSP amplitude is decreased, as illustrated in Figure 30. The precise timing at the millisecond level is an important factor: the time window is around 0 to 20 ms to

induce LTP (pre leads post) and around 0 to 20-100 ms to induce LTD (post leads pre) (Feldman, 2012). The description of such effects gave rise to several studies with paired stimulation in which the precise timing of activity was controlled in a manner to strengthen or weaken connections, for example on motor cortical output (Stefan *et al.*, 2000). Importantly, the duration of the stimulation time needs to be long enough to produce long-lasting plastic effects in the synaptic connections.

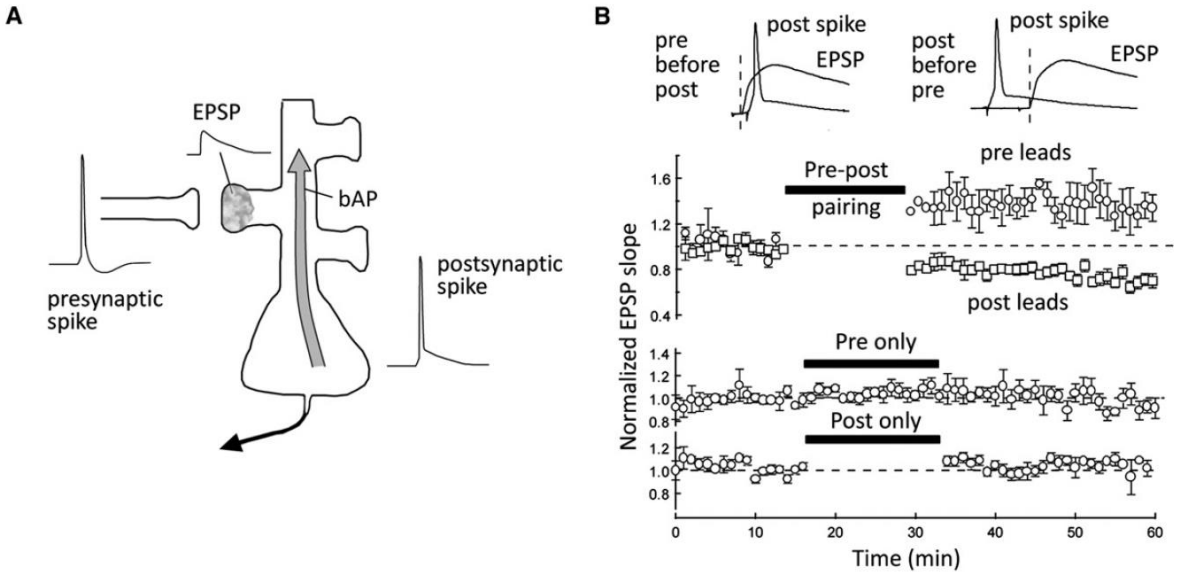

Figure 30. **A**, schematic representation of a presynaptic neuron that connects to a postsynaptic dendrite. **B**, demonstration of effects of paired pre and postsynaptic events. When presynaptic activity leads EPSP is increased, when postsynaptic activity leads EPSP is decreased and activation of pre and postsynaptic elements alone does not change EPSP. From Feldman (2012).

6.2. 3 Hypothesis

Phase cancellation occurring between oscillations at around 10 Hz in M1 and spinal cord is the reason why the amplitude of physiological tremor is small. Changes in tremor amplitude occur due to ineffective action of spinal cord circuitry to adjust the amplitude of its oscillations to variations in the amplitude of motor cortical oscillations (Williams *et al.*, 2010). It is hypothesized here that peripheral nerve stimulation could be used to induce plasticity in interneurons in the spinal cord, optimizing the phase cancellation between 10 Hz oscillations in spinal cord and M1, i.e., changing the amplitude of oscillations in spinal cord to match the amplitude of motor cortex oscillations and better cancelling them out at the motoneuron level. The measurement of EMG activity directly assess motoneuron firing and frequency

analysis can then reveal when motoneurones are firing. Peripheral nerve stimulation given at a specific phase of the detected EMG activity would travel through afferents reaching interneurons in the spinal cord strengthening this connection so the activity of these interneurons at that phase would be stronger. Since it is unknown which phase would be the correct one for phase cancellation with M1 four different phases were tested initially. Assuming one of these phases would be opposite to M1 oscillations (causing phase cancellation), it is hypothesized this one would reduce tremor by increasing amplitude of oscillations in spinal cord to match amplitude of M1 oscillations (Figure 31 shows a schematic representation of this hypothesis of optimization of phase cancellation). The phase opposite to that would increase tremor, since this phase would be strengthening the connection for interneurons to fire in phase with oscillations from M1, summing them up as oppose to cancelling them out. The remaining two phases would not alter tremor. On the other hand, if the amplitude of oscillations in the spinal cord was actually greater than the amplitude of M1 oscillations it would be necessary to weaken the activity of interneurons in the spinal cord at the phase opposite to M1 oscillations, therefore reducing the amplitude of oscillations in the spinal cord so they would match the smaller amplitude of oscillations in M1. Such weakening would occur if stimulation is delivered just after the firing of interneurons, causing LTD instead of LTP, according to the principles of STDP. Since tremor oscillations occur at around 10 Hz each cycle lasts 100ms so the difference between each phase tested here is 25ms, which would be appropriate to fall within time windows adequate to induce STDP. Therefore, by testing those four different phases it would be possible to investigate all these possibilities delivering stimulation right before and right after the firing of motoneurones, strengthening and weakening connections, respectively, and in-phase and anti-phase with M1 oscillations.

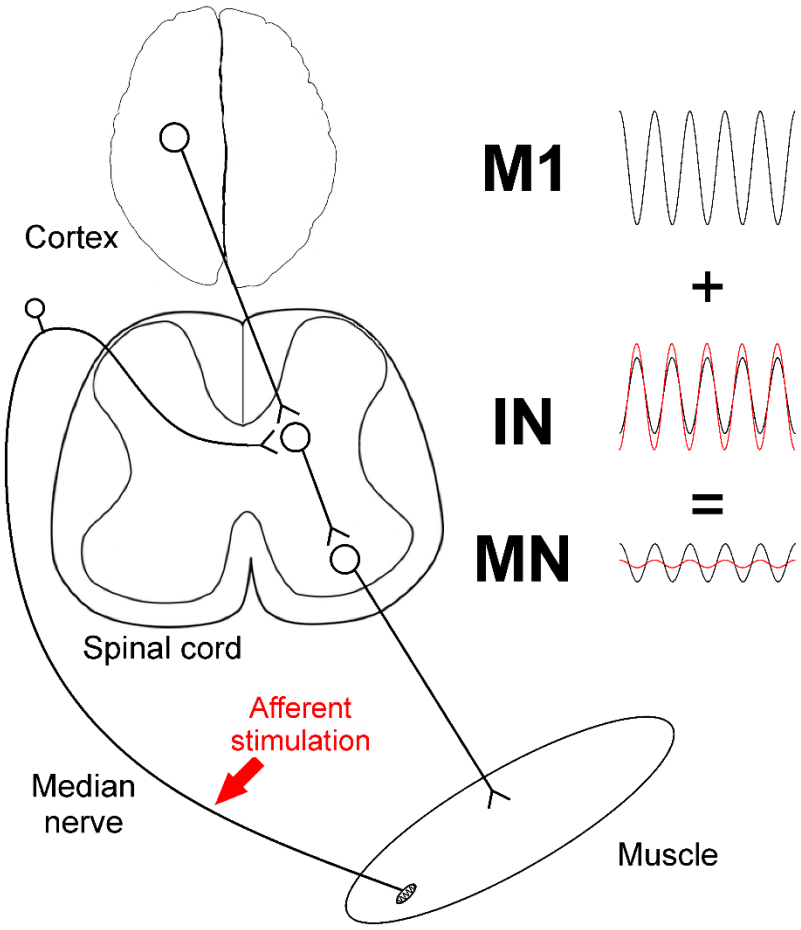

Figure 31. Schematic representation of the study's hypothesis. The reason why physiological tremor is small is the fact that oscillations at tremor frequency (~10Hz) exist in primary motor cortex (M1) and at the spinal cord (interneurons, IN) but are phase opposite to each other, so they cancel each other out at the motorneuon (MN) level (all three black traces). Afferent stimulation given at median nerve with precise timing could strength connections of IN at the spinal cord level, increasing the amplitude of spinal cord oscillations to better match the amplitude of M1 oscillations, improving even more the amount of cancellation of ~10Hz oscillations at the MN level (red traces), i.e., decreasing tremor.

6.2. 4 Aims

The overall purpose of this study was to develop a wearable electronic device protocol which would modify spinal circuits for tremor cancellation, making them more efficient. Such a protocol would be useful to develop further approaches in patients to ameliorate pathological tremor (e.g., Parkinsonian tremor, essential tremor, cerebellar tremor, amongst others).

In order to reach this goal first a tremor assessment was developed to be used to compare tremor before and after device intervention. Subsequently, this tremor assessment was used to conduct a wearable device study using stimulation at four

different phases to measure possible plastic effects causing changes in tremor. Since results from this stimulation intervention failed to show consistent and clear phase dependent modulation of tremor, subsequently a short version of the study was conducted with only two phases of stimulation. These three stages (i.e., tremor assessment, wearable device study and short version study) are described below.

6.3 Tremor assessment

The optimization of the tremor assessment included choosing the appropriate number of trials, task parameters, time of assessments, measurements, among other factors. Tremor assessments took place both before and after intervention with device stimulation.

While resting their right arm participants had a position sensor (Polhemus Inc.) attached to their index fingernail and this provided feedback on the finger position through a cursor on a screen. On the screen, a target cursor also appeared remaining in the centre for two seconds (centre phase), moving towards a different place during 2 seconds (tracking phase), and remaining in this new location for another 2 seconds (hold phase). Participants had to move their index finger to follow the target cursor the entire time as accurately as possible. The total 6 seconds of the 3 phases comprised one trial. A two-second rest period was provided in between trials and a total of 40 trials was recorded. In the tracking phase the target cursor could go from the centre to one of eight different locations – up, down, right, left, diagonally up and right, diagonally up and left, diagonally down and right, diagonally down and left – and the total finger displacement for each one was 20 mm (velocity of 10 mm/s). Figure 32 illustrates the task.

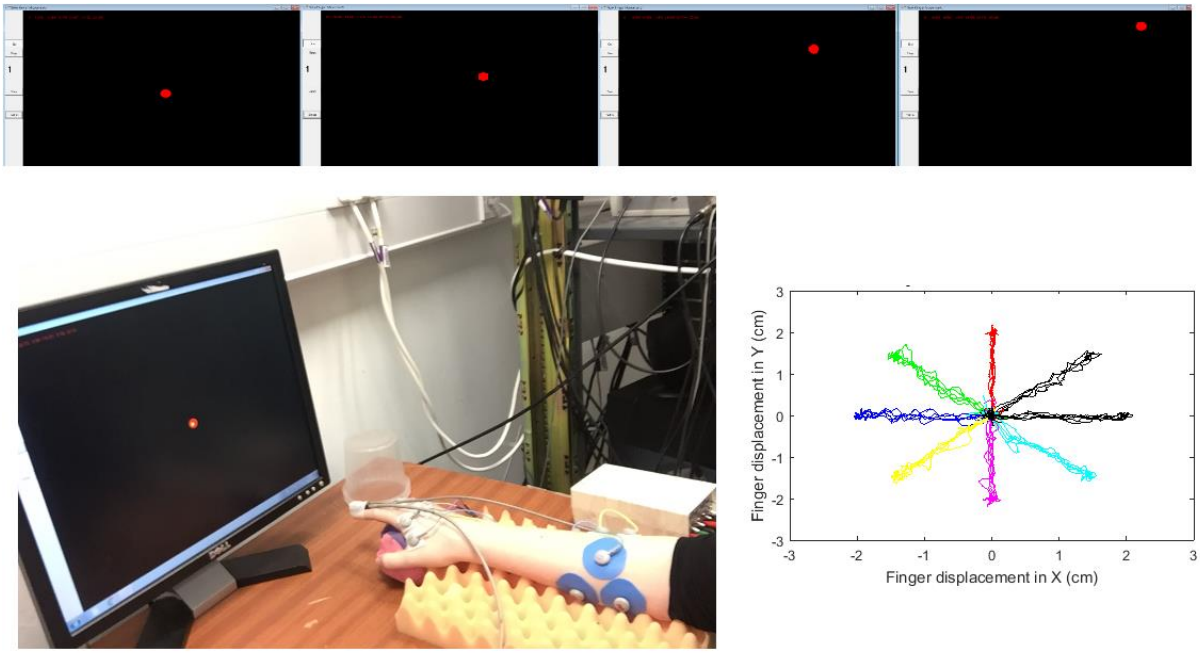

Figure 32. Illustration of the tremor task. Top figure shows example of target displacement from centre to final hold position for one target type (diagonally up and right). Bottom left figure shows a participant performing the task and bottom right shows an example of subject's performance with finger displacement data in vertical and horizontal axis with different colours for all 8 target types.

EMG and accelerometry were used to assess tremor. An accelerometer was attached to participants' right index finger nail providing information on acceleration in x, y and z axis with a sampling rate of 1000 Hz. EMG recordings were carried out in four muscles, first dorsal interosseous (1DI), second dorsal interosseous, flexor digitorum superficialis (FDS) and extensor digitorum comunis, however, only data from 1DI and FDS are shown throughout the study since these two muscles were representative of the overall EMG results. Sampling rate for EMG recordings was 5000 Hz. The software Spike2 was used for recordings of all signals. EMG signals were rectified for analysis. Data from the accelerometer and rectified EMG signals were separated in 1-second windows and subsequently the power spectra was calculated in each window using Fourier Transforms, according to the formula:

$$Power(f) = \frac{1}{N}\sum_{i=1}^{N} X_i(f)\, X_i^{*}(f) \quad (1)$$

, where $X_i(f)$ and $X_i^*(f)$ are the Fourier transform of the signal and the complex conjugate of the Fourier transform of the signal, respectively, for the *i*-th section of data at frequency *f*. Power spectra were then averaged across all 1-second windows

from all 40 trials, separately for each of the three phases of the task (centre, track and hold). In the case of the accelerometer data the power spectra from the accelerometer in the x direction were summed with the power spectra from the accelerometer in the y direction. Finally, the sum of the power between 6 and 13 Hz was calculated as the main variable used in the study. Figure 33 shows an example of the signals recorded depicting the different phases of the task and the 1-second windows used to calculate power spectra separately for each one of these phases.

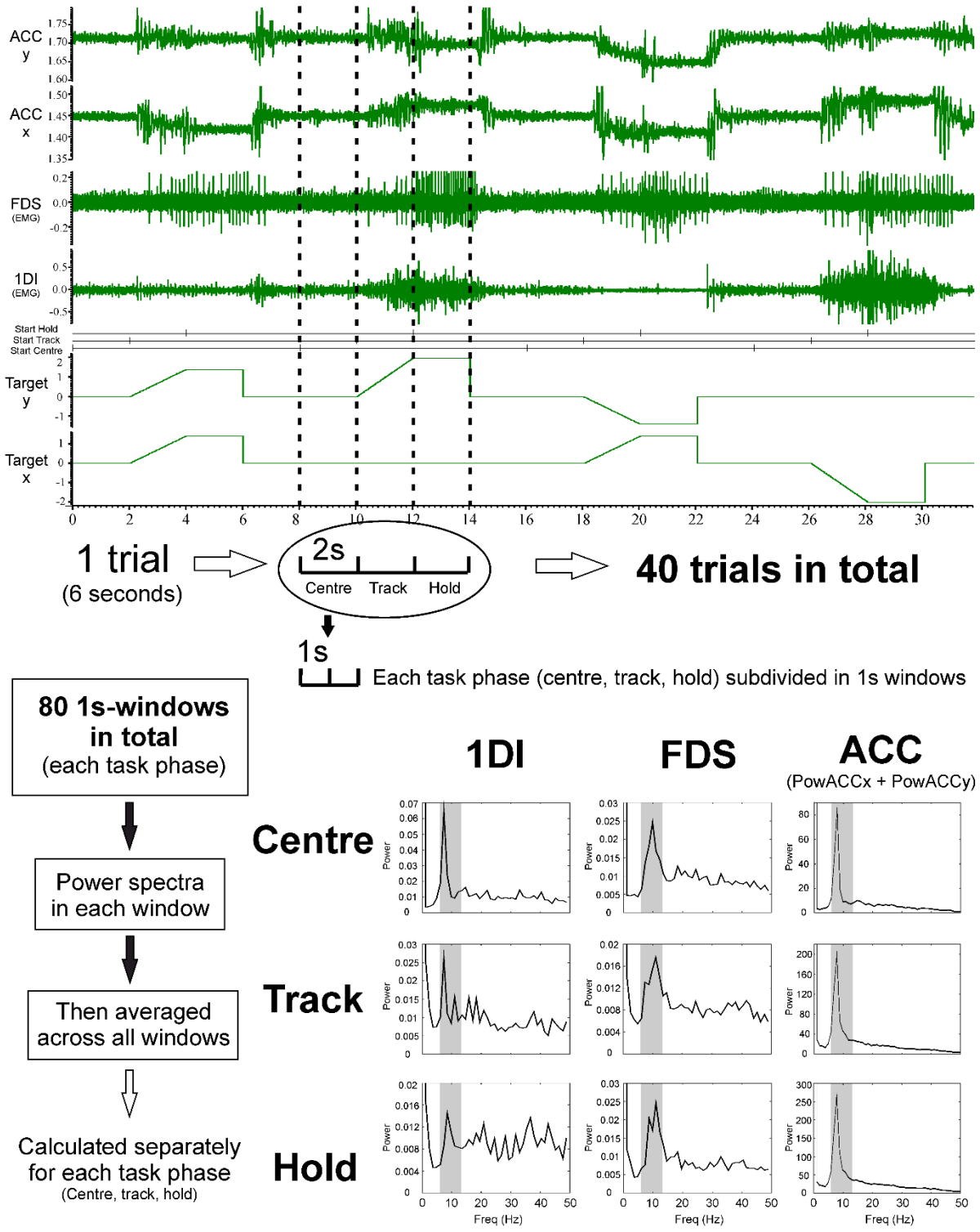

Figure 33. Example of recording of signals during tremor assessment. The task comprised 40 trials. Each trial lasted 6 seconds: 2 seconds on the centre phase, 2 seconds on the track phase and 2 seconds on the hold phase. For each task phase separately data was further divided in 1-second windows which were used to calculate power spectra. This analysis was conducted for EMG signals from 1DI and FDS and for accelerometer (ACC) data, in which power from ACC in the x axis was summed with power from ACC in the y axis.

6.4 Wearable device study

6.4. 1 Methods

- *Participants*

Participants were eight healthy adults aged between 23 and 31 years-old, with no history of neurological disease or pathological tremor, who signed a written consent form prior to participation. All experiments were covered by ethical approval from the Ethics Committee, Newcastle University Medical Faculty.

- *Wearable device protocol*

Measurements occurred at around lunch time, between 11am and 2pm, on two consecutive days (pre and post intervention) at the same time of day to avoid circadian variations in tremor interfering with results.

Participants wore the device during one day, excluding the period when they were sleeping, when the device was removed. After the first tremor assessment volunteers were fitted with the device and were free to go about their normal daily activities whilst wearing it. They received instructions on how to remove the device and fit it back on themselves. Subjects were advised to try to wear the device as long as possible, taking it off just before going to sleep and putting it back right after waking up in the next morning.

The wearable electronic device (Figure 34) is slightly bigger than a smartphone and operates with three AA batteries, which give about 15 hours function. A digital signal processor performs real-time analysis of signals recorded and those are stored in an SD card memory for later analysis. The device was programmed to record EMG signals from FDS and give stimulation to the median nerve at the wrist (intensity just below motor threshold). Recordings were made from FDS since pilot studies showed there was a clear peak at tremor frequency in the power spectrum from that muscle in the described tremor task.

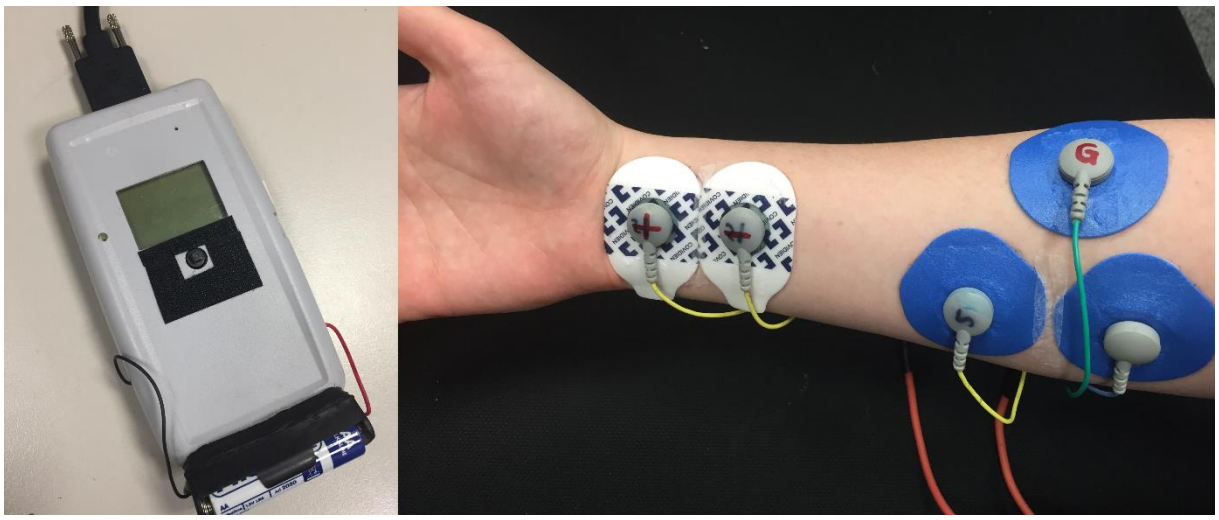

Figure 34. Wearable device (left) and electrodes location (right). Two electrodes (plus a ground electrode) recorded EMG from FDS (blue electrodes) and two electrodes (white) were used to give electrical stimulation to median nerve at wrist.

Five different conditions of wearable device intervention were tested in each subject: one control condition in which the device recorded EMG signals but gave no stimulation, and four other conditions with median nerve stimulation given at different phases of tremor oscillations (45°, 135°, 225° and 315°). A minimum of 1-week interval was used in between stimulation conditions to avoid possible plastic changes caused by previous stimulation interfering with results. The control condition was the first to be tested so EMG data recorded could be used to adjust parameters of stimulation for the subsequent stimulation conditions.

The gain of the EMG recording was adjusted on the device by recording a maximum voluntary contraction and that was used to choose the appropriate gain to detect mainly contractions between 0 and 50 % of maximum, since those are the most frequently observed in daily life activities (i.e., the device was not able to detect contractions above 50% of maximum and was very sensitive to register contractions below that).

- *Processing of EMG signal in the wearable device*

Signals were recorded with a sampling rate of 1000 Hz. Signals were first rectified and then filtered with a low-pass filter at 35 Hz using 40ms windows. A convolution was computed between filter coefficients and the rectified EMG data in 40ms windows. Real time analysis of the data was performed in windows of 400 ms updated every 1 ms. To optimize the performance of the device processing data in real time signals were down-sampled to 100 Hz to compute all analysis of tremor

parameters. The down-sampling of EMG data to 100 Hz after filtering was done by just considering the first values at every 10 registered values and ignoring the intervening ones. Even though the 400ms window of data used for analysis was down-sampled to 100 Hz, the calculation of parameters which determine whether stimulation would be given or not was computed every 1ms.

Real and imaginary wavelets were calculated specifically at tremor frequency. Tremor frequency was chosen as the frequency at the peak observed between 6 and 13 Hz in the EMG power spectrum from FDS during the tremor assessments, which could be different for each subject. An exponential function was multiplied by a cosine function to generate the real wavelet and by a sine function to generate the imaginary wavelet, according to the formulae:

$$\mathrm{W_R(t) = e^{1.2ft} \cos\ (2\pi ft)} \qquad -0.4s \le t \le 0 \tag{2}$$

$$W_I(t) = -e^{1.2ft}\, sin(2\pi ft) \qquad -0.4s \le t \le 0 \tag{3}$$

, where W_R is wavelet real, W_I is wavelet imaginary, f is the frequency of tremor (~10 Hz) measured individually for each subject and t is time (in steps of Δt=10ms). Mean values were subtracted from each wavelet to ensure zero-mean wavelets and a subsequent normalization– wavelet divided by the square root of the sum of the squares of wavelet – was conducted so both real and imaginary wavelets would have the same scale (power), as described in the formulae:

$$W_R(t) = W_R(t)\ -\ \frac{1}{N}\sum_{i=1}^{N} W_R(-i\Delta t) \tag{4}$$

$$W_I(t) = W_I\ (t) - \frac{1}{N}\sum_{i=1}^{N} W_I\ (-i\Delta t) \tag{5}$$

$$W_R(t) = \frac{W_R(t)}{\sqrt{\sum_{i=1}^{N} {W_R}^2(-i\Delta t)}} \tag{6}$$

$$W_I(t) = \frac{W_I(t)}{\sqrt{\sum_{i=1}^{N} {W_I}^2(-i\Delta t)}} \tag{7}$$

For real time analysis a convolution was then computed between EMG data and real wavelet and another one between EMG data and imaginary wavelet resulting in

real (Z_R) and imaginary parts (Z_I), respectively, according to the formulae (where *x* represents the EMG data):

$$Z_R = \sum_{i=-40}^{0} W_R(i\Delta t)\, x(i\Delta t) \qquad \Delta t = 10ms \tag{8}$$

$$Z_I = \sum_{i=-40}^{0} W_I(i\Delta t)\, x(i\Delta t) \qquad \Delta t = 10ms \tag{9}$$

Total power (S^2) was calculated as the sum of the squares of the EMG signal, as described in the formula:

$$S^2 = \sum_{i=-40}^{0} x^2(i\Delta t) \tag{10}$$

Fraction of power at tremor frequency (*FractPower*) was then defined as the sum of the squares of real and imaginary parts divided by the sum of the squares of the signal (total power, S^2), as described in the formula:

$$FractPower(t) = \frac{Z_I^2(t) + Z_R^2(t)}{S^2(t)} \tag{11}$$

Phase (θ) was defined using the real and imaginary parts, where:

$$tan(\theta) = \frac{Z_I}{Z_R} \tag{12}$$

These 3 parameters (fraction of power at tremor frequency, phase and total power) were calculated in real time and used to decide whether to give stimulation or not, as explained in detail below.

- *Parameters for stimulation*

Total power was computed as a measure of the amount of muscle activity, so periods of rest could be differentiated from periods of activity (even if of small magnitude) in order to give stimulation only when muscular activity was present. A threshold was set based on simple visual inspection of data from the control

condition. The first parameter to give stimulation was that total power had to be above this threshold, i.e., muscle is not at rest.

Phase was computed using the ratio between imaginary and real parts. Four different phases were tested in the study: 45°, 135°, 225° and 315°. Using the formulae

$$tan\left(\frac{\pi}{4} + 2\pi 0.01\right) = 1.13 \quad (13)$$

$$tan\left(\frac{\pi}{4} - 2\pi 0.01\right) = 0.88 \quad (14)$$

we determined a 1ms margin (more or less) in which phase would have to fall within for stimulation to be given. In the formulae 0.01 represents 1% of one cycle (1ms as a fraction of 100ms). The sign of the real part and these boundary values were then used to indicate each one of the four phase conditions, as described in Figure 35.

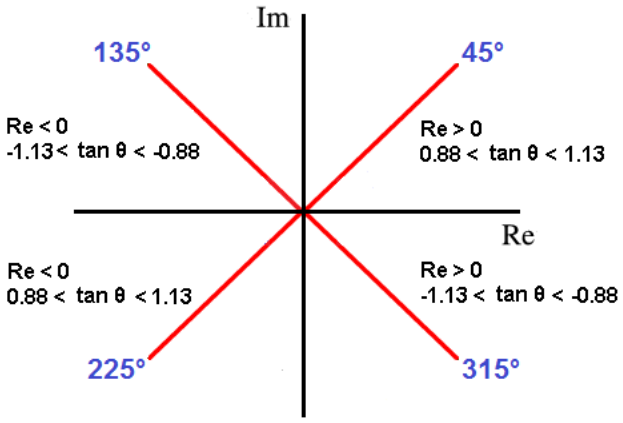

Figure 35. Schematic representation for the phase parameter in each of the fours conditions, 45°, 135°, 225° and 315°. Imaginary (Im) and Real (Re) parts are represented in vertical and horizontal axis, respectively.

Fraction of power at tremor frequency was computed to quantify oscillations at tremor frequency and a threshold was also set. The optimum value for this threshold would be one that is not too low that stimulation would be given too often when only small oscillations at tremor frequency are present, but also one that is not too high that the frequency of stimulation would be too small to induce plasticity. The

procedure to identify this value was to run a simulation with data from the control condition for each one of the 4 phases to be tested. In this simulation, with the fixed values for total power threshold and phase, different values for fraction of power at tremor frequency were tested; those values were percentages of the maximum value registered in the control condition, in steps of 1%. The simulation then provided the rate of stimulation λ that would be given at each value of fraction of power at tremor frequency. We defined an 'effectiveness' measure E as

$$E = FractPower.\lambda \quad (15)$$

We then chose the FractPower threshold to maximise E. The idea behind this was that a low stimulus rate during very strong oscillations might be equivalent to a higher rate during weaker oscillations. The stimulus rate at the maximum of E ranged from 0.13 to 0.28 Hz across all subjects tested.

The threshold was defined, therefore, as the value of fraction of power at tremor frequency which would result in this optimum rate of stimulation and this value was different for each one of the four phases tested. Since small changes in this optimum rate of stimulation could be observed between the four different phases, this value was adjusted to the average rate of all four phases so stimulation rate would be similar in all conditions.

The last parameter was the **minimum interval between stimuli**, which was set as 1 second. This means even if the three parameters above were fulfilled stimulation would not be given if the previous stimulus had occurred less than 1 second before.

In sum, every time the device detected muscular activity (total power) which contained reasonably strong oscillations at tremor frequency (fraction of power at tremor frequency) occurring at a particular phase (phase), stimulation was given, provided that the last stimulus occurred at least one second before (minimum interval). A flow chart describing this process is presented in Figure 36.

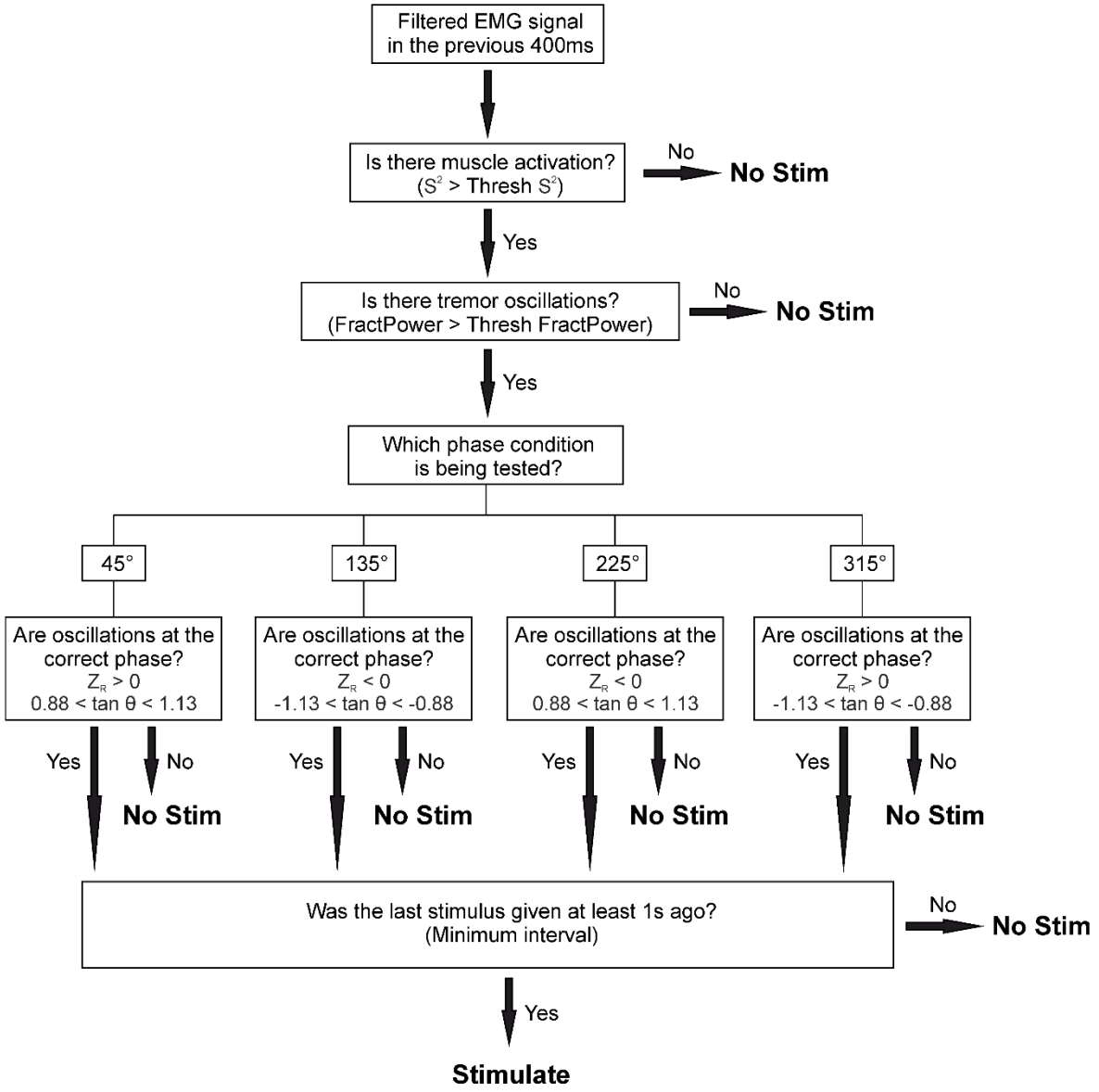

Figure 36. Flow chart describing how the processing of the EMG signal led to the decision, every 1ms, to deliver stimulation or not.

Figure 37 shows data from the wearable device depicting average of smoothed EMG from one subject triggered by stimulation applied with the parameters described in all four phases of stimulation.

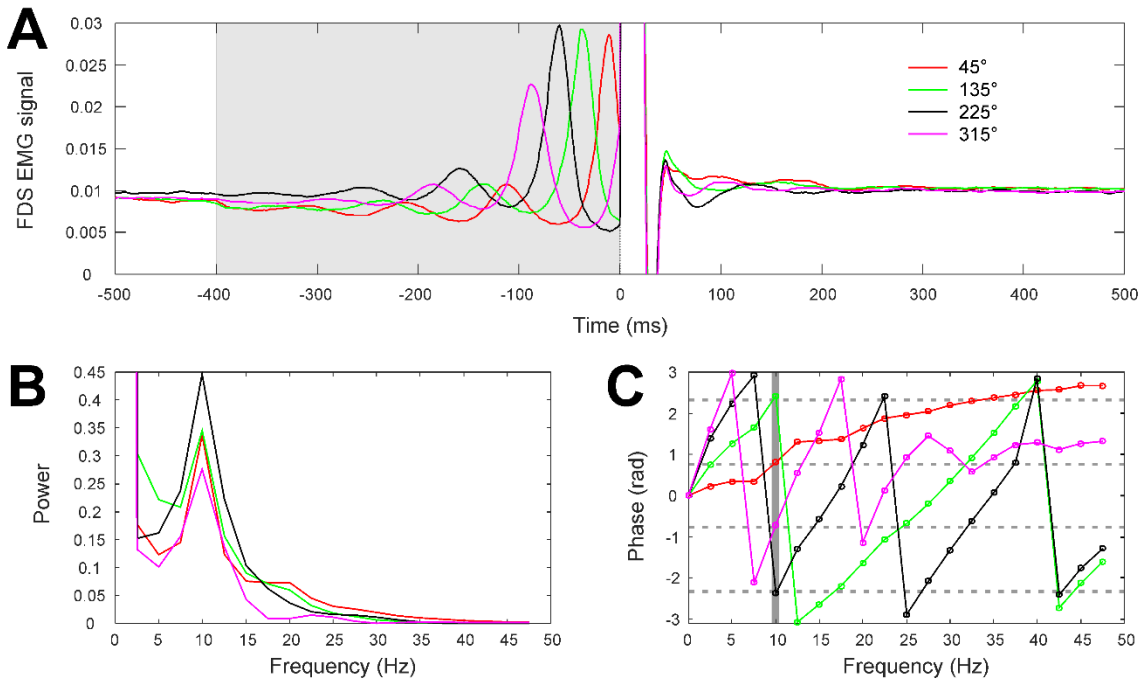

Figure 37. Example of recordings from the wearable device in one subject for all four phase stimulation conditions (45°, 135°, 225° and 315°). **A**, average of smoothed EMG data from FDS triggered by stimulation (Time 0 ms) given for oscillations detected at all four phases at 10 Hz. **B**, power at the 400 ms window preceding stimulation (grey shade in A). **C**, phase at the 400 ms window preceding stimulation (grey shade in A). Vertical grey bar highlights phase at 10 Hz, which is the frequency in which stimulation was given for this subject. Horizontal grey dashed lines highlight the four different target phases of stimulation (indicated in radians, corresponding to 45°, 135°, 225° and 315°).

- *Statistical analysis*

For group averages analysis, the sum of power between 6 and 13 Hz on the 40 trials was computed for all subjects. Post stimulation values, expressed as percentages of pre stimulation values (to reduce subject-by-subject variation), were compared to 100% through t tests, for each of the 5 different conditions. The alpha level was set to 0.05.

To analyse average results investigating possible differences between the 4 phases of stimulation, specifically searching for phase dependent modulation of tremor, Monte Carlo analysis was used. First, a sine wave was fitted to the average results from all four phases of stimulation. The amplitude of this sine wave was then measured. Subsequently the results from all phases of stimulation were shuffled for each subject and the amplitude calculated again 10,000 times. These results were then compared to the original amplitude of the sine wave to show whether this amplitude was significant (significance limit was set as 0.05).

Individual results analysis were conducted separately for each subject. Data from the 80 windows of each phase of the task (windows were 1 second long and each phase of the task lasted for two seconds, with 40 repetitions) was compared before and after stimulation through paired t tests (alpha level was also 0.05). This analysis answered the question of whether that particular subject's tremor had significantly changed after stimulation in each condition. Results from all subjects were put together to show how many subjects significantly reduced, increased or presented no change in tremor.

6.4. 2 Results

Figure 38 shows the average results for EMG and accelerometer data for all experimental conditions.

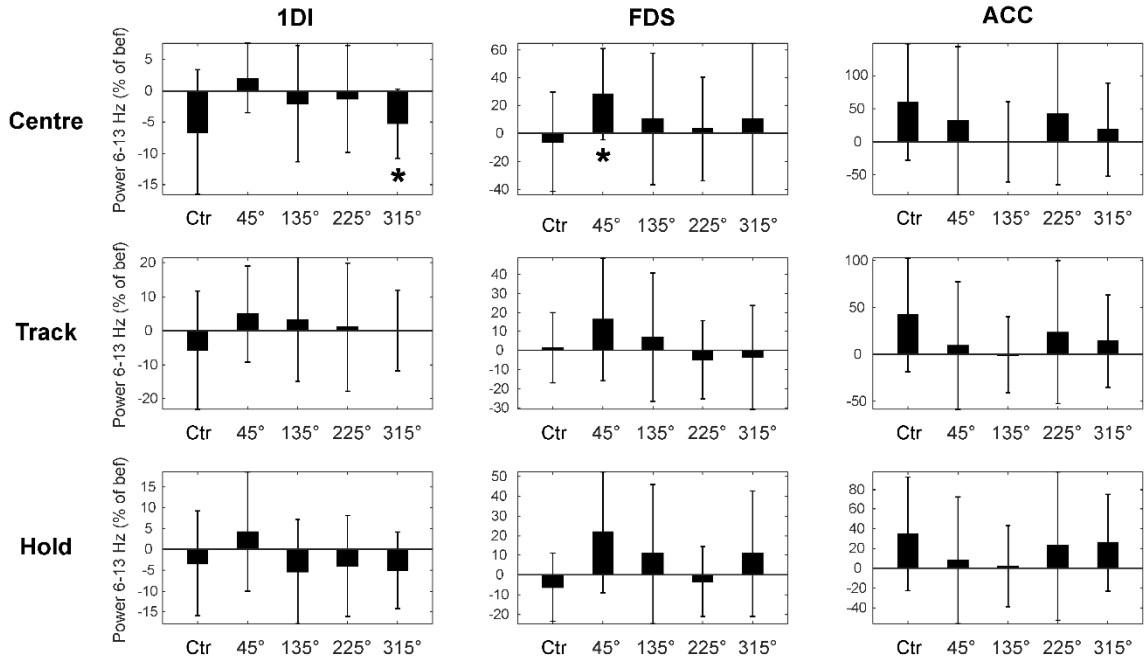

Figure 38. Average results in all five experimental conditions (control, 45°, 135°, 225°, 315°). Sum of power between 6 and 13 Hz, shown as percentage of before (pre- tremor assessment) and subtracted by 100 so that positive values represent increase and negative values represent decrease in tremor after stimulation intervention. Results are presented for all three phases of the task (centre, track, hold) and for EMG signals from 1DI and FDS and for accelerometer data (ACC). (*) indicates significant effect.

Results showed significant differences only for the centre task phase for 1DI in the 315° condition (decrease in tremor measurement after stimulation) and for FDS in

the 45° condition (increase in tremor measurement after stimulation). All the other measures showed no changes in tremor.

Figure 39 shows results from sine wave fit analysis.

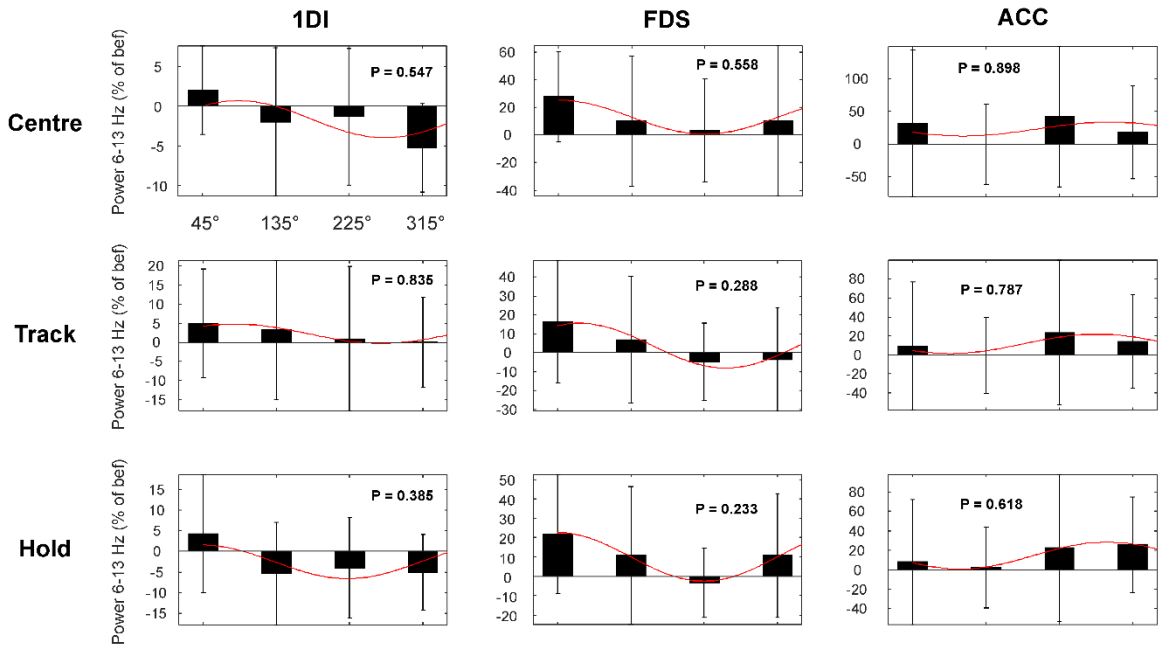

Figure 39. Average results from sine wave analysis. Sum of power between 6 and 13 Hz, shown as percentage of before (pre- tremor assessment) and subtracted by 100 is shown as for Figure 38 for all four phases of stimulation (45°, 135°, 225°, 315°) together with the fitted sine wave (red). Results are presented for all three phases of the task (centre, track, hold) and for EMG signals from 1DI and FDS and for accelerometer data (ACC). P values are shown in each graph displaying result from sine wave Monte Carlo analysis.

Sine wave analysis did not reach significance for any of the task phases on 1DI, FDS and accelerometer results (all $p > 0.05$, see Figure 39). This shows that no phase-dependent modulation of tremor was found for any of the measurements used in the study.

Figure 40 shows individual results for EMG and accelerometer data in all experimental conditions.

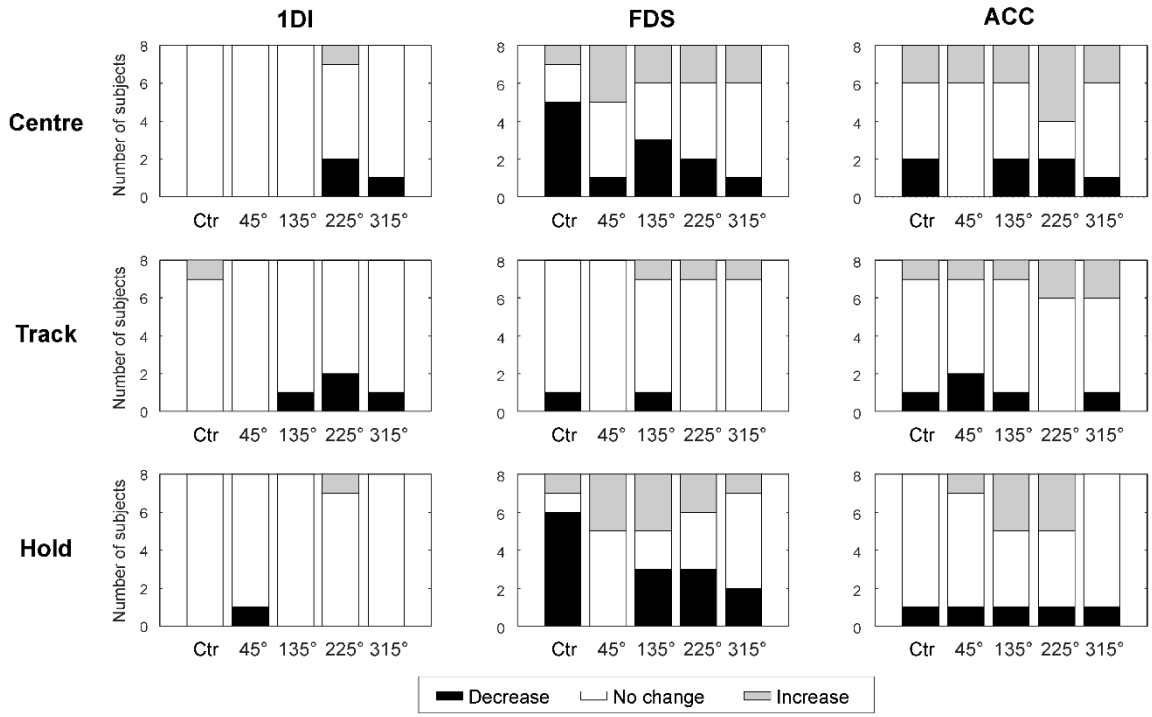

Figure 40. Individual results in all five experimental conditions (control, 45°, 135°, 225°, 315°). Number of subjects presenting significant decrease (black), no change (white) and increase (grey) in tremor assessed by sum of power between 6 and 13 Hz. Results are presented for all three phases of the task (centre, track, hold) and for EMG signals from 1DI and FDS and for accelerometer data (ACC).

The most apparent change in tremor occurred for the control condition, in which 5 to 6 subjects decreased tremor in FDS during the centre and hold phases. A balance between the number of subjects presenting decreases and increases in tremor was observed for FDS in all stimulation conditions. No apparent clear tendencies for increase or decrease in tremor are seen for data from 1DI and accelerometer.

As an additional measure, besides the described tremor assessment, data from the wearable device was analysed to track possible changes in tremor on the FDS muscle throughout the stimulation period. The same tremor measurement, sum of power between 6 and 13 Hz was calculated every approximately 17 minutes of the stimulation period in all five different experimental conditions. Figure 41 shows results from a representative subject.

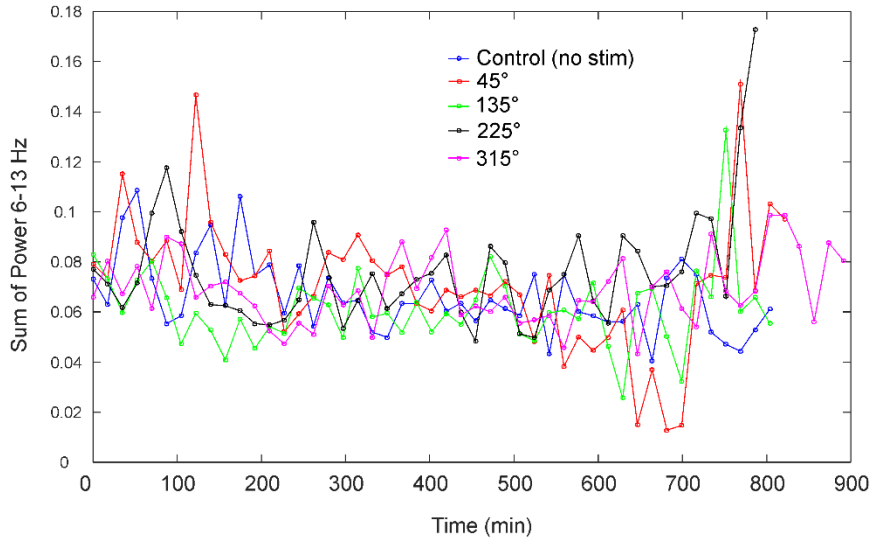

Figure 41. Results from tremor assessed from wearable device EMG data in one representative subject. Tremor, measured as sum of power between 6 and 13 Hz, was calculated every approximately 17 minutes during wearable device use in all five conditions: control (no stimulation, blue), 45° (red), 135° (green), 225° (black) and 315° (pink).

Results showed no clear tendencies differentiating the amount of tremor present in the five experimental conditions. Similar results were observed for the remaining subjects (not shown).

In sum, average results showed that significant changes were very rarely present. The two instances when these happened on average results analysis could be expected by chance. A possible trend for a sinusoidal modulation of tremor across all 4 tested phases was investigated with a sine wave analysis, but this showed that no phase-modulation of tremor was observed above chance levels. Individual results showed again no clear tendencies for tremor change except for the control condition, in which tremor in FDS increased after intervention with no stimulation. The additional analysis with tremor in FDS recorded with the wearable device during stimulation confirms the previously shown tendencies for no changes which differed across the different experimental conditions.

6.4. 3 Discussion

The overall purpose of this project was to develop a wearable device protocol which would modify spinal circuits for tremor cancellation, making them more

efficient. Specifically in this wearable device study the aim was to optimize parameters of device stimulation to generate the most effective protocol for physiological tremor reduction in healthy volunteers.

Although both EMG and accelerometer data were used in this study, pilot studies with this tremor assessment carried out on two days without device use in between showed that accelerometer measures varied a lot from one day to another, while EMG data remained constant in different assessments. For this reason EMG data was considered more reliable to detect changes in tremor. This high variability of tremor assessment using accelerometer might explain why the consistent increase in tremor was observed in the control condition in individual analysis for the EMG data in FDS but not in the accelerometer data.

Results were not clearly consistent with the hypothesis. There was no particular condition in which participants showed tremor reduction, except for the control condition, with no stimulation. Results from the control condition showing tremor reduction after device use are problematic because they could mean that the tremor assessment was not the most adequate or that a placebo effect might take place, which seems more likely since pilot studies using this same tremor assessment in two consecutive days but without device use in between showed no change in tremor.

Considering the first suggestion, that the tremor assessment is not the most adequate, tremor measurements were taken throughout the stimulation time using EMG data from the device. Results from sum of power between 6 and 13 Hz calculated every ~17 minutes of stimulation time showed no apparent differences between the conditions, which corroborates results from the tremor assessment (see Figure 41).

The sine wave analysis failed to disprove the null hypothesis of no phase-modulation of tremor. It is important to note the possibility that since physiological tremor amplitude is small, perhaps plastic changes could be able to cause only tremor increase and not reduction in healthy volunteers. This would still be a useful result since the use of the phase opposite to the one causing tremor increase could be tested in patients to achieve tremor reduction.

The tremor assessment used seems to be adequate to evaluate tremor before and after device intervention by using EMG signals. The code running on the device for the detection of oscillations at specific phases seems to work efficiently, as exemplified by Figure 37. However, the protocol of stimulation needed improvements

to induce plastic changes causing tremor reduction. For this reason, a short version of this experiment was conducted, changing parameters of stimulation including the increase of the rate of stimulation, in a lab based experiment (described below). The lab based experiments allowed faster test of stimulation parameters since the duration of the protocol was considerably shorter compared to the wearable device study protocol. This shorter duration, however, implied the possibility that the stimulation protocol would be less efficient in producing plastic changes to ameliorate tremor. The increase in stimulation rate was adopted as a strategy to attempt to overcome this problem.

6.5 Short version study

The short version of the experiment was conducted to allow better optimization of stimulation parameters. The long version implemented earlier had the advantage of being long enough to be expected to produce plastic changes in connectivity. However, the evaluation of the effectiveness of the stimulation parameters used was extremely time consuming. Since it was concluded that stimulation parameters needed to be optimized this short version could allow changes in such parameters before implementing a long-lasting stimulation protocol. Although the duration of stimulation was notably decreased in this short version, from one day to 45 minutes, stimulation was provided for this 45 minute-period while subjects performed the slow finger movements task described previously that has been proven to produce physiological tremor, which is the main requirement for the device to deliver stimulation adequately to induce plastic changes in circuits producing tremor. Additionally, the stimulation rate was increased considerably. By concentrating stimulation for 45 minutes with high stimulation rate during a task that produces physiological tremor it was expected that enough stimulation would be delivered to be comparable to the one in the long version applied previously. Finally, also with the intent of obtaining results and optimizing device use in a less time consuming manner, only two phases of stimulation were tested in this short version study, 45° and 225°. These two phases were chosen based on the previously obtained results, which indicated possible trends for tremor increase with stimulation at 45° phase and reduction with 225°.

6.5. 1 Methods

The tremor assessment was the exact same used in the previous study. Results from this assessment were compared before and after stimulation intervention.

- *Participants*

Participants were nine (for the control condition) and 15 (for the two simulation conditions) healthy adults aged between 23 and 31 years-old, with no history of neurological disease or pathological tremor, who signed a written consent form prior to participation. Experiments were covered by ethical approval from the Ethics Committee, Newcastle University Medical Faculty. Experimental sessions occurred either in the morning or afternoon, lasting approximately two hours.

- *Stimulation protocol*

The increase in stimulation rate is demonstrated by Figure 42. Instead of delivering a single stimuli at a particular phase of the detected tremor, we varied the number of stimuli given during the entire oscillation so that stimulus rate would peak at the desired phase of stimulation. In that way, stimulation is still delivered at a particular phase of detected tremor – 45° or 225° at approximately 10 Hz, depending on the individual physiological tremor peak frequency – but now the stimulation rate was substantially increased (around 20 Hz, described in more detail below).

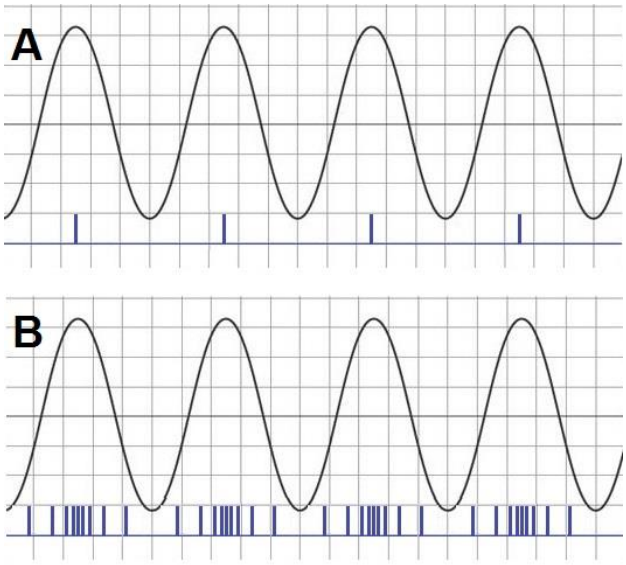

Figure 42. Increase in stimulation rate of short version study compared to previous study. **A** shows method applied previously and **B** shows new method applied in the short version study.

One implication of having this high stimulation rate was that the one second silent period with no stimulus after each stimulation (minimal interval between stimuli) was abolished. Immediately after each stimulation was given an artefact happened in the EMG signal making this piece of data inappropriate to be used in the analysis. The artefact after stimulation lasted approximately 1ms. For this reason we performed all of our calculations ignoring the 2ms subsequent to each stimulation given, as described in the formulae:

$$Z_R = \sum_{i=-40..0, i \notin S} W_R(i\Delta t)x(i\Delta t) \quad (16)$$

$$Z_I = \sum_{i=-40..0, i \notin S} W_I(i\Delta t)x(i\Delta t) \quad (17)$$

, where Z_R and Z_I are real and imaginary parts, respectively and S are data points contaminated by stimulus artefact.

Figure 43 contains a demonstration of the algorithm used for online processing of EMG data and the triggering of stimulation in these tremor experiments. Target stimulation rate was set as 20 Hz. In order to assure these stimulation rate was kept constant the algorithm used involved the following steps. First, the EMG signal was filtered to contain only data in the frequency of interest (~10Hz) and phase shifted to

the phase of interest (either 45° or 225°). Filter coefficients are described in the formula:

$$W(t) = [sin\theta\, sin(2\pi ft) + cos\theta\, cos(2\pi ft)].e^{2\pi ftk} \quad (18)$$

, where *k* was set as 1.2. A convolution was then computed between the EMG signal (*x*) and the filter (*W*), according to the formula:

$$y(t) = \sum_{i=-511}^{0} x(i\Delta t)W(i\Delta t) \qquad \Delta t = 2ms \quad (19)$$

Poisson probability (*P*) was used to determine whether stimulation would be given or not, every 2ms, according to the formulae:

$$\lambda(t) = Ay(t) + B \quad (20)$$

$$P = \lambda.\Delta t \quad (21)$$

, where *y* is the filtered EMG signal, *A* is a scale parameter and *B* is an offset value. Offset *B* was set as 10 Hz.

The product of formulae 19 and 20 (i.e., *P*) resulted in increased probability of triggering stimulation at the specific phase required (see Figure 43). In sum, a uniform random number *r*, chosen every 2ms, is compared with the stimulus probability *P*, which led to an inhomogeneous Poisson process, as described below:

$$r = uniform\ random\ [0,1] \quad (22)$$

$$r < P \quad | Stim \quad (23)$$

$$r \geq P \quad | No\ stim \quad (24)$$

In general, the filtered EMG *y(t)* will have an arbitrary scale, whereas the rate *λ(t)* is required to have a defined mean (here 20 Hz). We therefore needed to find a way to choose the scale parameter *A* correctly.

Scale *A* was equal to scale subtracted by a learning rate *σ* multiplied by the difference between actual stimulation rate *R* and target stimulation rate *R'* (which was set as 20 Hz), as described in the formula:

$$A(t) = A(t - \Delta t) - \sigma.(R(t) - R') \quad (25)$$

Rate of stimulation was defined according to the formulae:

$$R(t) = R(t - \Delta t).e^{\frac{-\Delta t}{\tau}} \qquad \tau = 10s \quad | If\ No\ stim \quad (26)$$

$$R(t) = R(t - \Delta t).e^{\frac{-\Delta t}{\tau}} + \left(1 - e^{\frac{-\Delta t}{\tau}}\right) \qquad \tau = 10s \quad | If\ stim \quad (27)$$

The exponential part of the equation and the τ value set as 10s meant that rate of stimulation was monitored in a long-lasting time scale in such a way that numbers computed 10s ago were less important than numbers computed 5s ago.

The learning rate *σ* was an important part of the algorithm, which could be changed by the experimenter during data collection (initially it was set as 5000). This change could be used at any time whenever a faster or slower learning would seem necessary to reach the target stimulation rate of 20 Hz, which was achieved by fluctuations in scale.

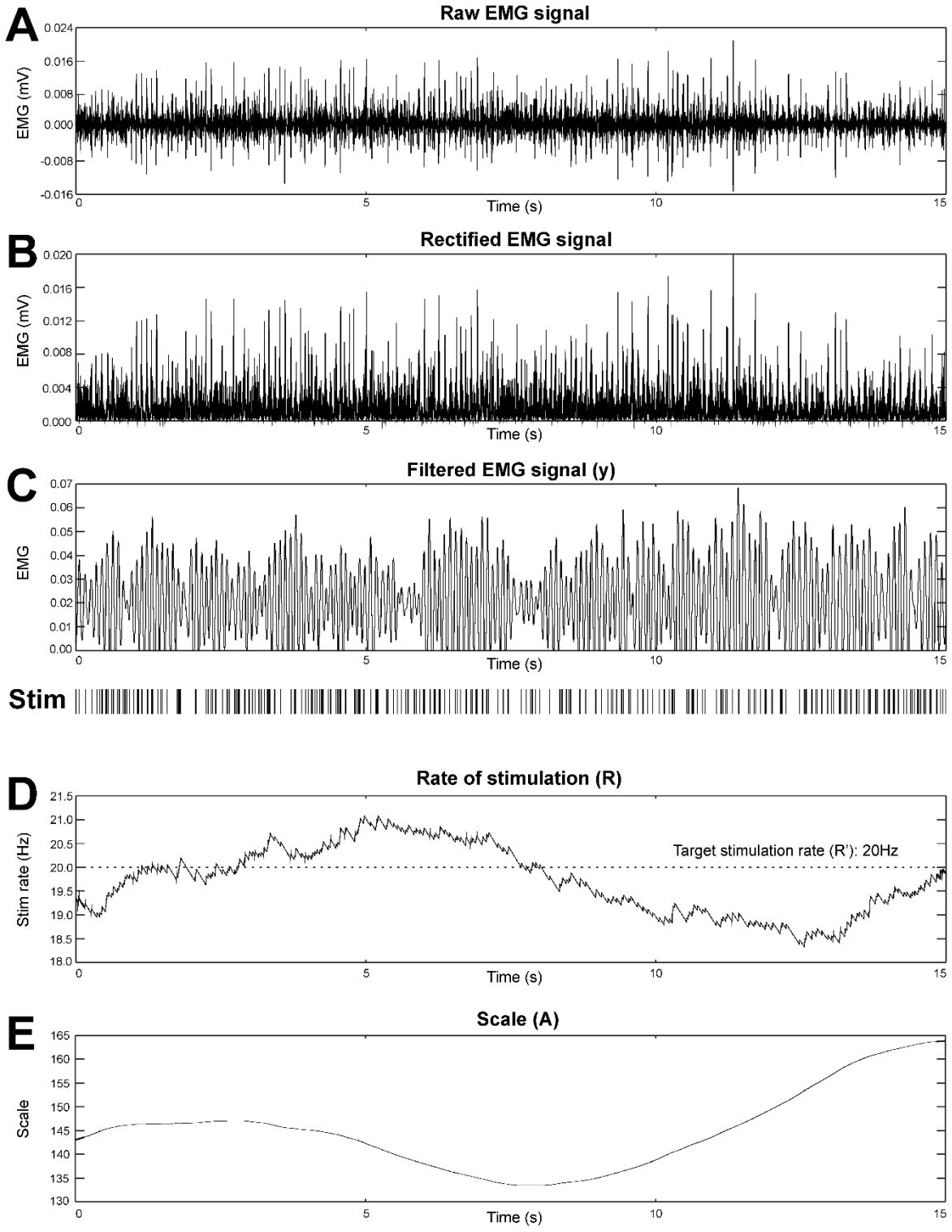

Figure 43. Demonstration of algorithm used to deliver stimulation phase locked with tremor oscillations. **A**, raw EMG signal. **B**, rectified EMG signal. **C**, filtered EMG signal (y) and stimuli delivered over the period based on these computations. **D**, rate of stimulation (R). Dashed horizontal line represent target rate of stimulation (R'), set as 20Hz. **E**, scale parameter (A).

In Figure 43 is clearly visible how fluctuations in scale were used to keep the rate of stimulation close to the target stimulation rate of 20Hz. The rate of stimulation

delivered in the experiments was 17.86 ± 0.07 Hz (Mean ± SD) for the 45° condition and 17.75 ± 0.12 Hz (Mean ± SD) for the 225° condition.

Figure 44 shows a simulation in which the algorithm was implemented two times, one for each stimulation phase (45° and 225°), on the same EMG signal recorded from a participant during approximately 5 minutes of the tremor task. Clear coherence was observed between the EMG signal and the stimulation (Figure 44A), and the correct phases of stimulation (which are opposite phases to each other) were achieved (Figure 44B).

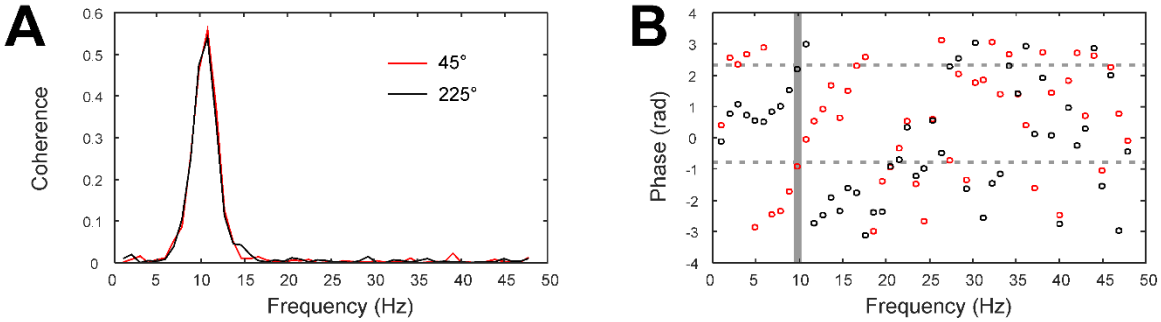

Figure 44. Demonstration of algorithm delivering stimulation at two different phases: 45° (red) and 225° (black). **A**, coherence between EMG signal and stimulation. **B**, phase between EMG signal and stimulation. Vertical grey line highlights frequency of stimulation (10Hz). Horizontal grey dashed lines highlight the two target phases of stimulation (indicated in radians, corresponding to 45° and 225°).

Three different conditions were tested: (1) control (no stimulation), in which participants performed the tremor task for the same amount of time as the stimulation conditions but received no stimulation, (2) 45°, in which stimulation was delivered at 45° phase of the detected tremor, and (3) 225°, in which stimulation was delivered at 225° phase of the detected tremor.

Participants performed one block of 40 trials of the task, which lasted approximately five minutes, as the pre-intervention measure (referred to as ‘before’), then nine more blocks while receiving stimulation (only for the 45° and 225° conditions) or not (only for the control condition), with a two minutes rest break in between these blocks. Total time of effective stimulation was therefore approximately 45 minutes. Finally, three more blocks were performed as the post-intervention measures. The first one was referred to as ‘after’ and performed immediately after the stimulation intervention. After a two minutes rest break period the second post intervention block was performed, which was referred to as ‘5min’ since it occurred

approximately 5 minutes after the intervention. Right after this block a 10 minutes rest break occurred, after which participants performed the third and last post intervention measure, referred to as ‘break’. The dependent variables used to represent tremor were the same ones used previously (i.e., sum of power between 6 and 13 Hz, expressed as percentage of measurements before intervention). The three post stimulation intervention measures (‘after’, ‘5min’ and ‘break’) were compared to the pre intervention measure to investigate changes in tremor caused by stimulation.

- *Statistical analysis*

For group averages analysis Monte Carlo simulations were used. We calculated the average tremor measure (sum of power between 6 and 13 Hz) for each subject in the ‘before’ evaluation and separately in the post intervention measurements (‘after’, ‘5min’ and ‘break’). To compare each of the post intervention measures with the before intervention the ratio between post and pre intervention values was calculated (each subject contributed with one value before and one after). The next step was to calculate the geometric mean of all ratio values. Subsequently the pre and post intervention values were shuffled across subjects randomly in order to destroy the time relationship of the measures relative to the stimulation intervention. After shuffling the ratio the geometric mean was calculated again. This procedure was repeated 1000 times, which provided 1000 values of geometric means of ratios. Then it was analysed in which part of the distribution of this 1000 geometric mean values the original geometric mean value (with no shuffle) was located, using a significance limit of 0.05. P values lower than 0.05 would then indicate the stimulation intervention changed tremor, demonstrating the causality of the relationship between pre and post intervention measures.

Additionally, one-way ANOVAs were implemented with factor condition comparing the three experimental conditions (control, 45°, and 225°) in each of our measurements (significance limit was set as 0.05). When ANOVA reached significance t-tests for independent samples were used for pairwise comparisons to locate which conditions were different from each other (significance limit was also set as 0.05).

Individual results analysis were conducted through paired samples t-tests in the same way used for the previous tremor study. The significance level was set as 0.05.

6.5. 2 Results

Figure 45 shows the average results for EMG and accelerometer data in all experimental conditions. Monte Carlo analyses were conducted to compare changes from before to after stimulation. ANOVA was conducted to compare the three experimental conditions (control, 45° and 225°).

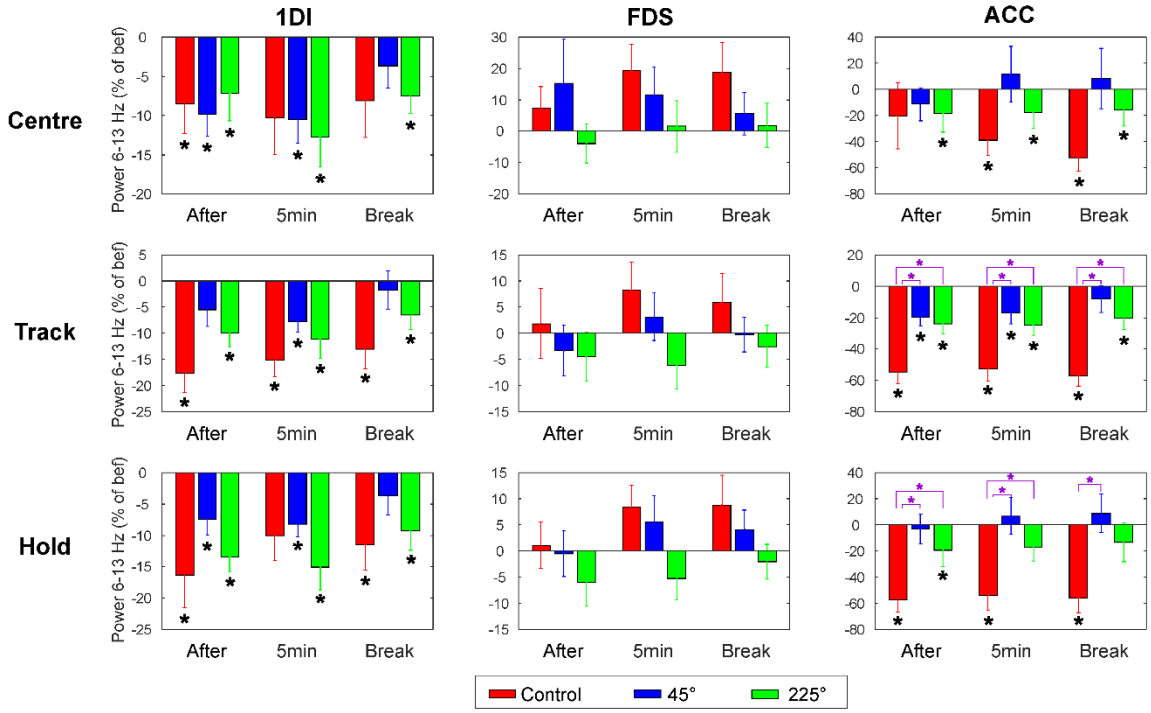

Figure 45. Average results in all three experimental conditions: control (red), 45° (blue) and 225° (green) for all three tremor assessments (after, 5min and Break). Sum of power between 6 and 13 Hz, shown as percentage of before (pre- tremor assessment) and subtracted by 100 so that positive values represent increase and negative values represent decrease in tremor after stimulation intervention. Results are presented for all three phases of the task (centre, track, hold) and for EMG signals from 1DI and FDS and for accelerometer data (ACC). Black (*) indicates significant effect shown by Monte Carlo analysis. Magenta brackets and (*) indicate significant difference between experimental conditions (control, 45°, 225°) assessed by t-tests implemented when ANOVA reached significance.

Results show a clear trend of tremor decrease in 1DI in all phases of the task regardless of the experimental condition. The accelerometer data also show a trend for tremor reduction in all phases of the task which seems slightly more evident for the control condition, with no stimulation. Results from FDS, which is the muscle used to trigger stimulation showed no significant effects in all experimental conditions.

ANOVA tests comparing the experimental conditions (control, 45°, and 225°) only reached significance for accelerometer data during the track and hold phases of the task in all measurements (after, 5min and break). Results from pairwise comparisons showed a clear tendency for larger reduction of tremor in the control condition compared to both stimulation conditions (45° and 225°) for accelerometer data during the track and hold phases of the task (see Figure 45).

Figure 46 shows individual results for EMG and accelerometer data in all experimental conditions. T tests were conducted separately for each participant across all trials.

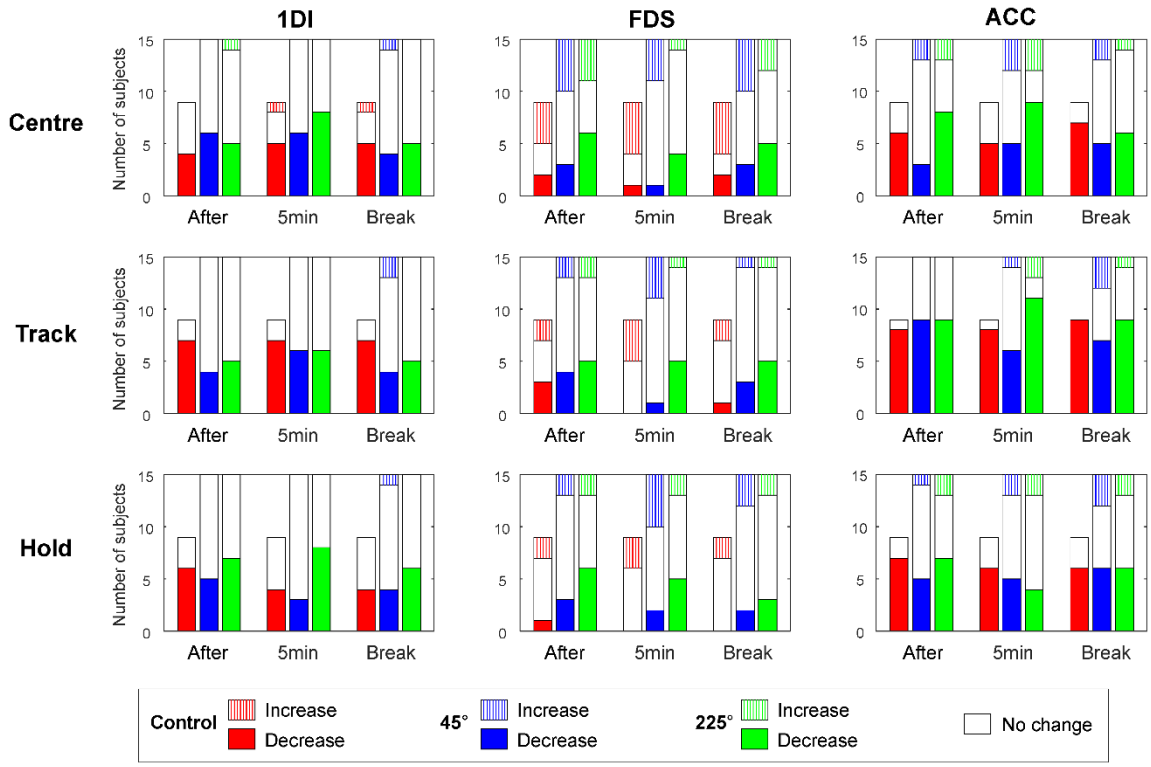

Figure 46. Individual results in all three experimental conditions: control (red), 45° (blue) and 225° (green) for all three tremor assessments (after, 5min and Break). Number of subjects presenting significant decrease, no change and increase in tremor assessed by sum of power between 6 and 13 Hz. Results are presented for all three phases of the task (centre, track, hold) and for EMG signals from 1DI and FDS and for accelerometer data (ACC).

Individual results show a similar trend to the one demonstrated on average results. Tremor was visibly smaller in 1DI regardless of the experimental condition. A similar trend was present in the accelerometer data. Results from FDS, the muscle used to trigger stimulation, seem to present a balance between the number of

subjects with decrease and increase in tremor for all of the experimental conditions and task phases.

In sum, results showed that although data from 1DI and accelerometer presented a tendency for tremor reduction, this was not phase dependent, since results were very similar for both 45° and 225° phases of stimulation. Furthermore, this tendency was also present in the control condition, in which no stimulation was given. Results from FDS, which should present the most relevant outcome since this was the muscle used to trigger stimulation, showed no clear tendency for changes in tremor, either increase or decrease, in any of the experimental conditions.

6.5. 3 Discussion

These results show that tremor reduction was observed, especially for data from 1DI and accelerometer. However, such reduction was not phase dependent since no difference was observed between the two different phases of stimulation (45° and 225°), which according to our hypothesis should produce opposite effects on tremor – i.e., one phase would increase tremor while the other would decrease it.

More importantly, results from the control condition showed clear reduction in tremor, especially for the accelerometer data which was often more pronounced than in the two stimulation conditions (45° and 225°). This means the tremor assessment with this protocol was not ideal since the simple act of performing the tremor task for this long period inside the lab was already capable of causing changes in tremor, which limits any conclusions that might be drawn from the two stimulation conditions in different phases.

6.6 Discussion

Results failed to demonstrate clear phase-dependent modulation of physiological tremor in both the long and short versions of stimulation intervention. Such results can be explained by limitations in our hypothesis and other limitations including short stimulation time, non-optimal phases of stimulation and the fact that physiological tremor might not be appropriate to test the potential of our intervention in

ameliorating pathological tremor. Nevertheless, the tremor assessment seemed to be adequate to measure tremor and the stimulation protocol was capable of accurately detecting tremor oscillations and stimulating at specific phases of ongoing tremor. The progress obtained here with this methodology can now be used to optimize intervention protocols with the goal of reducing pathological tremor.

One important achievement of this tremor study was the development of a task to assess changes in tremor after a long lasting intervention, as long as the assessment controls for two important factors. Firstly, EMG signals seemed to be a reliable measure when used at the same time of day, as in our first long version study, to avoid circadian variations. Secondly, a likely placebo effect was observed in the long version of the study. The no stimulation condition, which was the first one tested in all volunteers, produced tremor reduction, while the subsequently tested stimulation conditions did not show such a clear decrease in tremor. Therefore, it seems possible that the fact that participants were using the device for the first time changed the outcome of the tremor measurements, which is likely to be due to a placebo effect related to the novelty of the device. However, this is speculation and the possibility that all the stimulation conditions increased tremor while the control condition decrease tremor needs to be acknowledged. Therefore, it was concluded that the tremor assessment is appropriate for long lasting interventions as long as besides controlling for circadian variations (i.e., making sure the tremor assessment is implemented at the same time of day) it also controls for placebo effects regarding the novelty of the device (i.e., assuring participants familiarize themselves with the device before the actual intervention).

Another positive outcome of this intervention was the effectiveness of the stimulation protocols. For both long and short versions of the intervention the device accurately delivered stimulation in real time at the correct phase of the detected ongoing oscillations (for example see Figure 37). Specifically for the short version study, in which the stimulation rate was increased, the algorithm successfully performed all calculations ignoring EMG signals contaminated by artefact and still delivering stimulation at the correct phase (see Figure 44). The algorithm also worked accurately to ensure the device delivered stimulation at the desired stimulation rate (i.e., ~20 Hz on the second short version study; see Figure 43). Therefore, it is suggested that future studies should use the progress achieved in this study with real time processing of EMG signals, detection of ongoing tremor

oscillations, blanking of artefact and calculation of parameters of stimulation such as phase to improve stimulation interventions aiming at reduction of pathological tremor.

These two positive findings, the effectiveness of both the tremor assessment and the stimulation protocols, can now be used to explore possible shortcomings on our hypothesis of inducing plastic changes to reduce tremor with peripheral nerve stimulation. These shortcomings may include a number of factors. (1) The stimulation time might not have been long enough to produce plastic changes. In the first long version of the intervention stimulation was delivered for one day (excluding asleep time; effectively around 12 hours) at a rate of around 0.2 Hz, which gives a total of around 8,640 stimuli delivered. This rate was substantially increased on the second short version of the intervention using 20 Hz with a total stimulation time of around 45 minutes, which gives a total of around 54,000 stimuli delivered. It is uncertain whether the stimulation times used are long enough to induce plasticity in spinal cord circuits. (2) The stimulation phases chosen might not have been the most appropriate to induce phase cancellation between spinal cord and M1. The phases 45°, 135°, 225° and 315° were tested in the first long version study and again the 45° and 225° phases were tested on the second short version intervention. It is possible however that the optimal phase to produce phase cancellation and tremor reduction (and its opposite phase to produce phase summation and tremor increase) has not been tested thus far in this study. Testing eight different phases in steps of 45° in future studies could be an appropriate solution to investigate this further. (3) Physiological tremor might not be appropriate for initial tests aiming at pathological tremor reduction. The small amplitude of physiological tremor could make it extremely difficult to achieve tremor modulation. Slight differences in frequency and neural and physiological aspects of pathological tremor compared to physiological tremor might also play an important role in the phase modulation of tremor. Therefore, it is suggested that further investigations focus on patients with pathological tremor, use longer intervention times and test a wider range of phase stimulations. Unfortunately the time requirements for such an approach are unsuitable for this PhD thesis.

In similar lines of investigation as the experiments described here several studies used plasticity, neurophysiological intervention techniques and even robotic assistance devices with the goal of reducing tremor. The investigations using robotic devices rely on the effective cancellation of ongoing tremor oscillations. One of the main challenges, besides the engineering approach to develop the devices, is to compute algorithms which will detect tremor oscillations and cancel them in real time

by producing opposite forces on the limb but without affecting the natural muscle activity the patient might be trying to perform, such as writing or drinking a glass of water. Nevertheless, some initial progress has been observed in investigations of this type in trying to overcome these issues and achieve tremor reduction (e.g., As'arry *et al.*, 2013; Kiguchi and Hayashi, 2013; Taheri *et al.*, 2014; Chuanasa and Songschon, 2015). Unfortunately we are still not at the stage of having a commercialized tremor reduction robotic device on large scale with proved effectiveness for patients suffering from pathological tremor. Nevertheless, the progress that is being achieved in this field towards accomplishing such goal has been a source of excitement for the general public (see http://www.bbc.co.uk/news/av/magazine-38208814/the-invention-that-helped-me-write-again). Another area with promising outcomes for tremor treatment is brain stimulation. Deep brain stimulation has shown some tremor reduction with the implantation of electrodes in the thalamus of tremor patients providing stimulation at specific phases on ongoing oscillations (e.g., Kuncel *et al.*, 2012; Cagnan *et al.*, 2013). The invasive nature of such procedures has led authors to search for alternative non-invasive methods of brain stimulation and the results also seem promising. Techniques such as TMS and transcranial alternating current stimulation have been used in patients suffering from pathological tremor such as essential tremor and Parkinson's disease to non-invasively produce plastic changes based on phase-dependent stimulation of the brain and near 50% tremor reduction has been demonstrated (Hellriegel *et al.*, 2012; Brittain *et al.*, 2013). More closely related to this study are investigations using peripheral stimulation and interesting results also seem to demonstrate a great potential of this approach in ameliorating pathological tremor. Tremor reduction has been observed in studies which detect tremor oscillations in specific muscles and delivers electrical stimulation to antagonist muscles in an out-of-phase manner (Popovic Maneski *et al.*, 2011; Dosen *et al.*, 2015). Mechanical stochastic noise stimulation has also shown positive effects in reducing tremor (Trenado *et al.*, 2014). Recently, it has been shown that muscle electric stimulation could produce a 50% reduction in tremor in some patients provided it systematically adapts parameters of stimulation individually (Dideriksen *et al.*, 2017); methodological issues were present in this particular study however since the experiments did not conduct continuous tremor phase detection: once stimulation started being delivered the measurements were not taken into account anymore assuming oscillations did not change phase, which is less accurate then our approach detecting phase in real time whilst stimulating is being delivered.

Plastic induced changes in neural connections have been a topic of interest in neuroscience for many decades. Different approaches are used in experiments on this subject, including for example operant conditioning of spinal reflexes (e.g., Thompson and Wolpaw, 2015). Since the 1970s studies have been demonstrating that animals and humans are able to condition reflex responses such as the H-reflex with approaches based on reward or punishment (Thompson and Wolpaw, 2014a; Thompson and Wolpaw, 2014b). Great interest in these techniques emerges also from the therapeutic potential of such approaches to improve motor function in patients suffering from neurological conditions (Thompson and Wolpaw, 2015). Other forms of plasticity include STDP, the approach used in this study, which deals with the stimulation of pre and postsynaptic elements in a timely precise manner (Feldman, 2012). Regardless of the approach used to induce plastic changes, the success of its implementation will always be intimately related to the knowledge of the elements and function of the spinal circuits targeted.

It is important to highlight that even though our approach to induce plastic changes which would cause long-lasting changes in synapses inducing tremor reduction even after device use is much more sophisticated than approaches which simply cancel ongoing tremor, there are a number of assumptions included in the hypothesis which could be completely or partially incorrect jeopardizing the desired outcome of tremor improvement. First, the hypothesis that non-optimal phase cancellation between spinal cord and brain oscillations is the reason why pathological tremor shows high amplitude, as opposed to physiological tremor, might not be the case for some or all forms of pathological tremors. Factors including oscillations in different neural structures could play a more important role than this phase cancelling in one or more types of pathological tremor, which would make the phase cancelling approach of our experiments very inefficient in causing changes in tremor. Another assumption of the approach used here is that the median nerve stimulation used would induce plastic changes in spinal cord circuits which ultimately would make them more efficient to cancel brain oscillations. One important limitation of that is the fact that this approach did not target the specific spinal circuits which produce such phase cancellation; these include Renshaw cells (Williams and Baker, 2009), intermediate zone interneurons (Williams *et al.*, 2010), but not pre-synaptic inhibition (Galan and Baker, 2015). The assumption that the median nerve stimulation used here would affect these specific spinal circuits which generate phase cancellation of physiological tremor might be incorrect. Finally, more complex details such as the

capability of the plastic changes induced by stimulation to cause changes in tremor amplitude big enough to improve the quality of life of patients with pathological tremor is still unknown.

The investigation of the previously mentioned possible shortcomings in the experimental protocols shown here as well as the exploration of the knowledge gathered from other interventions aiming for pathological tremor reduction would be extremely time consuming, which makes further work on this topic unsuitable for this PhD thesis. Future research projects can now use the progress achieved by the work presented here specifically in terms of methodology and the one published in the literature to improve protocols and continue to explore the potential of non-invasive peripheral nerve stimulation to reduce pathological tremor through plastic changes in connectivity at the spinal cord level.

Chapter 7.
General discussion

7.1 Context

The non-invasive electrophysiological assessment of human spinal circuitry is crucial not only to understand function but to comprehend and possibly treat pathology. In the past decades great progress has been achieved in the motor control field with studies describing spinal circuits and their non-invasive assessment in humans. Nevertheless, there is still progress to be made for example in the exploration of easier methods for assessment in humans and the investigation of circuits which are still not well described and/or still do not have an experimental protocol for their assessment in humans. This thesis focused on the assessment of human spinal circuits with the overall goal of understanding their function in health and disease. A novel spinal circuit and its assessment are described here, as well as some of its changes in pathology. In addition, it is shown that spinal cord circuits are capable of producing low frequencies intermuscular coherence. Finally, peripheral nerve stimulation was preliminarily explored as a potential strategy in producing plastic changes in the spinal cord to ameliorate tremor; although we did not obtain positive results in tremor improvement, methodological advances were accomplished towards this goal.

7.2 Summary and future directions

The main contribution of this thesis was the description of a novel spinal circuit with converging input from flexor afferent and extensor Ib afferents to the wrist flexor, which can be easily assessed in the human upper limb (chapter 2). Such a spinal pathway is responsible for the facilitation of the FCR H-reflex by conditioning ECR stimulation at 30ms interval. Extensive work with human and monkey experiments was necessary to uncover the components of this spinal circuit. This shows the crucial importance of invasive animal experiments to complement the human data,

which made it possible to discover an easily implemented non-invasive assessment of Ib pathways in the human upper limb. This assessment is possible since it was proven that the circuit is at least partially mediated by Ib pathways. The specificity of Ib function assessment can be improved by implementing the experimental protocol with subjects having their wrist held flexed (chapter 2), since in this case the facilitation of the FCR H-reflex is cause by ECR Ib afferents with minimal or no contribution of FCR afferents. With this study an important gap in the literature could be closed, since previously there was no efficient and clear method for the assessment of Ib pathways in the human upper limb.

A later inhibition, at 70ms interval, of the FCR H-reflex with conditioning ECR stimulation was also observed. Although the specific components of the spinal circuit mediating such inhibition are still to be uncovered, an important discovery was the fact that in stroke survivors such inhibition is weak or absent (chapter 3), which could represent either excessive facilitation or loss of inhibition. The earlier facilitation (30ms interval) remained unchanged in stroke survivors. Interestingly, preliminary unpublished data shows that patients with Parkinson's disease have a tendency to follow the same pattern of results as stroke patients. The lack of significant changes in both facilitation and inhibition effects in spinal cord injury patients (chapter 3) shows the diverse effects that spinal cord lesions can produce on both spinal circuits. Results with patient populations were important to show how pathology could affect both spinal circuits causing facilitation and inhibition of the FCR H-reflex with conditioning ECR stimulation.

TMS experiments showed that the corticospinal tract gives input to both spinal circuits described (chapter 4). This opens possibilities for the exploration of plasticity protocols which could target for example the 70ms inhibition. Plasticity protocols with TMS stimulation at appropriate intervals conditioning the FCR H-reflex preceded by ECR stimulation could aim at reducing the excessive facilitation or loss of inhibition present in stroke survivors, exploiting the principle of spike-timing dependent plasticity. If successful, such studies could investigate the potential that this reduction in either excess of facilitation or loss of inhibition could have in affecting spasticity. On the other hand, it was shown that the reticulospinal tract does not give input to both spinal circuits (chapter 4), but such interpretation needs caution since the results might be related to specific details of the experimental design used. Nevertheless, the implementation of click sound stimulation to activate the

reticulospinal tract is a novel method with proven efficacy, which should be explored further in the motor control field.

Spinal circuits can also be investigated through the analysis of oscillations using for example intermuscular coherence. Although the cortical origin of intermuscular coherence in the beta-band (15-30Hz) is well documented and understood, the mechanisms and source of intermuscular coherence at lower frequencies is still under debate. With the analysis of spasms in spinal cord injury patients in long-lasting (24h) EMG recordings it was shown for the first time that the spinal cord is capable of producing low frequencies intermuscular coherence (chapter 5). Studies exploring intermuscular coherence in different motor tasks as well as different populations can now consider the role that the spinal cord might play in generating these oscillations.

Oscillations in the spinal cord have been well documented at tremor frequency (~10 Hz) and interestingly these are phase opposite to ~10 Hz oscillations in the brain, which causes phase cancellation at the motoneuron level, resulting in small amplitude of physiological tremor. In chapter 6 a plasticity protocol was used with peripheral nerve stimulation with the aim of modifying spinal circuits, making them more efficient in causing phase cancellation and consequently tremor reduction. The preliminary results shown in this thesis provide an important contribution but future studies need to explore further the potential of long-lasting peripheral nerve stimulation in ameliorating pathological tremor. Important methodological details are provided in this thesis (chapter 6), including the algorithms used for stimulation, which can help with the implementation and improvement of stimulation intervention protocols.

7.3 Conclusions

This thesis describes a putative spinal circuit with converging excitatory input from flexor afferents and extensor Ib afferents to the wrist flexor. Such circuit can be easily assessed non-invasively in humans. This discovery represents a significant contribution since it helps fulfil the previous gap in the literature regarding the assessment of Ib function on the human upper limb. Using the same method a later inhibition of the wrist flexor was shown, which is weak or absent in stroke survivors;

specific components of this circuit need further investigation. Both spinal circuits, causing facilitation and inhibition of the wrist flexor, receive input from the corticospinal tract, which opens possibilities for plasticity protocols with the aim of modifying the circuits using TMS to ameliorate excessive facilitation or loss of inhibition in stroke survivors. It was also shown using analysis of spasms in spinal cord injury that the spinal cord is capable of producing intermuscular coherence at low frequencies, which has never been reported before and provides an important contribution to studies investigating the origin of intermuscular coherence in different motor tasks and populations. Finally, preliminarily exploration of the potential of peripheral nerve stimulation to cause plastic changes in spinal circuits to reduce tremor was shown, producing knowledge that can be used in further investigations to optimize the efficiency of the stimulation protocol.

References

Abbott, L.F. and Nelson, S.B. (2000) 'Synaptic plasticity: taming the beast', *Nature neuroscience*, 3 Suppl, pp. 1178-83.

Aguiar, S.A. and Baker, S.N. (2018) 'Convergent Spinal Circuits Facilitating Human Wrist Flexors', *The Journal of neuroscience : the official journal of the Society for Neuroscience*, in press.

Aguiar, S.A. and Baker, S.N. (submitted) 'Descending inputs to spinal circuits facilitating and inhibiting human wrist flexors'.

Alstermark, B., Isa, T., Ohki, Y. and Saito, Y. (1999) 'Disynaptic pyramidal excitation in forelimb motoneurons mediated via C(3)-C(4) propriospinal neurons in the Macaca fuscata', *Journal of neurophysiology*, 82(6), pp. 3580-5.

Araki, T., Eccles, J.C. and Ito, M. (1960) 'Correlation of the inhibitory post-synaptic potential of motoneurones with the latency and time course of inhibition of monosynaptic reflexes', *The Journal of physiology*, 154, pp. 354-77.

As'arry, A., Md Zain, M.Z., Mailah, M. and Hussein, M. (2013) 'Hybrid learning control for improving suppression of hand tremor', *Proceedings of the Institution of Mechanical Engineers. Part H, Journal of engineering in medicine*, 227(11), pp. 1171-80.

Baker, S.N. (2011) 'The primate reticulospinal tract, hand function and functional recovery', *The Journal of physiology*, 589(Pt 23), pp. 5603-12.

Baker, S.N., Chiu, M. and Fetz, E.E. (2006) 'Afferent encoding of central oscillations in the monkey arm', *Journal of neurophysiology*, 95(6), pp. 3904-10.

Baker, S.N., Kilner, J.M., Pinches, E.M. and Lemon, R.N. (1999) 'The role of synchrony and oscillations in the motor output', *Experimental brain research*, 128(1-2), pp. 109-17.

Baker, S.N., Pinches, E.M. and Lemon, R.N. (2003) 'Synchronization in monkey motor cortex during a precision grip task. II. effect of oscillatory activity on corticospinal output', *Journal of neurophysiology*, 89(4), pp. 1941-53.

Baker, S.N., Zaaimi, B., Fisher, K.M., Edgley, S.A. and Soteropoulos, D.S. (2015) 'Pathways mediating functional recovery', *Progress in brain research*, 218, pp. 389-412.

Baldissera, F. and Cavallari, P. (1993) 'Short-latency subliminal effects of transcranial magnetic stimulation on forearm motoneurones', *Experimental brain research*, 96(3), pp. 513-8.

Bannatyne, B.A., Edgley, S.A., Hammar, I., Jankowska, E. and Maxwell, D.J. (2003) 'Networks of inhibitory and excitatory commissural interneurons mediating crossed reticulospinal actions', *The European journal of neuroscience*, 18(8), pp. 2273-84.

Barker, A.T., Jalinous, R. and Freeston, I.L. (1985) 'Non-invasive magnetic stimulation of human motor cortex', *Lancet*, 1(8437), pp. 1106-7.

Bear, M.F., Connors, B.W. and Paradiso, M.A. (2007) *Neuroscience : exploring the brain*. 3rd edn. Philadelphia, Pa.: Lippincott Williams & Wilkins.

Berardelli, A., Day, B.L., Marsden, C.D. and Rothwell, J.C. (1987) 'Evidence favouring presynaptic inhibition between antagonist muscle afferents in the human forearm', *The Journal of physiology*, 391, pp. 71-83.

Boonstra, T.W. (2013) 'The potential of corticomuscular and intermuscular coherence for research on human motor control', *Frontiers in human neuroscience*, 7, p. 855.

Boonstra, T.W., Daffertshofer, A., Roerdink, M., Flipse, I., Groenewoud, K. and Beek, P.J. (2009a) 'Bilateral motor unit synchronization of leg muscles during a simple dynamic balance task', *The European journal of neuroscience*, 29(3), pp. 613-22.

Boonstra, T.W., Daffertshofer, A., van As, E., van der Vlugt, S. and Beek, P.J. (2007) 'Bilateral motor unit synchronization is functionally organized', *Experimental brain research*, 178(1), pp. 79-88.

Boonstra, T.W., van Wijk, B.C., Praamstra, P. and Daffertshofer, A. (2009b) 'Corticomuscular and bilateral EMG coherence reflect distinct aspects of neural synchronization', *Neuroscience letters*, 463(1), pp. 17-21.

Boulenguez, P., Liabeuf, S., Bos, R., Bras, H., Jean-Xavier, C., Brocard, C., Stil, A., Darbon, P., Cattaert, D., Delpire, E., Marsala, M. and Vinay, L. (2010) 'Down-regulation of the potassium-chloride cotransporter KCC2 contributes to spasticity after spinal cord injury', *Nature medicine*, 16(3), pp. 302-7.

Brittain, J.S., Probert-Smith, P., Aziz, T.Z. and Brown, P. (2013) 'Tremor suppression by rhythmic transcranial current stimulation', *Current biology : CB*, 23(5), pp. 436-40.

Brown, K.I., Williams, E.R., de Carvalho, F. and Baker, S.N. (2016) 'Plastic Changes in Human Motor Cortical Output Induced by Random but not Closed-Loop Peripheral Stimulation: the Curse of Causality', *Frontiers in human neuroscience*, 10, p. 590.

Burke, D. (2016) 'Clinical uses of H reflexes of upper and lower limb muscles', *Clinical Neurophysiology Practice*, (1), pp. 9-17.

Burke, D., Gandevia, S.C. and McKeon, B. (1983) 'The afferent volleys responsible for spinal proprioceptive reflexes in man', *The Journal of physiology*, 339, pp. 535-52.

Burne, J.A. and Lippold, O.C. (1996) 'Reflex inhibition following electrical stimulation over muscle tendons in man', *Brain*, 119 (Pt 4), pp. 1107-14.

Bussel, B. and Pierrot-Deseilligny, E. (1977) 'Inhibition of human motoneurons, probably of Renshaw origin, elicited by an orthodromic motor discharge', *The Journal of physiology*, 269(2), pp. 319-39.

Cagnan, H., Brittain, J.S., Little, S., Foltynie, T., Limousin, P., Zrinzo, L., Hariz, M., Joint, C., Fitzgerald, J., Green, A.L., Aziz, T. and Brown, P. (2013) 'Phase dependent modulation of tremor amplitude in essential tremor through thalamic stimulation', *Brain : a journal of neurology*, 136(Pt 10), pp. 3062-75.

Calancie, B., Broton, J.G., Klose, K.J., Traad, M., Difini, J. and Ayyar, D.R. (1993) 'Evidence that alterations in presynaptic inhibition contribute to segmental hypo- and hyperexcitability after spinal cord injury in man', *Electroencephalography and clinical neurophysiology*, 89(3), pp. 177-86.

Cavallari, P., Fournier, E., Katz, R., Malmgren, K., Pierrot-Deseilligny, E. and Shindo, M. (1985) 'Cutaneous facilitation of transmission in Ib reflex pathways in the human upper limb', *Experimental brain research*, 60(1), pp. 197-9.

Chuanasa, J. and Songschon, S. (2015) 'Essential tremor suppression by a novel self-balancing device', *Prosthetics and orthotics international*, 39(3), pp. 219-25.

Conway, B.A., Halliday, D.M., Farmer, S.F., Shahani, U., Maas, P., Weir, A.I. and Rosenberg, J.R. (1995) 'Synchronization between motor cortex and spinal motoneuronal pool during the performance of a maintained motor task in man', *The Journal of physiology*, 489 (Pt 3), pp. 917-24.

Coppin, C.M., Jack, J.J. and MacLennan, C.R. (1970) 'A method for the selective electrical activation of tendon organ afferent fibres from the cat soleus muscle', *The Journal of physiology*, 210(1), pp. 18P-20P.

Crossman, A.R. and Neary, D. (2010) *Neuroanatomy : an illustrated colour text*. 4th edn. Edinburgh ; New York: Churchill Livingstone/Elsevier.

Day, B.L., Dressler, D., Maertens de Noordhout, A., Marsden, C.D., Nakashima, K., Rothwell, J.C. and Thompson, P.D. (1989) 'Electric and magnetic stimulation of

human motor cortex: surface EMG and single motor unit responses', *The Journal of physiology*, 412, pp. 449-73.

Day, B.L., Marsden, C.D., Obeso, J.A. and Rothwell, J.C. (1984) 'Reciprocal inhibition between the muscles of the human forearm', *The Journal of physiology*, 349, pp. 519-34.

de Vries, I.E., Daffertshofer, A., Stegeman, D.F. and Boonstra, T.W. (2016) 'Functional connectivity in the neuromuscular system underlying bimanual coordination', *Journal of neurophysiology*, 116(6), pp. 2576-2585.

Delwaide, P.J. (2001) 'Parkinsonian rigidity', *Functional neurology*, 16(2), pp. 147-56.

Di Lazzaro, V. and Rothwell, J.C. (2014) 'Corticospinal activity evoked and modulated by non-invasive stimulation of the intact human motor cortex', *The Journal of physiology*, 592(19), pp. 4115-28.

Dideriksen, J.L., Laine, C.M., Dosen, S., Muceli, S., Rocon, E., Pons, J.L., Benito-Leon, J. and Farina, D. (2017) 'Electrical Stimulation of Afferent Pathways for the Suppression of Pathological Tremor', *Frontiers in neuroscience*, 11, p. 178.

Dosen, S., Muceli, S., Dideriksen, J.L., Romero, J.P., Rocon, E., Pons, J. and Farina, D. (2015) 'Online tremor suppression using electromyography and low-level electrical stimulation', *IEEE transactions on neural systems and rehabilitation engineering : a publication of the IEEE Engineering in Medicine and Biology Society*, 23(3), pp. 385-95.

Eccles, J.C., Eccles, R.M. and Lundberg, A. (1957) 'Synaptic actions on motoneurones caused by impulses in Golgi tendon organ afferents', *The Journal of physiology*, 138(2), pp. 227-52.

Elble, R.J. (2013) 'What is essential tremor?', *Current neurology and neuroscience reports*, 13(6), p. 353.

Elble, R.J. and Koller, W.C. (1990) *Tremor*. Baltimore: John Hopkins University Press.

Evans, C.M. and Baker, S.N. (2003) 'Task-dependent intermanual coupling of 8-Hz discontinuities during slow finger movements', *The European journal of neuroscience*, 18(2), pp. 453-6.

Fasano, A. and Deuschl, G. (2015) 'Therapeutic advances in tremor', *Movement disorders*, 30(11), pp. 1557-65.

Feldman, D.E. (2012) 'The spike-timing dependence of plasticity', *Neuron*, 75(4), pp. 556-71.

Ferbert, A., Priori, A., Rothwell, J.C., Day, B.L., Colebatch, J.G. and Marsden, C.D. (1992) 'Interhemispheric inhibition of the human motor cortex', *The Journal of physiology*, 453, pp. 525-46.

Fetz, E.E., Jankowska, E., Johannisson, T. and Lipski, J. (1979) 'Autogenetic inhibition of motoneurones by impulses in group Ia muscle spindle afferents', *The Journal of physiology*, 293, pp. 173-95.

Fisher, K.M., Zaaimi, B. and Baker, S.N. (2012a) 'Reticular formation responses to magnetic brain stimulation of primary motor cortex', *The Journal of physiology*, 590(Pt 16), pp. 4045-60.

Fisher, K.M., Zaaimi, B., Williams, T.L., Baker, S.N. and Baker, M.R. (2012b) 'Beta-band intermuscular coherence: a novel biomarker of upper motor neuron dysfunction in motor neuron disease', *Brain : a journal of neurology*, 135(Pt 9), pp. 2849-64.

Foncke, E.M., Bour, L.J., van der Meer, J.N., Koelman, J.H. and Tijssen, M.A. (2007) 'Abnormal low frequency drive in myoclonus-dystonia patients correlates with presence of dystonia', *Movement disorders : official journal of the Movement Disorder Society*, 22(9), pp. 1299-307.

Foysal, K.M., de Carvalho, F. and Baker, S.N. (2016) 'Spike Timing-Dependent Plasticity in the Long-Latency Stretch Reflex Following Paired Stimulation from a Wearable Electronic Device', *The Journal of neuroscience : the official journal of the Society for Neuroscience*, 36(42), pp. 10823-10830.

Frigon, A. (2017) 'The neural control of interlimb coordination during mammalian locomotion', *Journal of neurophysiology*, 117(6), pp. 2224-2241.

Galan, F. and Baker, S.N. (2015) 'Pre-Synaptic Inhibition of Afferent Feedback in the Macaque Spinal Cord Does Not Modulate with Cycles of Peripheral Oscillations Around 10 Hz', *Frontiers in neural circuits*, 9, p. 76.

Gracies, J.M., Meunier, S. and Pierrot-Deseilligny, E. (1994) 'Evidence for corticospinal excitation of presumed propriospinal neurones in man', *The Journal of physiology*, 475(3), pp. 509-18.

Grefkes, C. and Ward, N.S. (2014) 'Cortical reorganization after stroke: how much and how functional?', *The Neuroscientist : a review journal bringing neurobiology, neurology and psychiatry*, 20(1), pp. 56-70.

Grey, M.J., Ladouceur, M., Andersen, J.B., Nielsen, J.B. and Sinkjaer, T. (2001) 'Group II muscle afferents probably contribute to the medium latency soleus stretch reflex during walking in humans', *The Journal of physiology*, 534(Pt 3), pp. 925-33.

Grosse, P. and Brown, P. (2003) 'Acoustic startle evokes bilaterally synchronous oscillatory EMG activity in the healthy human', *Journal of neurophysiology*, 90(3), pp. 1654-61.

Grosse, P., Cassidy, M.J. and Brown, P. (2002) 'EEG-EMG, MEG-EMG and EMG-EMG frequency analysis: physiological principles and clinical applications', *Clinical neurophysiology : official journal of the International Federation of Clinical Neurophysiology*, 113(10), pp. 1523-31.

Grosse, P., Edwards, M., Tijssen, M.A., Schrag, A., Lees, A.J., Bhatia, K.P. and Brown, P. (2004) 'Patterns of EMG-EMG coherence in limb dystonia', *Movement disorders : official journal of the Movement Disorder Society*, 19(7), pp. 758-69.

Hagbarth, K.E. and Young, R.R. (1979) 'Participation of the stretch reflex in human physiological tremor', *Brain : a journal of neurology*, 102(3), pp. 509-26.

Halliday, D.M., Conway, B.A., Christensen, L.O., Hansen, N.L., Petersen, N.P. and Nielsen, J.B. (2003) 'Functional coupling of motor units is modulated during walking in human subjects', *Journal of neurophysiology*, 89(2), pp. 960-8.

Hellriegel, H., Schulz, E.M., Siebner, H.R., Deuschl, G. and Raethjen, J.H. (2012) 'Continuous theta-burst stimulation of the primary motor cortex in essential tremor', *Clinical neurophysiology : official journal of the International Federation of Clinical Neurophysiology*, 123(5), pp. 1010-5.

Hindle, A.R., Lou, J.W. and Collins, D.F. (2014) 'The pulse duration of electrical stimulation influences H-reflexes but not corticospinal excitability for tibialis anterior', *Can J Physiol Pharmacol*, 92(10), pp. 821-5.

Hunt, C.C. and Kuffler, S.W. (1951) 'Stretch receptor discharges during muscle contraction', *The Journal of physiology*, 113(2-3), pp. 298-315.

Jabre, J.F. (1981) 'Surface recording of the H-reflex of the flexor carpi radialis', *Muscle Nerve*, 4(5), pp. 435-8.

Jackson, A., Baker, S.N. and Fetz, E.E. (2006) 'Tests for presynaptic modulation of corticospinal terminals from peripheral afferents and pyramidal tract in the macaque', *The Journal of physiology*, 573(Pt 1), pp. 107-20.

Jami, L. (1992) 'Golgi tendon organs in mammalian skeletal muscle: functional properties and central actions', *Physiological reviews*, 72(3), pp. 623-66.

Jankowska, E., Bannatyne, B.A., Stecina, K., Hammar, I., Cabaj, A. and Maxwell, D.J. (2009) 'Commissural interneurons with input from group I and II muscle afferents in feline lumbar segments: neurotransmitters, projections and target cells', *The Journal of physiology*, 587(2), pp. 401-18.

Jenner, J.R. and Stephens, J.A. (1982) 'Cutaneous reflex responses and their central nervous pathways studied in man', *The Journal of physiology*, 333, pp. 405-19.

Kamke, M.R., Nydam, A.S., Sale, M.V. and Mattingley, J.B. (2016) 'Associative plasticity in the human motor cortex is enhanced by concurrently targeting separate muscle representations with excitatory and inhibitory protocols', *Journal of neurophysiology*, 115(4), pp. 2191-8.

Katz, R., Penicaud, A. and Rossi, A. (1991) 'Reciprocal Ia inhibition between elbow flexors and extensors in the human', *The Journal of physiology*, 437, pp. 269-86.

Khosrawi, S., Taheri, P. and Hashemi, S.H. (2015) 'Proposed equation between flexor carpi radialis H-reflex latency and upper limb length', *Iranian journal of neurology*, 14(1), pp. 41-6.

Kiguchi, K. and Hayashi, Y. (2013) 'Upper-limb tremor suppression with a 7DOF exoskeleton power-assist robot', *Conference proceedings : ... Annual International Conference of the IEEE Engineering in Medicine and Biology Society. IEEE Engineering in Medicine and Biology Society. Annual Conference*, 2013, pp. 6679-82.

Kilner, J.M., Baker, S.N., Salenius, S., Jousmaki, V., Hari, R. and Lemon, R.N. (1999) 'Task-dependent modulation of 15-30 Hz coherence between rectified EMGs from human hand and forearm muscles', *The Journal of physiology*, 516 (Pt 2), pp. 559-70.

Klomjai, W., Katz, R. and Lackmy-Vallee, A. (2015) 'Basic principles of transcranial magnetic stimulation (TMS) and repetitive TMS (rTMS)', *Annals of physical and rehabilitation medicine*, 58(4), pp. 208-13.

Kloter, E., Wirz, M. and Dietz, V. (2011) 'Locomotion in stroke subjects: interactions between unaffected and affected sides', *Brain : a journal of neurology*, 134(Pt 3), pp. 721-31.

Kozelj, S. and Baker, S.N. (2014) 'Different phase delays of peripheral input to primate motor cortex and spinal cord promote cancellation at physiological tremor frequencies', *Journal of neurophysiology*, 111(10), pp. 2001-16.

Kuncel, A.M., Birdno, M.J., Swan, B.D. and Grill, W.M. (2012) 'Tremor reduction and modeled neural activity during cycling thalamic deep brain stimulation', *Clinical neurophysiology : official journal of the International Federation of Clinical Neurophysiology*, 123(5), pp. 1044-52.

Lamy, J.C., Russmann, H., Shamim, E.A., Meunier, S. and Hallett, M. (2010) 'Paired associative stimulation induces change in presynaptic inhibition of Ia terminals in wrist flexors in humans', *Journal of neurophysiology*, 104(2), pp. 755-64.

Lemon, R.N. (2008) 'Descending pathways in motor control', *Annual review of neuroscience*, 31, pp. 195-218.

Li, S. and Francisco, G.E. (2015) 'New insights into the pathophysiology of post-stroke spasticity', *Frontiers in human neuroscience*, 9, p. 192.

Lundberg, A. and Winsbury, G. (1960) 'Selective adequate activation of large afferents from muscle spindles and Golgi tendon organs', *Acta physiologica Scandinavica*, 49, pp. 155-64.

Magladery, J.W. and Mc, D.D., Jr. (1950) 'Electrophysiological studies of nerve and reflex activity in normal man. I. Identification of certain reflexes in the electromyogram and the conduction velocity of peripheral nerve fibers', *Bulletin of the Johns Hopkins Hospital*, 86(5), pp. 265-90.

Magladery, J.W., Porter, W.E., Park, A.M. and Teasdall, R.D. (1951) 'Electrophysiological studies of nerve and reflex activity in normal man. IV. The two-neurone reflex and identification of certain action potentials from spinal roots and cord', *Bulletin of the Johns Hopkins Hospital*, 88(6), pp. 499-519.

Maier, M.A., Illert, M., Kirkwood, P.A., Nielsen, J. and Lemon, R.N. (1998) 'Does a C3-C4 propriospinal system transmit corticospinal excitation in the primate? An investigation in the macaque monkey', *The Journal of physiology*, 511 (Pt 1), pp. 191-212.

Markram, H., Gerstner, W. and Sjostrom, P.J. (2011) 'A history of spike-timing-dependent plasticity', *Frontiers in synaptic neuroscience*, 3, p. 4.

Marque, P., Nicolas, G., Simonetta-Moreau, M., Pierrot-Deseilligny, E. and Marchand-Pauvert, V. (2005) 'Group II excitations from plantar foot muscles to human leg and thigh motoneurones', *Experimental brain research*, 161(4), pp. 486-501.

Matthews, P.B.C. (1972) *Mammalian muscle receptors and their central actions*. London,: Edward Arnold.

McAuley, J.H. and Marsden, C.D. (2000) 'Physiological and pathological tremors and rhythmic central motor control', *Brain : a journal of neurology*, 123 (Pt 8), pp. 1545-67.

Mercuri, B., Wassermann, E.M., Ikoma, K., Samii, A. and Hallett, M. (1997) 'Effects of transcranial electrical and magnetic stimulation on reciprocal inhibition in

the human arm', *Electroencephalography and clinical neurophysiology*, 105(2), pp. 87-93.

Meunier, S. (1999) 'Modulation by corticospinal volleys of presynaptic inhibition to Ia afferents in man', *Journal of physiology, Paris*, 93(4), pp. 387-94.

Meunier, S. and Pierrot-Deseilligny, E. (1998) 'Cortical control of presynaptic inhibition of Ia afferents in humans', *Experimental brain research*, 119(4), pp. 415-26.

Minassian, K., Hofstoetter, U.S., Dzeladini, F., Guertin, P.A. and Ijspeert, A. (2017) 'The Human Central Pattern Generator for Locomotion', *The Neuroscientist : a review journal bringing neurobiology, neurology and psychiatry*, p. 1073858417699790.

Mizuno, Y., Tanaka, R. and Yanagisawa, N. (1971) 'Reciprocal group I inhibition on triceps surae motoneurons in man', *Journal of neurophysiology*, 34(6), pp. 1010-7.

Morgante, F. and Klein, C. (2013) 'Dystonia', *Continuum*, 19(5 Movement Disorders), pp. 1225-41.

Morita, H., Petersen, N., Christensen, L.O., Sinkjaer, T. and Nielsen, J. (1998) 'Sensitivity of H-reflexes and stretch reflexes to presynaptic inhibition in humans', *Journal of neurophysiology*, 80(2), pp. 610-20.

Muir, R.B. and Lemon, R.N. (1983) 'Antidromic excitation of motoneurons by intramuscular electrical stimulation', *Journal of neuroscience methods*, 8(1), pp. 73-86.

Nakashima, K., Rothwell, J.C., Day, B.L., Thompson, P.D., Shannon, K. and Marsden, C.D. (1989) 'Reciprocal inhibition between forearm muscles in patients with writer's cramp and other occupational cramps, symptomatic hemidystonia and hemiparesis due to stroke', *Brain : a journal of neurology*, 112 (Pt 3), pp. 681-97.

Nazarpour, K., Barnard, A. and Jackson, A. (2012) 'Flexible cortical control of task-specific muscle synergies', *The Journal of neuroscience : the official journal of the Society for Neuroscience*, 32(36), pp. 12349-60.

Nielsen, J. and Petersen, N. (1994) 'Is presynaptic inhibition distributed to corticospinal fibres in man?', *The Journal of physiology*, 477(Pt 1), pp. 47-58.

Norton, J.A., Wood, D.E. and Day, B.L. (2004) 'Is the spinal cord the generator of 16-Hz orthostatic tremor?', *Neurology*, 62(4), pp. 632-4.

Parmigiani, S., Zattera, B., Barchiesi, G. and Cattaneo, L. (2018) 'Spatial and Temporal Characteristics of Set-Related Inhibitory and Excitatory Inputs from the Dorsal Premotor Cortex to the Ipsilateral Motor Cortex Assessed by Dual-Coil Transcranial Magnetic Stimulation', *Brain topography*.

Paus, T., Jech, R., Thompson, C.J., Comeau, R., Peters, T. and Evans, A.C. (1997) 'Transcranial magnetic stimulation during positron emission tomography: a new method for studying connectivity of the human cerebral cortex', *The Journal of neuroscience : the official journal of the Society for Neuroscience*, 17(9), pp. 3178-84.

Pearson, K.G. and Collins, D.F. (1993) 'Reversal of the influence of group Ib afferents from plantaris on activity in medial gastrocnemius muscle during locomotor activity', *Journal of neurophysiology*, 70(3), pp. 1009-17.

Peterson, B.W. (1979) 'Reticulospinal projections to spinal motor nuclei', *Annual review of physiology*, 41, pp. 127-40.

Pierrot-Deseilligny, E. and Burke, D. (2005) 'Ib pathways', in Pierrot-Deseilligny, E. and Burke, D. (eds.) *The circuitry of the spinal cord: Its role in motor control and movement disorders*. Cambridge: Cambridge University Press.

Pierrot-Deseilligny, E. and Burke, D.J. (2012) *The circuitry of the human spinal cord : spinal and corticospinal mechanisms of movement*. Cambridge, England ; New York: Cambridge University Press.

Popovic Maneski, L., Jorgovanovic, N., Ilic, V., Dosen, S., Keller, T., Popovic, M.B. and Popovic, D.B. (2011) 'Electrical stimulation for the suppression of pathological tremor', *Medical & biological engineering & computing*, 49(10), pp. 1187-93.

Power, H.A., Norton, J.A., Porter, C.L., Doyle, Z., Hui, I. and Chan, K.M. (2006) 'Transcranial direct current stimulation of the primary motor cortex affects cortical drive to human musculature as assessed by intermuscular coherence', *The Journal of physiology*, 577(Pt 3), pp. 795-803.

Priori, A., Berardelli, A., Inghilleri, M., Pedace, F., Giovannelli, M. and Manfredi, M. (1998) 'Electrical stimulation over muscle tendons in humans. Evidence favouring presynaptic inhibition of Ia fibres due to the activation of group III tendon afferents', *Brain*, 121 (Pt 2), pp. 373-80.

Prochazka, A., Gillard, D. and Bennett, D.J. (1997) 'Implications of positive feedback in the control of movement', *Journal of neurophysiology*, 77(6), pp. 3237-51.

Raffalt, P.C., Alkjaer, T. and Simonsen, E.B. (2015) 'Changes in soleus H-reflex during walking in middle-aged, healthy subjects', *Muscle & nerve*, 51(3), pp. 419-25.

Ramos-Murguialday, A. and Birbaumer, N. (2015) 'Brain oscillatory signatures of motor tasks', *Journal of neurophysiology*, 113(10), pp. 3663-82.

Riddle, C.N. and Baker, S.N. (2010) 'Convergence of pyramidal and medial brain stem descending pathways onto macaque cervical spinal interneurons', *Journal of neurophysiology*, 103(5), pp. 2821-32.

Riddle, C.N., Edgley, S.A. and Baker, S.N. (2009) 'Direct and indirect connections with upper limb motoneurons from the primate reticulospinal tract', *The Journal of neuroscience : the official journal of the Society for Neuroscience*, 29(15), pp. 4993-9.

Rosenzweig, E.S., Brock, J.H., Culbertson, M.D., Lu, P., Moseanko, R., Edgerton, V.R., Havton, L.A. and Tuszynski, M.H. (2009) 'Extensive spinal decussation and bilateral termination of cervical corticospinal projections in rhesus monkeys', *The Journal of comparative neurology*, 513(2), pp. 151-63.

Rudomin, P. and Schmidt, R.F. (1999) 'Presynaptic inhibition in the vertebrate spinal cord revisited', *Experimental brain research*, 129(1), pp. 1-37.

Sakai, K., Ugawa, Y., Terao, Y., Hanajima, R., Furubayashi, T. and Kanazawa, I. (1997) 'Preferential activation of different I waves by transcranial magnetic stimulation with a figure-of-eight-shaped coil', *Experimental brain research*, 113(1), pp. 24-32.

Sakai, S.T., Davidson, A.G. and Buford, J.A. (2009) 'Reticulospinal neurons in the pontomedullary reticular formation of the monkey (Macaca fascicularis)', *Neuroscience*, 163(4), pp. 1158-70.

Schepens, B. and Drew, T. (2006) 'Descending signals from the pontomedullary reticular formation are bilateral, asymmetric, and gated during reaching movements in the cat', *Journal of neurophysiology*, 96(5), pp. 2229-52.

Soteropoulos, D.S., Edgley, S.A. and Baker, S.N. (2013) 'Spinal commissural connections to motoneurons controlling the primate hand and wrist', *The Journal of neuroscience : the official journal of the Society for Neuroscience*, 33(23), pp. 9614-25.

Soteropoulos, D.S., Williams, E.R. and Baker, S.N. (2012) 'Cells in the monkey ponto-medullary reticular formation modulate their activity with slow finger movements', *The Journal of physiology*, 590(16), pp. 4011-27.

Stefan, K., Kunesch, E., Cohen, L.G., Benecke, R. and Classen, J. (2000) 'Induction of plasticity in the human motor cortex by paired associative stimulation', *Brain*, 123 Pt 3, pp. 572-84.

Taheri, B., Case, D. and Richer, E. (2014) 'Robust controller for tremor suppression at musculoskeletal level in human wrist', *IEEE transactions on neural*

systems and rehabilitation engineering : a publication of the IEEE Engineering in Medicine and Biology Society, 22(2), pp. 379-88.

Tazoe, T. and Perez, M.A. (2014) 'Selective activation of ipsilateral motor pathways in intact humans', *The Journal of neuroscience : the official journal of the Society for Neuroscience*, 34(42), pp. 13924-34.

Thomas, C.K., Bakels, R., Klein, C.S. and Zijdewind, I. (2014a) 'Human spinal cord injury: motor unit properties and behaviour', *Acta physiologica*, 210(1), pp. 5-19.

Thomas, C.K., Dididze, M., Martinez, A. and Morris, R.W. (2014b) 'Identification and classification of involuntary leg muscle contractions in electromyographic records from individuals with spinal cord injury', *Journal of electromyography and kinesiology : official journal of the International Society of Electrophysiological Kinesiology*, 24(5), pp. 747-54.

Thompson, A.K. and Wolpaw, J.R. (2014a) 'Operant conditioning of spinal reflexes: from basic science to clinical therapy', *Frontiers in integrative neuroscience*, 8, p. 25.

Thompson, A.K. and Wolpaw, J.R. (2014b) 'The simplest motor skill: mechanisms and applications of reflex operant conditioning', *Exercise and sport sciences reviews*, 42(2), pp. 82-90.

Thompson, A.K. and Wolpaw, J.R. (2015) 'Restoring walking after spinal cord injury: operant conditioning of spinal reflexes can help', *The Neuroscientist : a review journal bringing neurobiology, neurology and psychiatry*, 21(2), pp. 203-15.

Toda, T., Ishida, K., Kiyama, H., Yamashita, T. and Lee, S. (2014) 'Down-regulation of KCC2 expression and phosphorylation in motoneurons, and increases the number of in primary afferent projections to motoneurons in mice with post-stroke spasticity', *PloS one*, 9(12), p. e114328.

Trenado, C., Amtage, F., Huethe, F., Schulte-Monting, J., Mendez-Balbuena, I., Baker, S.N., Baker, M., Hepp-Reymond, M.C., Manjarrez, E. and Kristeva, R. (2014) 'Suppression of enhanced physiological tremor via stochastic noise: initial observations', *PLoS One*, 9(11), p. e112782.

Turco, C.V., El-Sayes, J., Savoie, M.J., Fassett, H.J., Locke, M.B. and Nelson, A.J. (2018) 'Short- and long-latency afferent inhibition; uses, mechanisms and influencing factors', *Brain stimulation*, 11(1), pp. 59-74.

van der Meer, J.N., Schouten, A.C., Bour, L.J., de Vlugt, E., van Rootselaar, A.F., van der Helm, F.C. and Tijssen, M.A. (2010) 'The intermuscular 3-7 Hz drive is not

affected by distal proprioceptive input in myoclonus-dystonia', *Experimental brain research*, 202(3), pp. 681-91.

van der Stouwe, A.M., Conway, B.A., Elting, J.W., Tijssen, M.A. and Maurits, N.M. (2015) 'Usefulness of intermuscular coherence and cumulant analysis in the diagnosis of postural tremor', *Clinical neurophysiology : official journal of the International Federation of Clinical Neurophysiology*, 126(8), pp. 1564-9.

Wargon, I., Lamy, J.C., Baret, M., Ghanim, Z., Aymard, C., Penicaud, A. and Katz, R. (2006) 'The disynaptic group I inhibition between wrist flexor and extensor muscles revisited in humans', *Experimental brain research*, 168(1-2), pp. 203-17.

Williams, E.R. and Baker, S.N. (2009) 'Renshaw cell recurrent inhibition improves physiological tremor by reducing corticomuscular coupling at 10 Hz', *The Journal of Neuroscience*, 29(20), pp. 6616-24.

Williams, E.R., Soteropoulos, D.S. and Baker, S.N. (2010) 'Spinal interneuron circuits reduce approximately 10-Hz movement discontinuities by phase cancellation', *Proceedings of the National Academy of Sciences of the United States of America*, 107(24), pp. 11098-103.

Willis, W.D., Nunez, R. and Rudomin, P. (1976) 'Excitability changes of terminal arborizations of single Ia and Ib afferent fibers produced by muscle and cutaneous conditioning volleys', *Journal of neurophysiology*, 39(6), pp. 1150-9.

Winslow, J., Martinez, A. and Thomas, C.K. (2015) 'Automatic identification and classification of muscle spasms in long-term EMG recordings', *IEEE journal of biomedical and health informatics*, 19(2), pp. 464-70.

Witham, C.L., Fisher, K.M., Edgley, S.A. and Baker, S.N. (2016) 'Corticospinal Inputs to Primate Motoneurons Innervating the Forelimb from Two Divisions of Primary Motor Cortex and Area 3a', *The Journal of neuroscience : the official journal of the Society for Neuroscience*, 36(9), pp. 2605-16.

Wynne, M.M., Burns, J.M., Eland, D.C., Conatser, R.R. and Howell, J.N. (2006) 'Effect of counterstrain on stretch reflexes, hoffmann reflexes, and clinical outcomes in subjects with plantar fasciitis', *The Journal of the American Osteopathic Association*, 106(9), pp. 547-56.

Yi, X., Fisher, K.M., Lai, M., Mansoor, K., Bicker, R. and Baker, S.N. (2014) 'Differences between Han Chinese and Caucasians in transcranial magnetic stimulation parameters', *Experimental brain research*, 232(2), pp. 545-53.

Zaaimi, B., Dean, L.R. and Baker, S.N. (2018) 'Different contributions of primary motor cortex, reticular formation, and spinal cord to fractionated muscle activation', *Journal of neurophysiology*, 119(1), pp. 235-250.

Ziemann, U., Ishii, K., Borgheresi, A., Yaseen, Z., Battaglia, F., Hallett, M., Cincotta, M. and Wassermann, E.M. (1999) 'Dissociation of the pathways mediating ipsilateral and contralateral motor-evoked potentials in human hand and arm muscles', *The Journal of physiology*, 518 (Pt 3), pp. 895-906.